NOSC

Naval Ocean Systems Center
San Diego California 92152-5000

Technical Document 936
September 1986

The New MININEC (Version 3): A Mini-Numerical Electromagnetic Code

J. C. Logan and J. W. Rockway

AD-A181 682

Contents

1 Introduction

The "MINI" Electromagnetics Code, or MININEC, is a method of moments computer program for analysis of thin wire antennas [1]. A Galerkin procedure is applied to an electric field integral equation to solve for the wire currents following an approach suggested by Wilson [2]. This formulation results in an unusually short computer program suitable for implementation on a microcomputer. Hence, MININEC is written in a BASIC language compatible with many popular microcomputers.

MININEC solves for impedance and currents on arbitrarily oriented wires, including configurations with multiple wire junctions, in free space and over a perfectly conducting ground plane. Options include lumped parameter impedance loading of wires and calculation of near zone and far zone fields. Both near electric fields and near magnetic fields can be determined for free space and over a perfectly conducting ground. The far zone electric fields and radiation pattern (power pattern) can also be determined for free space and perfectly conducting ground.

Additional radiation pattern options include a Fresnel reflection coefficient correction to the patterns, for finite conducting grounds (real earth surface impedance). Up to five changes in surface impedance due to real ground are allowed in a linear or circular "cliff" model. The cliff may take on any elevation (including zero, i.e., a flat surface), however, there is no correction for diffraction from cliff edges. In the case of a circular cliff model, the first media may include a correction for the surface impedance of a densely spaced, buried, radial wire ground screen.

The first version of MININEC given by NOSC TD 516 [1], calculated currents and radiation patterns for wire antennas in free space and over a perfectly conducting ground plane. Wires attached to ground were required to intersect at a right angle and could not be impedance loaded at the connection point. Subsequent revisions corrected these shortcomings culminating in version 2 of MININEC(2), given by Li, et al. [3]. All previous versions of MININEC require user specification of wire end connections. However, MININEC(3) determines connection information for itself from user defined wire end coordinates. MININEC(3) also displays the currents wire by wire, and at all wire ends, including wire junctions. MININEC(3) features an improved, faster solution routine and has been completely restructured using a more modular programming style, including the use of helpful comment statements.

1.1 Background

The Numerical Electromagnetics Code (NEC) found in reference [4] is the most adavanced computer code available for the analysis of thin wire antennas. It is a highly user-oriented computer code offering a comprehensive capability for analysis of the interaction of electromagnetic waves with conducting structures. The program is based on the numerical solution of integral equations for the currents induced on the structure by an exciting field.

NEC combines an integral equation for smooth surfaces with one for wires to provide convenient and accurate modeling for a wide range of applications. A NEC model may include nonradiating networks and transmission lines, perfect and imperfect conductors, lumped element loading, and ground planes. The ground planes may be perfectly or imperfectly conducting. Excitation may be via an applied voltage source or incident plane wave. The output may include induced currents and charges, near or far zone electric or magnetic fields, and impedance or admittance. Many other commonly used parameters such as gain and directivity, power budget, and antenna to antenna coupling are also available.

NEC is a powerful tool for many engineering applications. It is ideal for modeling co-site antenna environments in which the interaction between antenna and environment cannot be ignored. In many problems, however, the extensive full capability of NEC is not really required because the antenna and its environment are not very complex or the information sought requires only a simplified model. In addition, NEC requires the support of and access to a large main-frame computer system. These computer systems are expensive and not always readily available at remote field activities. Even when the computer facilities are available, heavy demand usage may result in slow turnaround, even for relatively simple (or small) NEC runs. One viable solution is a "stripped down" version of NEC that would retain only the basic solution and the most frequently used options and which could be implemented on a mini- or microcomputer with an advanced FORTRAN language capability. MININEC(3) offers many of the required NEC options, but makes use of a BASIC language that is compatible with many popular microcomputers. MININEC(3) is only suitable for small problems less than 75 unknowns and 10 wires, depending on the computer memory and BASIC compiler.

1.2 Computer Requirements

Occasionally a technology develops which is destined to produce significant changes in the way people think and conduct their business. For many decades, scientists and engineers struggled with unmanageable equations and data using trial and error techniques, employing logarithmic tables and inadequate slide rule calculations. Then came the digital computer.

In the 1950s and 60s, physically large and expensive computing machines that were relatively slow, with limited capability compared to today's standards, became available to few. At first, stored programs were accessible through direct connection of individual terminals a short distance away. The revolution had begun.

In the 70s, technologists rushed to convert proven algorithms into computer programs or to develop new algorithms suitable for efficient computer programming for use as analysis and synthesis tools by the scientific community. These tools, for the most part, required the support of large central machines. Meanwhile, slide rules were being replaced by hand-held calculators with trigonometric functions, some of which could be programmed for simple repetitive algorithms.

Today, large central processing systems are being supplemented with small powerful mini- and microcomputers. The development of the low cost microprocessor chip means that computers with capabilities that equal or exceed those of the earlier main frame machines of the 60s are now available in compact size. Sizes range from suitcase, or desktop, machines the microcomputer to file cabinet machines the minicomputer that can be expanded or configured to meet specialized needs. The microcomputer is becoming more and more affordable as a personal computing tool. The microcomputer, or "home computer", is emerging as today's most important engineering and scientific tool, allowing widespread networking. Anyone with a microcomputer or terminal with an acoustic coupler and telephone has access to a wide variety of computing facilities around the country, as well as an almost limitless source of information.

MININEC has been written with the microcomputer in mind. But, it can also be implemented on mini- or larger computers that have the BASIC language capability. However, some changes in the program may be required. Programming has been kept simple, with few machine-dependent program statements, so that it will be compatible with most BASIC languages.

NEC is suitable for both small and large numeric models. The upper limit is determined by the cost factors and memory size of the mainframe on which it resides. A model containing up to 2000 unknowns (segments) seems to be the practical upper limit. On the other hand, MININEC is suitable only for small problems. The upper limit is determined by the memory size and speed of the microcomputer employed. Practical limits seem to be 30 to 40 unknowns (current pulses) when using interpreter BASIC, due to the time required to obtain a solution. However, if one is willing to wait an hour or more for the solution, a model with 65 to 75 unknowns is possible. Serious antenna modeling requires the use of a BASIC compiler. In addition, a math co-processor board is recommended. Present microcomputer memory size limits MININEC to models with less than 100 unknowns. For problems of 100 or more unknowns, a mainframe is recommended, and in that case, the use of NEC is the natural choice.

2 The Theory of MININEC

The MININEC program is based on the numerical solution of an integral equation representation of the electric fields. Discussion of similar formulations can be found elsewhere, for example, see Harrington [5]. The real advantage is that the solution techniques as implemented in MININEC results in a relatively compact (i.e., short) computer code. The discussion that follows in this section is condensed from reference [2].

2.1 The Electric Field Integral Equation and its Solution

It has become customary in solving wire antenna problems to make several assumptions which are valid for thin wires. They are that the wire radius, a, is very small with respect to the wavelength and the wire length. Because it is necessary to subdivide wires into short segments, the radius is assumed small with respect to the segment lengths as well, so that the currents can be assumed to be axially directed; i.e., there are no azimuthal components of current.

Figure 1 gives the geometry of a typical, arbitrarily oriented wire. Assume that the wire is straight, even though the theory applies equally to

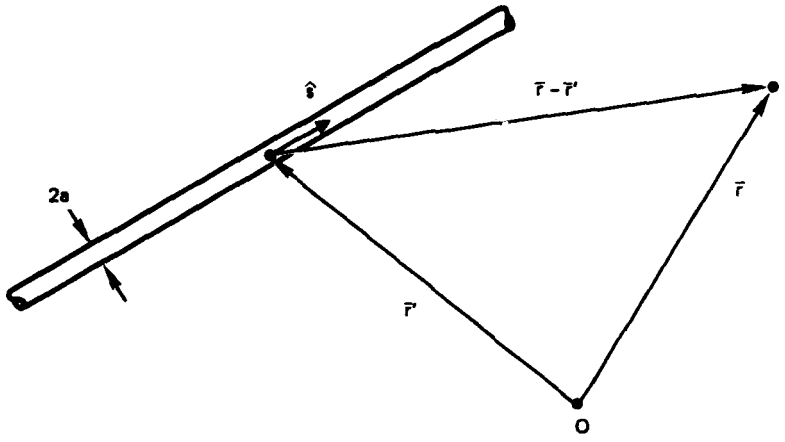

(a) An arbitrarily oriented wire.

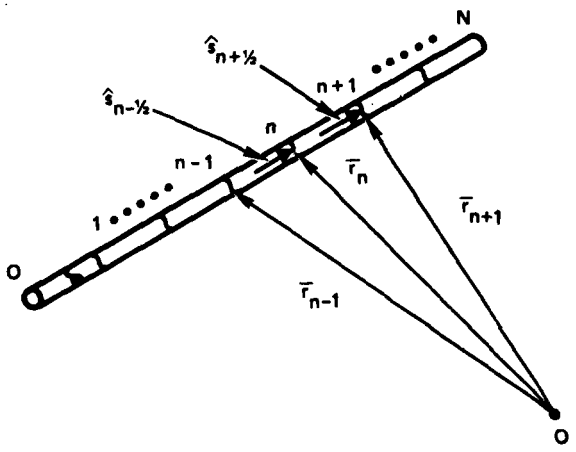

(b) Segmentation scheme for the same wire.

Figure 1: Definition of the position vectors with respect to the global origin O

bent configurations. The same wire is also shown broken into segments or subsections.

In equations (1), (2), and (3) below, the vector and scalar potentials are given by

$$\bar{A} = \frac{\mu}{4\pi} \int_c I(s)\hat{s}(s)k(s-s')\mathrm{d}s \tag{1}$$

$$\Phi = \frac{1}{4\pi\varepsilon} \int_c q(s)k(s-s')\mathrm{d}s \tag{2}$$

where

$$k(s-s\prime) = \frac{1}{2\pi} \int_{-\pi}^{\pi} \frac{e^{-jkr}}{r}\mathrm{d}\phi$$

$$r = \left((s-s')^2 + 4a^2 \sin^2 \frac{\phi}{2}\right)^{\frac{1}{2}}$$

and the linear charge density (via the continuity equation) is

$$q(s) = \frac{-1}{j\omega}\frac{\mathrm{d}I}{\mathrm{d}s} \tag{3}$$

The kernel k becomes the "exact kernel" when $\bar{r} \to \bar{r'}$ on c, but can be accurately replaced by the "reduced kernel," $k_0 = e^{-jkr}/r$, $r = (|\bar{r} - \bar{r}'|^2 + a^2)^{1/2}$ for $|\bar{r} - \bar{r'}| \gg a$.

The integral equation relating the incident field, $\bar{E}_{\mathrm{inc}}$, and the vector and scalar potentials is

$$-\bar{E}_{\mathrm{inc}} \cdot \hat{s} = -j\omega\bar{A} \cdot \hat{s} - \hat{s} \cdot \nabla\Phi \quad . \tag{4}$$

Equation (4), above, is solved in MININEC by using the following procedure.

The wires are divided into equal segments, and, as shown in Figure 1, the vectors $\bar{r}_n, n = 0, 1, \ldots N+1$ are defined, with respect to the global coordinate origin, 0. The unit vectors parallel to the wire axis for each segment shown are defined as

$$\hat{s}_{n+1/2} = \frac{\bar{r}_{n+1} - \bar{r}_n}{|\bar{r}_{n+1} - \bar{r}_n|} \quad . \tag{5}$$

Pulse testing and pulse expansion functions used in MININEC are defined as

$$P_n(s) = \begin{cases} 1, & s_{n-1/2} < s < s_{n+1/2} \\ 0, & \text{otherwise} \end{cases} \tag{6}$$

where the points $s_{n\pm1/2}$ designate segment midpoints,

$$s_{n+1/2} = \frac{s_{n+1} + s_n}{2} \tag{7}$$

or in terms of the global coordinates,

$$\bar{r}_{n+1/2} = \frac{\bar{r}_{n+1} + \bar{r}_n}{2} \quad . \tag{8}$$

It is assumed that the components of the vectors $\bar{E}_{\text{inc}}$ and $\bar{A}$ in equation (4) are sufficiently smooth over each segment that their respective values on each segment may be replaced by those taken at the point s_m. The pulse functions of (6) are then used as testing functions on (4), resulting in

$$\begin{aligned} &\bar{E}_{\text{inc}}(s_m) \cdot \left[\left(\frac{s_m - s_{m-1}}{2} \right) \hat{s}_{m-1/2} + \left(\frac{s_{m+1} - s_m}{2} \right) \hat{s}_{m+1/2} \right] = \\ &j\omega \bar{A}(s_m) \cdot \left[\left(\frac{s_m - s_{m-1}}{2} \right) \hat{s}_{m-1/2} + \left(\frac{s_{m+1} - s_m}{2} \right) \hat{s}_{m+1/2} \right] + \\ &\Phi(s_{m+1/2}) - \Phi(s_{m-1/2}) \end{aligned} \tag{9}$$

The vector quantities in brackets are simply $(\bar{r}_{m+1/2} - \bar{r}_{m-1/2})$, so (9) can be written as

$$\begin{aligned} \bar{E}_{\text{inc}}(s_m) \cdot (\bar{r}_{m+1/2} - \bar{r}_{m-1/2}) = \\ j\omega \bar{A}(s_m) \cdot (\bar{r}_{m+1/2} - \bar{r}_{m-1/2}) + \Phi(s_{m+1/2}) - \Phi(s_{m-1/2}) \quad . \end{aligned} \tag{10}$$

The currents are expanded in pulses centered at the junctions of adjacent segments as illustrated in figure 2(a). Note that pulses are omitted from the wire ends. This is equivalent to placing a half pulse of zero amplitude at each end, thus imposing the boundary condition for zero current at unattached wire ends. The current expansion can be written as

$$I(s) = \sum_{n=1}^{N} I_n P_n(s) \quad . \tag{11}$$

A difference approximation is applied to equation (3) to compute the charge. Thus, as shown in Figure 2(b), the charge can be represented as pulses displaced from the current pulses by a half pulse width.

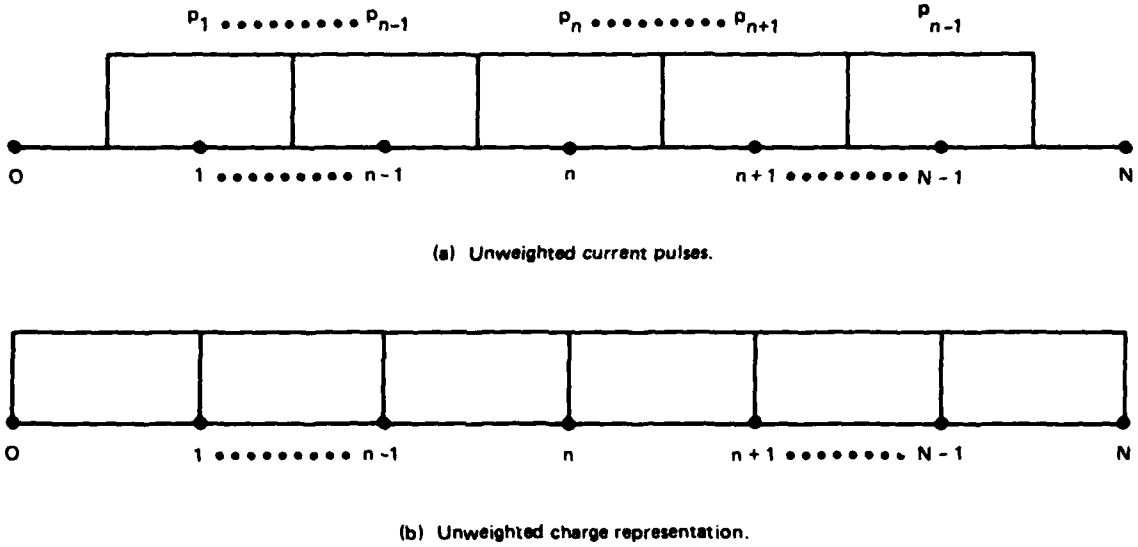

Figure 2: Wire segmentation scheme illustrating equally weighted pulses for current and charge

Substituting (11) into (10) produces a system of equations that can be expressed in matrix form. Each matrix element, Z_{mn}, associated with the n-th current and the s_m observation point involves scalar and vector potential terms with integrals of the form

$$\Phi_{m,u,v} = \int_{s_u}^{s_v} k(s_m - s')\mathrm{d}s' \tag{12}$$

where

$$k(s - s') = \frac{1}{2\pi}\int_{-\pi}^{\pi} \frac{e^{-jkr_m}}{r_m}\mathrm{d}\phi \tag{13}$$

and

$$r_m = \left((s_m - s')^2 + 4a^2 \sin^2 \frac{\phi}{2}\right)^{1/2} \quad . \tag{14}$$

Equation (12) does not lend itself to straightforward integration because of the singularity at $r = 0$. The $1/r$ can be subtracted from the integrand and then added as a separate term to yield

$$k(s - s') = \frac{1}{2\pi} \int_{-\pi}^{\pi} \frac{\mathrm{d}\phi}{r_m} + \frac{1}{2\pi} \int_{-\pi}^{\pi} \frac{e^{-jkr_m} - 1}{r_m} \mathrm{d}\phi \quad . \tag{15}$$

The first term of (15) can be rewritten as an elliptic integral of the first kind [6].

$$\frac{\beta}{\pi a} F\left(\frac{\pi}{2}, \beta\right) = \frac{1}{2\pi} \int_{-\pi}^{\pi} \frac{\mathrm{d}\phi}{r_m} \tag{16}$$

where

$$\beta = \frac{2a}{\left[(s_m - s')^2 + 4a^2\right]^{1/2}}$$

$F(\frac{\pi}{2}, \beta)$ has an approximation [6].

$$\begin{aligned} F\left(\frac{\pi}{2}, \beta\right) \cong\ & [a_0 + a_1 m + a_2 m^2 + a_3 m^3] \cdot \\ & [b_0 + b1_m + b_2 m^2 + b_3 m^3] \ln(1/m) \end{aligned} \tag{17}$$

where

$$m = 1 - \beta^2 = \frac{(s_m - s')^2}{(s_m - s')^2 + 4a^2}$$

$$\begin{array}{lll} a_0 = & 1.38629\ 436112 & b_0 = .5 \\ a_1 = & .09666\ 344259 & b_1 = .12498\ 59397 \\ a_2 = & .03590\ 092383 & b_2 = .06880\ 248576 \\ a_3 = & .03742\ 563713 & b_3 = .03328\ 355346 \\ a_4 = & .01451\ 196212 & b_4 = .00441\ 787012 \end{array}$$

Thus

$$\frac{\beta}{\pi a} F\left(\frac{\pi}{2}, \beta\right) \overrightarrow{s \to s'} - \frac{1}{\pi a} \ln\left[\frac{|s_m - s'|}{8a}\right] \tag{18}$$

and this singularity is also subtracted from $k(s_m - s')$.

Thus

$$k(s_m - s') = -\frac{1}{\pi a}\ln\left[\frac{|s_m - s'|}{8a}\right] + \frac{\beta F(\frac{\pi}{2},\beta) + \ln\left[\frac{|s_m - s'|}{8a}\right]}{\pi a} + \frac{1}{2\pi}\int_{-\pi}^{\pi}\frac{e^{-jkr}-1}{r}\mathrm{d}\phi \tag{19}$$

This equation is substituted into equation (12) and written as

$$\int_{s_u}^{s_v} k(s - s')\mathrm{d}s' = I_1 + I_2 + I_3 \quad . \tag{20}$$

I_1, I_2, and I_3 are defined as

$$I_1 = -\frac{1}{\pi a}\int_{s_u}^{s_v}\ln\left[\frac{|s - s'|}{8a}\right]\mathrm{d}s' \;=\; \frac{8}{\pi}u(1 - \ln|u|)\Big|_{u_1}^{u_2} \tag{21}$$

where

$$u_1 = \frac{s_u - s}{8a} \text{ and } u_2 = \frac{s_v - s}{8a} \quad .$$

Similarly,

$$I_2 = \int_{s_u}^{s_v}\frac{\beta F\left(\frac{\pi}{2},\beta\right) + \ln\frac{|s-s'|}{8a}}{\pi a}\mathrm{d}s' \tag{22}$$

This integral has a well behaved integrand and can be integrated numerically. The integration is broken up into two integrals over the ranges (s_u, s) and (s, s_v) for best accuracy. Gaussian quadrature is used for the numerical integration [7]. The number of points used in the integration routine is automatically selected by consideration of the pulse accuracy required for the source to observation distance. The final integral is

$$I_3 = \frac{1}{2\pi}\int_{s_u}^{s_v}\int_{-\pi}^{\pi}\frac{e^{-jkr}-1}{r}\mathrm{d}\phi \quad . \tag{23}$$

The integrand is nonsingular and can be integrated numerically. To obviate the need for double integration, it is convenient to approximate the integral by replacing r by a reduced kernel approximation of equation (14). Thus

$$I_3 = \int_{s_u}^{s_v} \frac{e^{-jkr_a} - 1}{r_a} \mathrm{d}s' \tag{24}$$

where

$$r_a = \sqrt{(s_v - s') + a^2} \quad .$$

The integral can be integrated numerically by the same procedure as for I_2.

Thus, equation (12) with its singularity problem is evaluated by adding I_1 of equation (21), I_2 of equation (22), and I_3 of equation (24).

This approach to evaluate (12) is accurate for a wide range of wire radii but breaks down when the radius becomes very small. For very small radii, equation (12) may be expressed as a single integral and evaluated using two terms of a Maclaurin series, after Harrington [5]. This approximation for the Φ terms is:

$$\left.\begin{array}{ll} \Phi \approx \frac{1}{2\pi\Delta s} \ln\left(\frac{\Delta s}{a}\right) - j\frac{k}{4\pi} & \text{for } m = n \\ \Phi \approx \frac{e^{-jkr_m}}{4\pi r_m} & \text{for } m \neq n \end{array}\right\} \quad . \tag{25}$$

Figure 3 demonstrates the range and validity with and without the small radius correction. Without the correction, MININEC gives acceptable answers for wire radii between 10^{-2} and 10^{-5} wave lengths. Note that MININEC is within 10% or better of the data published by King [8] [9], for radii between 10^{-3} and 10^{-2} wave lengths. The small radius correction provides correct results for radii of 10^{-4} wave lengths or smaller. In MININEC, the switch to the small radius approximations occurs automatically for radii of 10^{-4} and smaller.

By substitution, the matrix equation to be solved is

$$[Z_{mn}] = [I_n] = [V_m] \tag{26}$$

where

$$[Z_{mn}] = \frac{-1}{4\pi j\omega\varepsilon}\left[k^2(\bar{r}_{m+1/2} - \bar{r}_{m-1/2}) \cdot (\hat{s}_{n+1/2}\Phi_{m,n,n+1/2} + \hat{s}_{n-1/2}\Phi_{m,n-1/2,n}) \right.$$
$$\left. -\frac{\Phi_{m+1/2,n,n+1}}{s_{n+1} - s_n} + \frac{\Phi_{m+1/2,n-1,n}}{s_n - s_{n-1}} + \frac{\Phi_{m+1/2,n,n+1}}{s_{n+1} - s_n} - \frac{\Phi_{m+1/2,n-1,n}}{s_n - s_{n-1}} \right] \tag{27}$$

and

$$V_m = \bar{E}_{\text{inc}}(s_m) \cdot (\bar{r}_{m+1/2} - \bar{r}_{m-1/2}) \quad . \tag{28}$$

$[Z_{mn}]$ is a square matrix and $[I_n]$ and $[V_m]$ are column matrices with $n = 1, 2, \ldots N$ and $m = 1, 2, \ldots N$ total unknowns (N is the total number of current pulses). The extension of these equations to two or more coupled wires follows the same line of development and will not be covered here.

The column vector $[V_m]$ represents an applied voltage that superimposes a constant tangential electric field along the wire for a distance of one segment length centered coincident with the location of the current pulses. Hence, for a transmitting antenna, all elements of $[V_m]$ are set to zero except for the element(s) corresponding to the segment(s) located at the desired feed point(s). For an incident plane wave, all elements of $[V_m]$ must be assigned a value depending on the strength, polarization (or orientation), and angle of incidence of the plane wave. The applied voltage source (transmit case), however, is the only ready-made, or programmed, option in MININEC.

As stated above, the $[Z_{mn}]$ matrix in equation (26) is filled by the evaluation of an elliptic integral and use of Gaussian quadrature for numerical integration. The solution of (26) can be accomplished by using any one of a number of standard matrix solution techniques. MININEC(3) uses a triangular decomposition (LU decomposition) with the Gauss elimination procedure with partial pivoting [7].

2.2 Wire Junctions

The theory developed thus far for straight wires is equally applicable to bent wires. However, for coding simplicity in MININEC, bent wires are treated in the same way as the junctions of multiple numbers of wires. That is, a bend in an otherwise straight wire is treated as the junction between two straight wires.

It has been generally accepted that the currents at junctions of thin wires conform to Kirchoff's current law [10]. Rather than explicitly enforcing this condition in MININEC, an overlapping segment scheme [11] is employed at junctions of two or more wires. A detailed discussion of this approach, including arguments for validity, appears in both references [8] and [9]. Only those aspects essential to the use of MININEC are discussed here.

Consider a wire having no connections at either end. The wire is subdivided into segments and the current is expanded in pulses centered at adja-

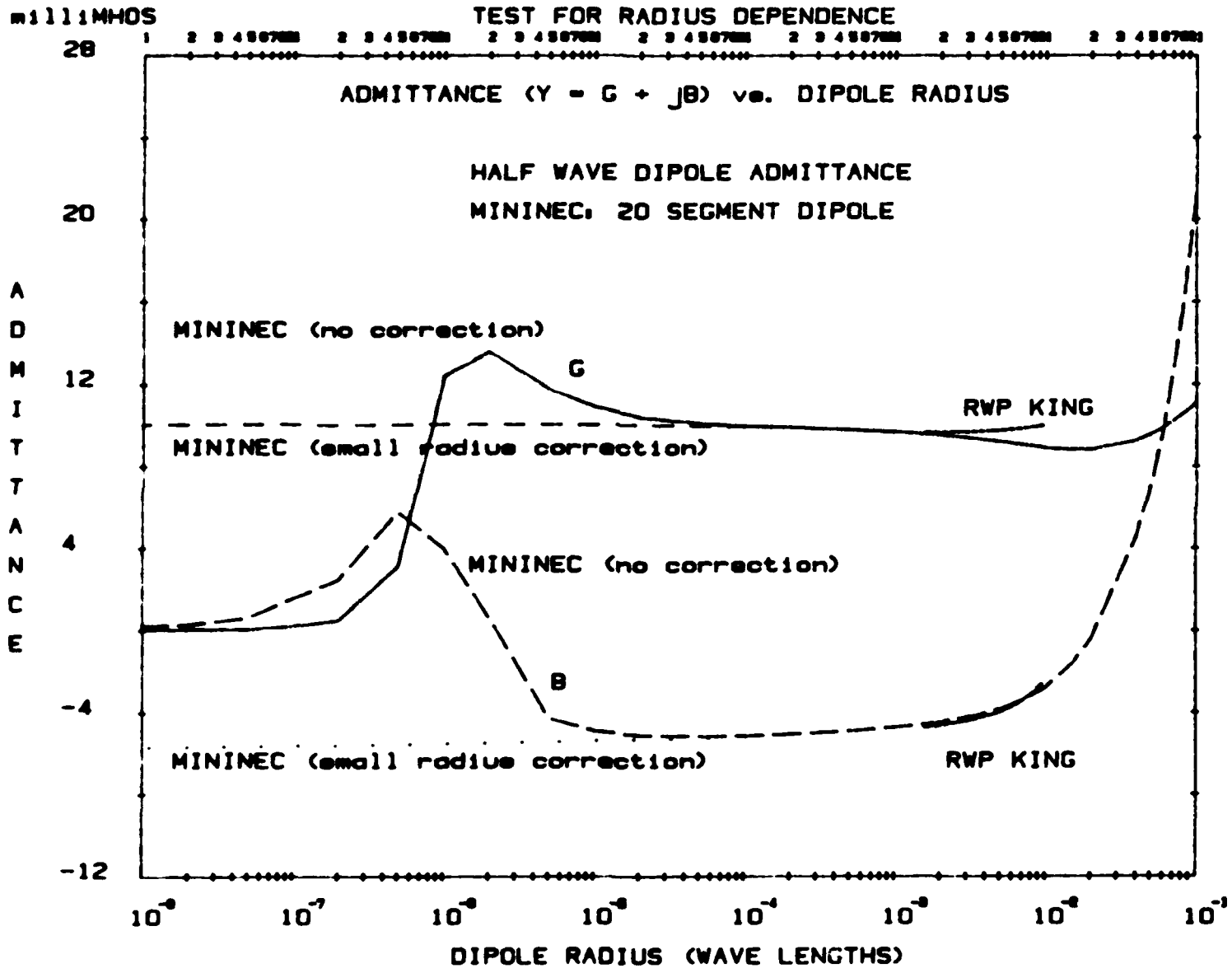

Figure 3: Variation of dipole admittance with wire radius for MININEC with and without the small radius correction. Data from King [8], [9] is also shown.

cent segment junctions as described above and illustrated in Figure 4(a). The end points have no pulses, or alternatively the end points have half pulses with zero amplitude. A second wire is to be attached to one end of the first. The second wire is subdivided into segments with pulses for currents located as in the first case. However, a full pulse is located at the attachment end, with half the pulse extending onto wire two, and half onto wire one, as illustrated in Figure 4(b). The half on wire one assumes the dimensions (length and radius) of the half segment on wire one, while the half on wire two assumes the dimensions appropriate to wire two. Wire two overlaps onto wire one with a full pulse centered at the junction end. Note that the free end of the wire has a zero half pulse. A third wire may be assumed to also overlap onto wire one, as illustrated in Figure 4(c). It can be shown (see [8] and [9]) that for a junction of N wires, only $N-1$ overlapping pulses are required to satisfy Kirchoff's current law. Alternatively, wire three could have overlapped onto wire two (not illustrated here).

The convention in MININEC(3) is that the overlap occurs onto the earliest wire specified at a given junction. It is assumed that a wire can overlap onto another wire, provided that another wire was previously specified. It cannot overlap onto a wire not yet specified. Either end of a wire may overlap onto either end of another wire. All that is required to impose the continuity conditions at the junction is that there be $N-1$ overlaps for a junction of N wires.

Current reference directions are assumed to be based on the order in which the coordinates of a wire are specified. A positive wire current is from the end first specified, end one, towards the other end, end two. By use of Kirchoff's current law and the current reference direction, the currents at the junction can be found. For example, suppose the wires in Figure 4(c) are all specified from left to right. Let the pulse amplitudes for the first pulse on wires two and three be I_2 and I_3, respectively. Then the currents out of the junction into wires two and three are the complex amplitudes of the first pulses, the overlapping pulses, on wires two and three, respectively. Hence, the current on wire one into the junction is the sum of these currents; i.e., $I_1 = I_2 + I_3$.

MININEC(3) automatically determines, during geometry input, whether there is a connection on either end of a wire, and if so, to which wire and wire end it is connected. After solving for the current pulse amplitudes, MININEC(3) then computes the junction currents, if any, for each wire end. The final display indicates free ends by the letter `E` (for free end) and junction

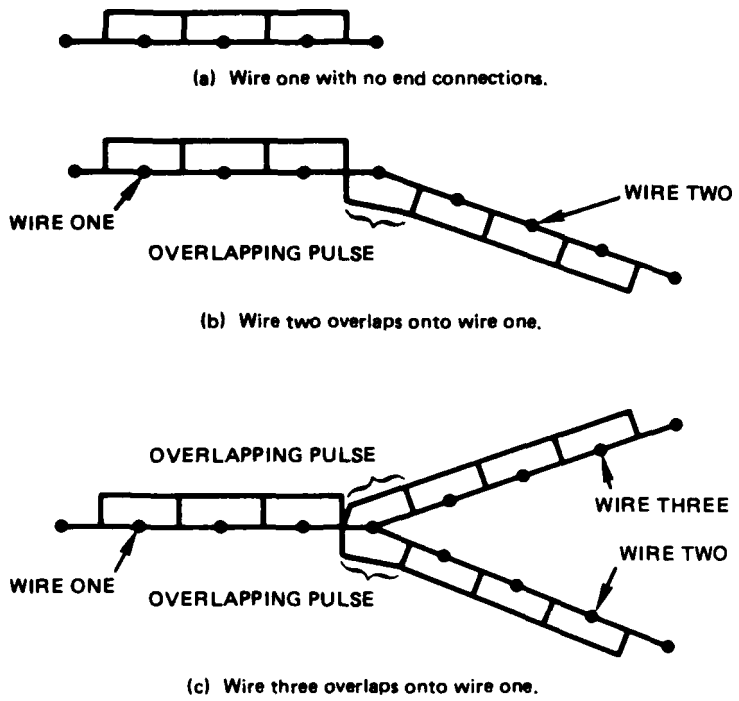

Figure 4: Illustration of the overlap scheme used at multiple wire junctions

ends by the letter J. The geometry and currents are displayed wire by wire.

2.3 The Ground Plane

The method of images is used in MININEC to solve for currents in wires located over a perfectly conducting ground plane.

Consider a wire structure represented by N segments. In the presence of a perfectly conducting ground plane, by image theory, the structure and ground plane may be replaced by the original structure and its image. Hence, there are now $2N$ segments and $2N$ unknowns to be determined. Equation (26) can be written as

$$\begin{bmatrix} V_1 \\ \vdots \\ V_N \\ \vdots \\ V_{2N} \end{bmatrix} = \begin{bmatrix} Z_{11} & \cdots & Z_{1N} & \cdots & Z_{1,2N} \\ \vdots & & \vdots & & \vdots \\ Z_{N1} & \cdots & Z_{NN} & \cdots & Z_{N,2N} \\ \vdots & & \vdots & & \vdots \\ Z_{2N,1} & \cdots & \cdot & \cdots & Z_{2N,2N} \end{bmatrix} = \begin{bmatrix} I_1 \\ \vdots \\ I_N \\ \vdots \\ I_{2N} \end{bmatrix} \tag{29}$$

The image current, $I_{N+1} \cdots I_{2N}$, are equal to the currents on the original structure, $I_1 \cdots I_N$, so that $I_n = I_{2N-n+1}$. Half the equations represented in (29) contain redundant information and may be discarded. It may be reduced to a square matrix again by adding appropriate columns; i.e., by using the current identity. Hence (29) becomes

$$V = [Z'_{ij}]I \tag{30}$$

where $Z'_{ij} = Z_{ij} + Z_{i\ 2N-j+1}$.

For a wire attached to ground, a current pulse is automatically added to the wire end point connected to ground so that current continuity with its image is observed; i.e., a non-zero half pulse is placed on both the wire end and its image. The voltage in equation (30) is divided by two in this case. Either end of a wire may be attached to ground.

2.4 Lumped Parameter Loading

The wire structures discussed so far consist of perfectly conducting wires. If an impedance due to a fixed load, $Z_L = R + jX$, is added to the structure so that its location coincides with that of one or more of the non-zero-current pulse functions (i.e., a lumped load is placed on the wire at the junction of two segments), then the load introduces an additional voltage (a voltage drop) equal to the product of the current pulse magnitude and Z_L. Hence, equation (26) becomes

$$[Z'_{mn}][I_n] = [V_m] \tag{31}$$

where $Z'_{mn} = Z_{mn}$ for $m \neq n$ and $Z'_{mn} = Z_{mn} + Z_L$ for $m = n$. Hence, a specified impedance represented as the sum of a resistance and a reactance, and located on a wire coincident with a current pulse is simply added to the diagonal impedance element or self-term corresponding to that pulse. A distributed impedance such as wire conductivity can be treated in the same way by use of an equivalent, lumped-circuit, element-impedance relationship.

2.5 Near Fields

The electric near fields and the magnetic near fields can be determined from the current distribution obtained in the solution of equation (26).

The near electric fields are computed by the method described by A. T. Adams, et al., [12]. Using MININEC, the current on the wire structure is approximated using the computed current pulses. To determine the electric field at a given point in the near field, a small, virtual thin-wire dipole is placed at the point with its axis parallel to the appropriate vector component. The open-circuit voltage at the near field point can be calculated from the knowledge of the current distribution over the wire structure and the mutual impedance between the wire structure and the virtual dipole. In other words,

$$V_d = \sum_{i=1}^{N} Z_{di} I_i \quad . \tag{32}$$

The virtual dipole is open-circuited. V_d is the open-circuit voltage. I_i are the MININEC computed current pulses of the wire structure. Z_{di} are the mutual impedances between the wire structure and the virtual dipole. The mutual impedances are calculated using the MININEC method of equation (27). The electric field strength along the direction of the virtual dipole is given by

$$E_d = -\frac{V_d}{\text{length of dipole}} \quad . \tag{33}$$

This equation is evaluated once for each electric field vector component in the x, y and z directions at the near field point of interest. In MININEC, a virtual dipole of length .001 wave length is used.

MININEC calculates the three vector components E_x, E_y and E_z, as real and imaginary terms, from which the magnitude and phase are determined. The average value is determined by

$$E_{\text{ave}} = \left[\frac{1}{2}(E_x^2 + E_y^2 + E_z^2)\right]^{1/2} \tag{34}$$

which is a conservative estimate of the maximum value. The maximum or peak electric field is determined by the method described by Adams and Mendelovicz [13]. The peak electric field is

$$E_{\text{peak}} = \left[\frac{1}{2}(E_x^2 + E_y^2 + E_z^2) + \frac{1}{2}(A^2 + B^2)^{1/2}\right]^{1/2} \tag{35}$$

where

$$A = E_x^2 \cos 2\theta_x + E_y^2 \cos 2\theta_y + E_z^2 \cos 2\theta_z$$

$$B = E_x^2 \sin 2\theta_x + E_y^2 \sin 2\theta_y + E_z^2 \sin 2\theta_z$$

and where θ_x, θ_y, and θ_z are the phase angles for the corresponding field component.

The near magnetic fields are computed by a comparable method. As is the case for electric near fields, the currents on the wires are approximated by the current pulses of the MININEC solution. A virtual, thin-wire dipole is placed at the near field point with its axis parallel to the appropriate vector component. The near magnetic field is then calculated using the MININEC current distribution and the difference between the appropriate components of the vector potential.

The vector potential is generally defined such that

$$\overset{+}{H} = \frac{1}{\mu} \nabla X \overset{+}{A} \tag{36}$$

expressed in rectangular coordinates, becomes

$$\mu \overset{+}{H} = \left(\frac{\partial A_z}{\partial y} - \frac{\partial A_y}{\partial z}\right)\hat{i} + \left(\frac{\partial A_x}{\partial z} - \frac{\partial A_z}{\partial x}\right)\hat{j} + \left(\frac{\partial A_y}{\partial x} - \frac{\partial A_x}{\partial y}\right)\hat{k} \tag{37}$$

whre $\hat{i}$, $\hat{j}$, $\hat{k}$ are the unit vectors parallel to the x, y, z coordinate axis, respectively. And where A_x, A_y, A_z are the corresponding components of the vector potential evaluated at the location of the virtual dipole (i.e., the near field point). If the virtual dipoles are electrically short enough so that the fields vary continuously and smoothly over the dipole length, the partial derivatives of equation (37) can be replaced by differences:

$$\mu \overset{+}{H} = \left(\frac{\Delta A_z}{\Delta y} - \frac{\Delta A_y}{\Delta z}\right)\hat{i} + \left(\frac{\Delta A_x}{\Delta z} - \frac{\Delta A_z}{\Delta x}\right)\hat{j} + \left(\frac{\Delta A_y}{\Delta x} - \frac{\Delta A_x}{\Delta y}\right)\hat{k} \tag{38}$$

such that, for example, $\Delta A_z/\Delta_y$ is the change in the Z-component of the vector potential along a y-directed virtual dipole of length Δy, located at

the near field point, etc. In MININEC, the virtual dipole length is .001 wave length for both the near electric and near magnetic field calculations.

MININEC calculates the three vector components, H_x, H_y and H_z as real and imaginary terms, from which the magnitude and phase are determined. The average and peak values of the magnetic near fields are found in the same way as they are for the electric near fields. Thus,

$$H_{\text{ave}} = \left[\frac{1}{2}(H_x^2 + H_y^2 + H_z^2)\right]^{1/2} \tag{39}$$

and

$$H_{\text{peak}} = \left[\frac{1}{2}(H_x^2 + H_y^2 + H_z^2) + \frac{1}{2}(A^2 + B^2)^{1/2}\right]^{1/2} \tag{40}$$

where

$$A = H_x^2 \cos 2\theta_x + H_y^2 \cos 2\theta_y + H_z^2 \cos 2\theta_z$$
$$B = H_x^2 \sin 2\theta_x + H_y^2 \sin 2\theta_y + H_z^2 \sin 2\theta_z$$

and θ_i are the corresponding phase angles.

Both the electric and magnetic near fields can be scaled for any desired radiated power from the wire structure since the near fields are directly proportional to the square root of the power radiated.

2.6 Far Zone Radiation Patterns

Once the induced currents on the wires have been determined from equation (25), the radiated electric fields are computed by

$$\bar{E}(\bar{r}_0) = \int_L \frac{jk\eta}{4\pi} + \frac{e^{-jkr_0}}{r_0} + \left[\hat{k} + \bar{I}(s)\hat{k} - \bar{I}(s)\right] e^{i\bar{K}\cdot\bar{r}} \mathrm{d}s \tag{41}$$

where $\bar{r}_0$ is the position vector at the observation point, $\bar{k} = \bar{r}_0/|\bar{r}_0|$, and $\bar{K} = k\hat{k} = \frac{2\pi}{\lambda}\hat{k}$. The integral is evaluated in closed form over each straight wire segment for each current pulse and is reduced to the summation over the wire segments. The fields are then evaluated as real and imaginary parts of the θ and ϕ components at a specified radial distance. If the radial distance is zero, the factor e^{-jkr_0}/r_0 defaults to unity.

The power gain in MININEC is evaluated with the e^{-jkr_0}/r_0 factor set to one in an approach similar to that in NEC [4]. The power gain in a given direction (θ, ϕ) in spherical coordinates is

$$G = 10 \log \left(\frac{4\pi P(\theta, \phi)}{P_{\text{IN}}} \right) \tag{42}$$

where $P(\theta, \phi)$ is the power radiated per unit steradian in the direction (θ, ϕ) and P_{IN} is the total input power to the antenna. Note that directive gain could be obtained by replacing P_{IN} by the total power radiated. This step is not done in MININEC. P_{IN} is calculated from the applied voltages and the corresponding feed point currents as

$$P_{\text{IN}} = \sum_{i=1}^{N} (1/2) \text{Re}(V_n I_n^*) \tag{43}$$

where I_n^* denotes complex conjugate and n is the number of sources. $P(\theta, \phi)$ is determined from

$$P(\theta, \phi) = \frac{1}{2} r_0^2 \text{Re}[\bar{E} \times \bar{H}] = \frac{r_0^2}{2\eta} \bar{E} \cdot \bar{E}^* \tag{44}$$

where r_0 is the magnitude of the position vector $\bar{r}_0$ in the (θ, ϕ) direction. In MININEC, the gains are calculated for the individual orthogonal components of the field determined from equation (41). The power gain thus obtained from (42) is in dB above the gain of an isotropic antenna (sometimes denoted as dBi).

MININEC includes an option to correct the far fields and gain for the effects of real ground using a Fresnel reflection coefficient. The method is similar to the far field corrections used in NEC [4], but is not limited to one or two mediums. The surface of the ground is divided into a finite number of zones with a constant conductivity and dielectric constant in each zone, i.e., a constant surface impedance for each zone. The zones are defined by circular boundaries concentric about the origin or linear boundaries parallel to the y-axis and spaced along the positive x-axis. Thus, in the latter case, the ground surface is divided into "strips" at user defined x-axis intercepts. In the former case, the ground surface is divided into concentric rings at user specified radii. In this case, the first ring, or zone, may include a radial wire ground screen. For both circular and linear zone grounds, each zone may have a different surface impedance and each zone may have a different height

(Z-coordinate) relative to the first zone. In MININEC, the number of zones is limited by an array dimension and is currently set to 5.

In the Fresnel reflection coefficient method, the far field is obtained by summing the contributions of a direct ray and a reflected ray from each current pulse. The field, due to the reflected ray, is modified by the Fresnel plane wave reflection coefficient, which depends on the ground surface impedance at the bounce point, or specular point, and the angle of incidence.

The Fresnel reflection coefficients have not been applied to the MININEC current calculation. When a real ground is specified, the currents are calculated by using the perfectly conducting image theory (described in section 2.3). The real ground corrections are applied to the far field calculations only. This compromise is designed to keep MININEC relatively compact and provide accurate results whenever the ground directly beneath the antenna is a good conductor.

Following along the lines of the development given by Burke and Poggio [4], a wave incident upon a finite ground (i.e., a real ground) yields a reflected field, $\bar{E}_r$, given by

$$\bar{E}_R = R_H \left[(\bar{E}_I \cdot \hat{P}) \hat{P} \right] + R_V \left[\bar{E}_I - (\bar{E}_I \cdot \hat{P}) \hat{P} \right] \tag{45}$$

or

$$\bar{E}_R = R_V \bar{E}_I + (R_H - R_V)(\bar{E}_I \cdot \hat{P}) \hat{P} \tag{46}$$

where $\hat{P}$ is a unit vector perpendicular to the plane of incidence. $\bar{E}_I$ is the incident field and R_V and R_H are the vertical and horizontal reflection coefficients, respectively.

The two terms in square brackets in equation (44) correspond to horizontally and vertically polarized waves. The reflected field is obtained by decomposing the incident field into horizontally and vertically polarized waves, computing a reflected wave for each, and recombining the two.

The vertical and horizontal coefficients are

$$R_V = \frac{\cos\theta - z\sqrt{1 - z^2 \sin^2\theta}}{\cos\theta + z\sqrt{1 - z^2 \sin^2\theta}} \tag{47}$$

$$R_H = \frac{-\left(z\cos\theta - \sqrt{1 - z^2 \sin^2\theta} \right)}{\cos\theta + z\sqrt{1 - z^2 \sin^2\theta}} \tag{48}$$

where θ is the angle of incidence and Z is the relative impedance of the ground surface (relative to the free space impedance).

For a given observation direction (θ, ϕ), the $\hat{P}$ vector normal to the plane of incidence is

$$\hat{P} = (-\sin\theta, \cos\phi) \tag{49}$$

as may be seen in Figure 5(c). In addition, the $\hat{r}_0$ vector, pointing in the observation direction, is

$$\hat{r}_0 = (\sin\theta\cos\phi, sin\theta\sin\phi, \cos\theta) \tag{50}$$

To obtain the far fields, the integral in equation (40) implies the summation over all the current pulses. For the direct field, the currents and vectors pointing to the current pulse centers are calculated and stored in arrays by MININEC during the matrix solution process. The incident field on the ground surface is also computed from a summation over the currents, but this requires the coordinates of the specular point (the bounce point). For the geometry illustrated in Figure 5, the specular point is given by

$$r_{\text{bounce}} = \sqrt{x_{\text{bounce}}^2 + y_{\text{bounce}}^2} \tag{51}$$

$$x_{\text{bounce}} = x_i + d\cos\phi \tag{52}$$

$$y_{\text{bounce}} = y_i + d\sin\phi \tag{53}$$

$$d = Z_i \tan\theta \tag{54}$$

The value of x_{bounce} or r_{bounce} is used appropriately for the case of linear or circular zone boundaries to determine in which media the bounce occurs. The height of the ground at this point is used to locate the image of the source.

The ground surface impedance in any zone is given by

$$Z_g = \frac{1}{\sqrt{\frac{\varepsilon}{\varepsilon_0} - j\frac{\sigma}{\omega\varepsilon_0}}} \tag{55}$$

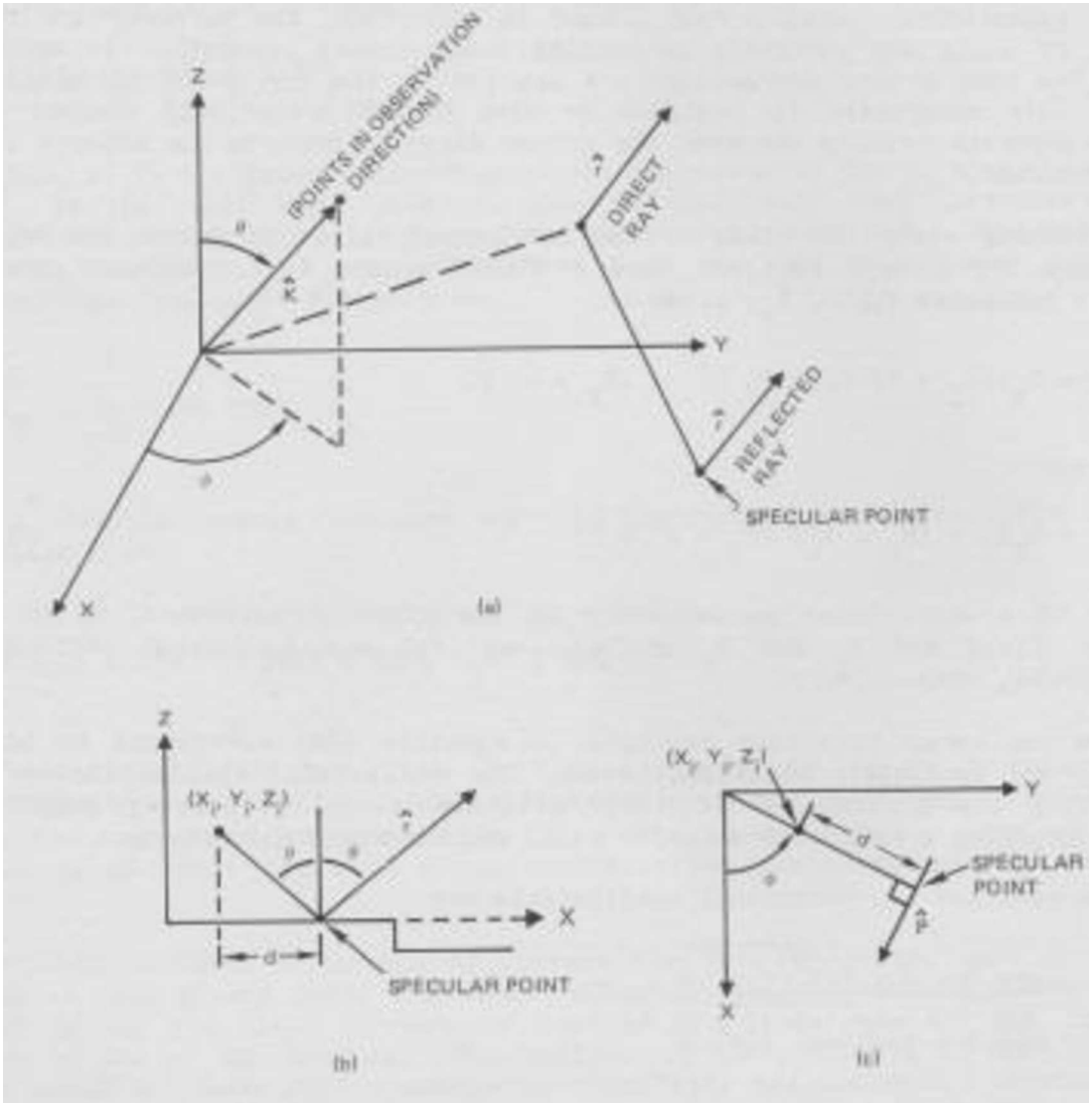

Figure 5: Definition of position vectors for Fresnel reflection coefficient

The surface impedance, when a ground screen is present and the specular point lies on the ground screen, is given by Wait [14], (also see [4]). The impedance of the ground screen by itself is

$$Z_{gs}(r_{\text{bounce}}) = j\sqrt{\varepsilon_0\mu_0}\,\frac{\omega r_{\text{bounce}}}{N}\ln\frac{r_{\text{bounce}}}{NC_0}$$

where N is the number of wires in the ground screen and C_0 is the radius of each wire. The effective ground impedance is formed by computing the parallel impedance of the ground without the ground screen and the impedance of the ground screen without the ground, or

$$Z = \frac{Z_g Z_{gs}}{Z_g + Z_{gs}} \tag{56}$$

(where $Z = Z_g$ if no ground screen is present).

The total field at a point (θ, ϕ, r) is the vector sum of the direct and reflected fields as described. When the range r is set to zero or the power gain option is selected, the e^{-jkr}/r term is set to unity. The total resulting field is used in equation (43) to calculate the power gain.

3 Validation and Modeling Guidance

The solution to an antenna problem generated by a method of moments computer program is, at best, an approximation. How close the solution is to reality depends in part on (1) the numerical methods employed in the code (and how well these methods are implemented), (2) the inherent accuracy (i.e., the number of significant digits) of the computer, (3) how well the antenna being modeled conforms to the limitations (i.e., simplifying assumptions) of the electromagnetics formulation used to create the computer program, and (4) the user's experience. Nonetheless, highly acurate answers can be obtained by careful modeling of the antenna configuration, taking into account the inherent limitations of the computer program.

Reliable, accurate answers are obtained when the user has accumulated sufficient experience from frequent and systematic exercise of the program to recognize problem areas. He must be fully aware of potential difficulties throughout the modeling process, from initially setting up a problem to interpreting the results. It is recommended that the user run MININEC for a number of elementary problems, comparing the results to independent solutions or real world measurements, until he has the confidence to apply the code to a problem for which the answer is unknown. The examples in this section provide a good place to start.

Development of confidence in the computer solution is a process of discovery of the limitations of the computer program. This entails the modeling of a number of simple antenna structures found in standard texts on antenna

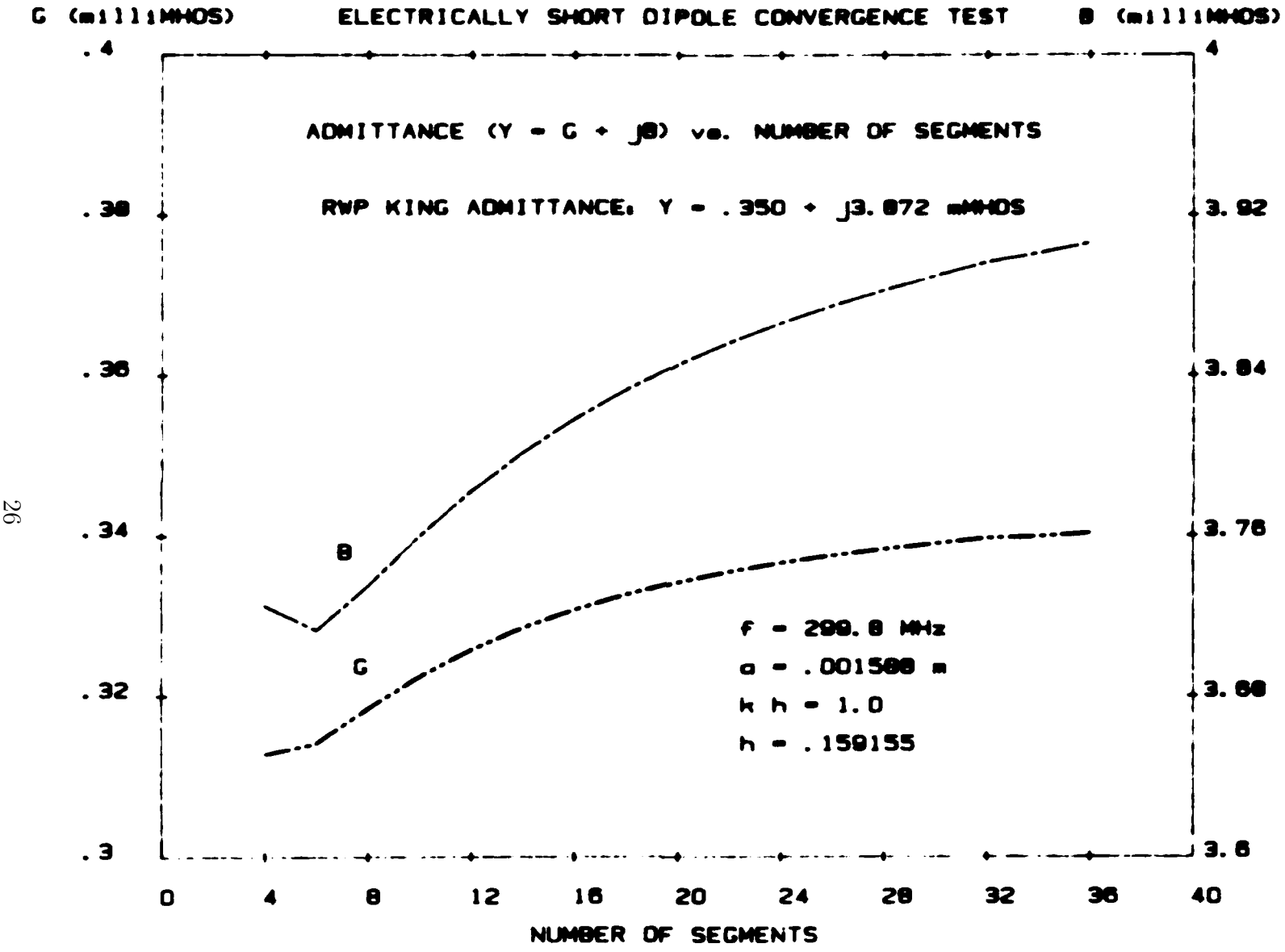

Figure 6: Convergence test for an electrically short dipole when admittance is given (Part a)

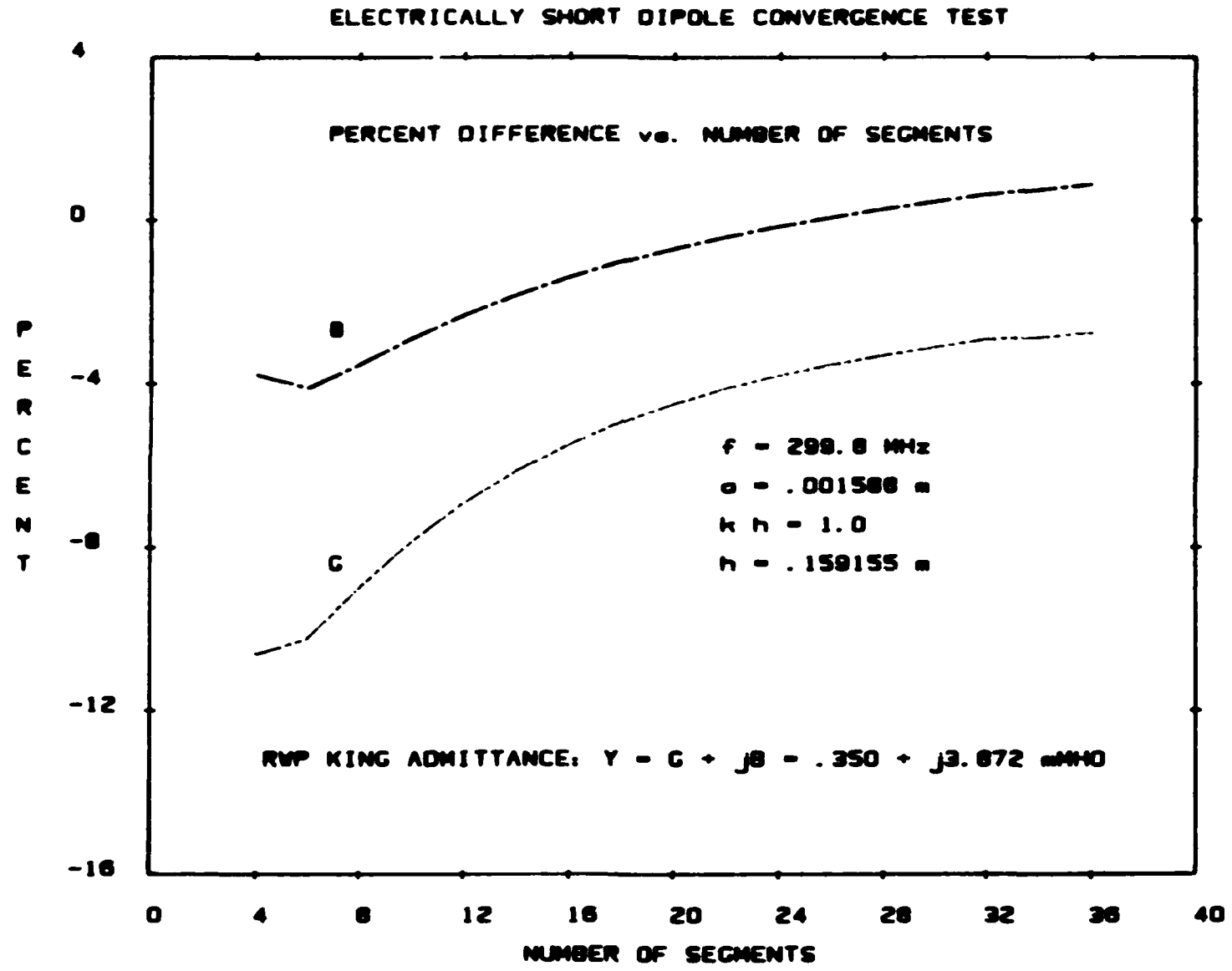

Figure 7: Convergence test for an electrically short dipole showing the percent difference in admittance between MININEC and R. W. P. King [8], [9] (Part b)

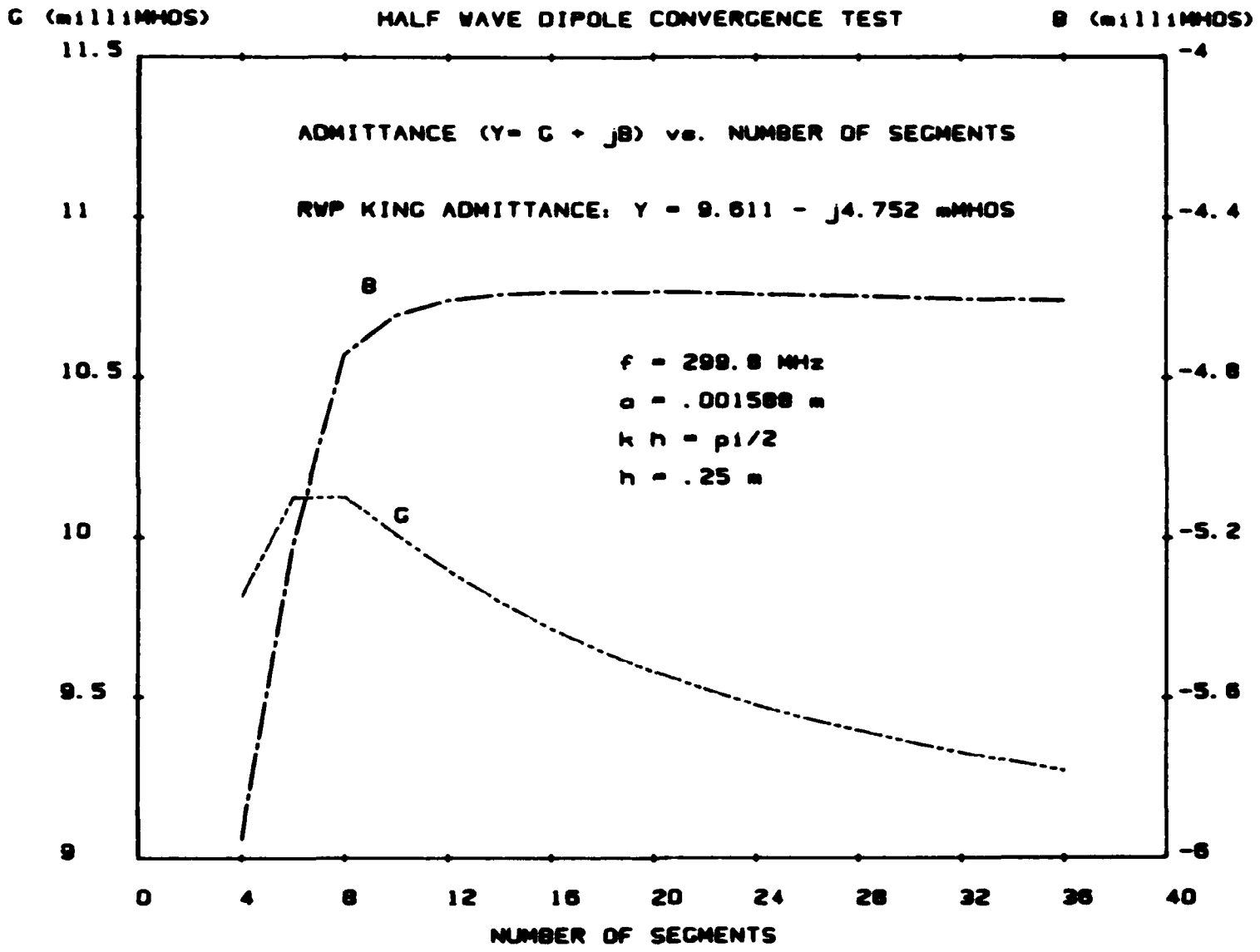

Figure 8: Convergence test for a half wave dipole when admittance is given (Part a)

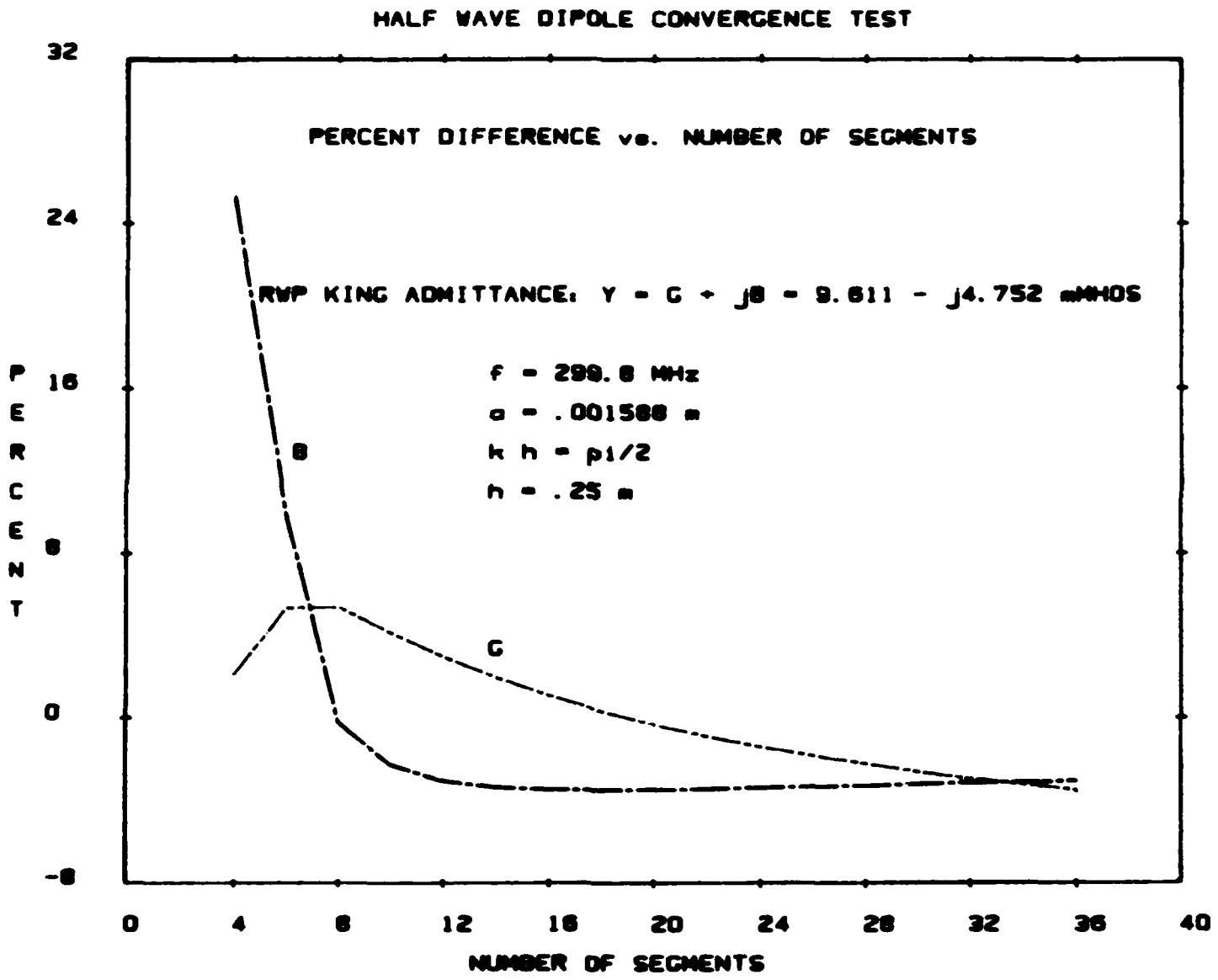

Figure 9: Convergence test for a half wave dipole showing the percent difference in admittance between MININEC and R. W. P. King [8], [9] (Part b)

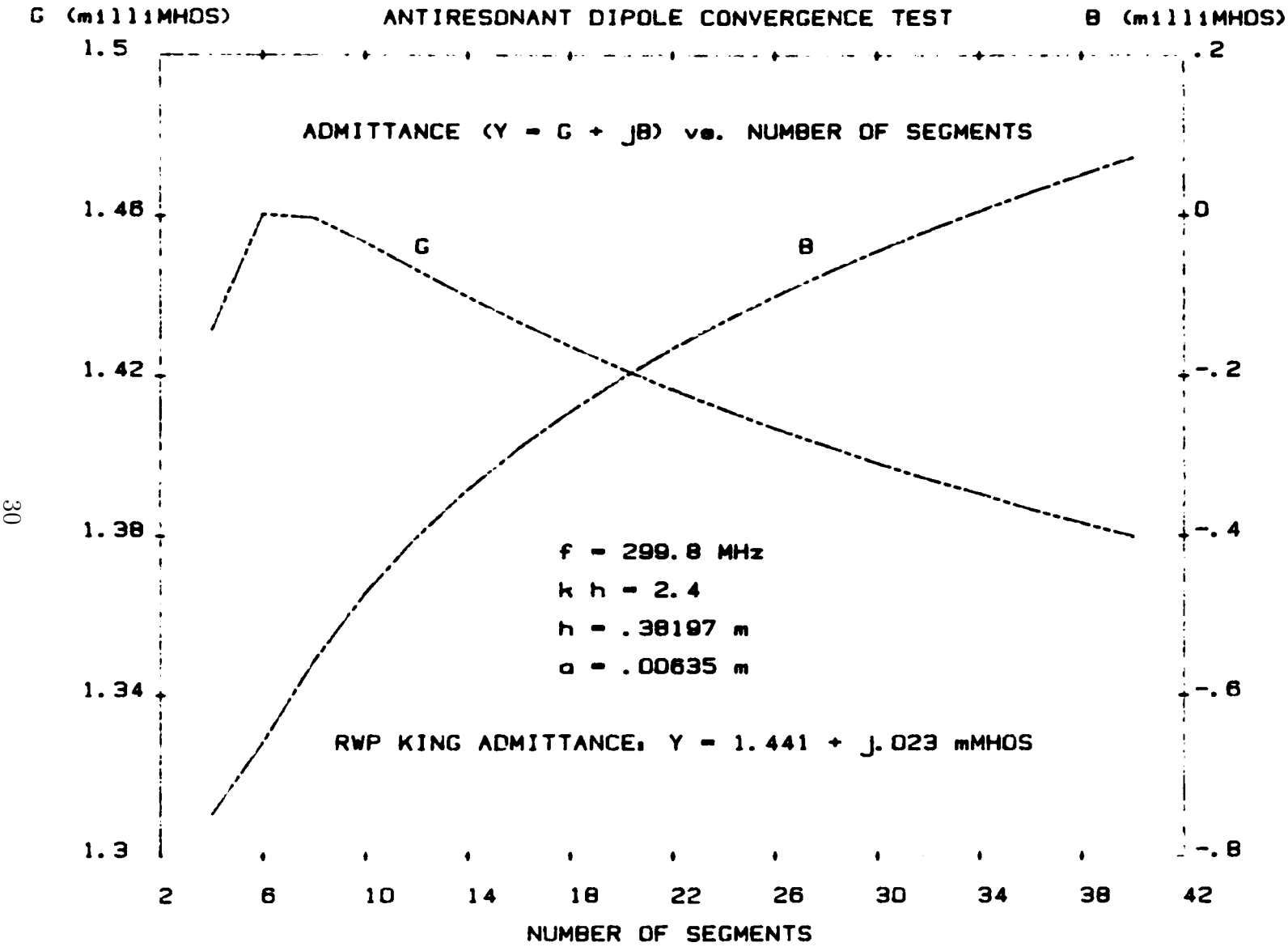

Figure 10: Convergence test for an antiresonant dipole when admittance is given (Part a)

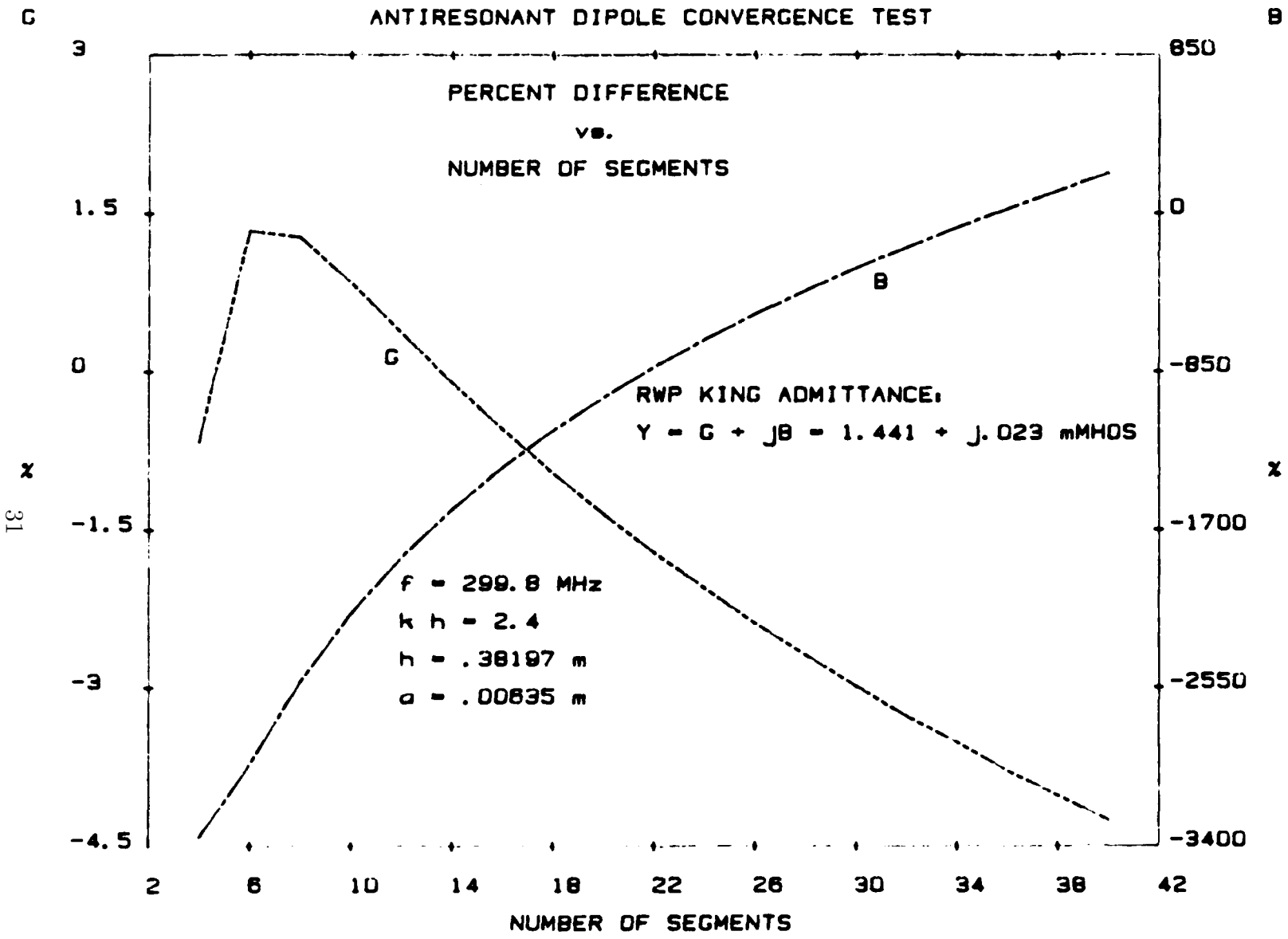

Figure 11: Convergence test for an antiresonant dipole showing the percent difference in admittance between MININEC and R. W. P. King [8], [9] (Part b)

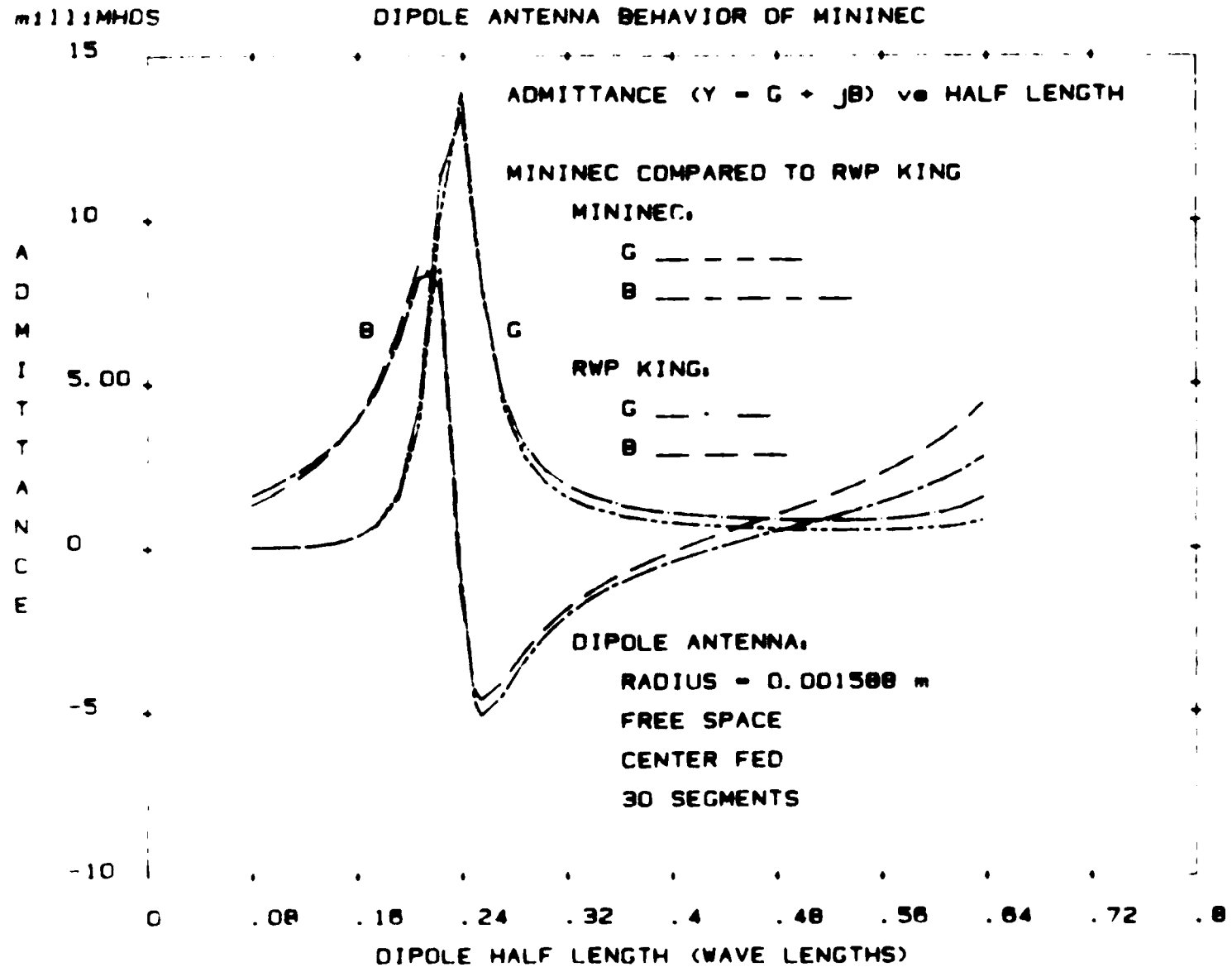

Figure 12: Dipole admittance predicted by MININEC (compared to the theory of R. W. P. King [8], [9])

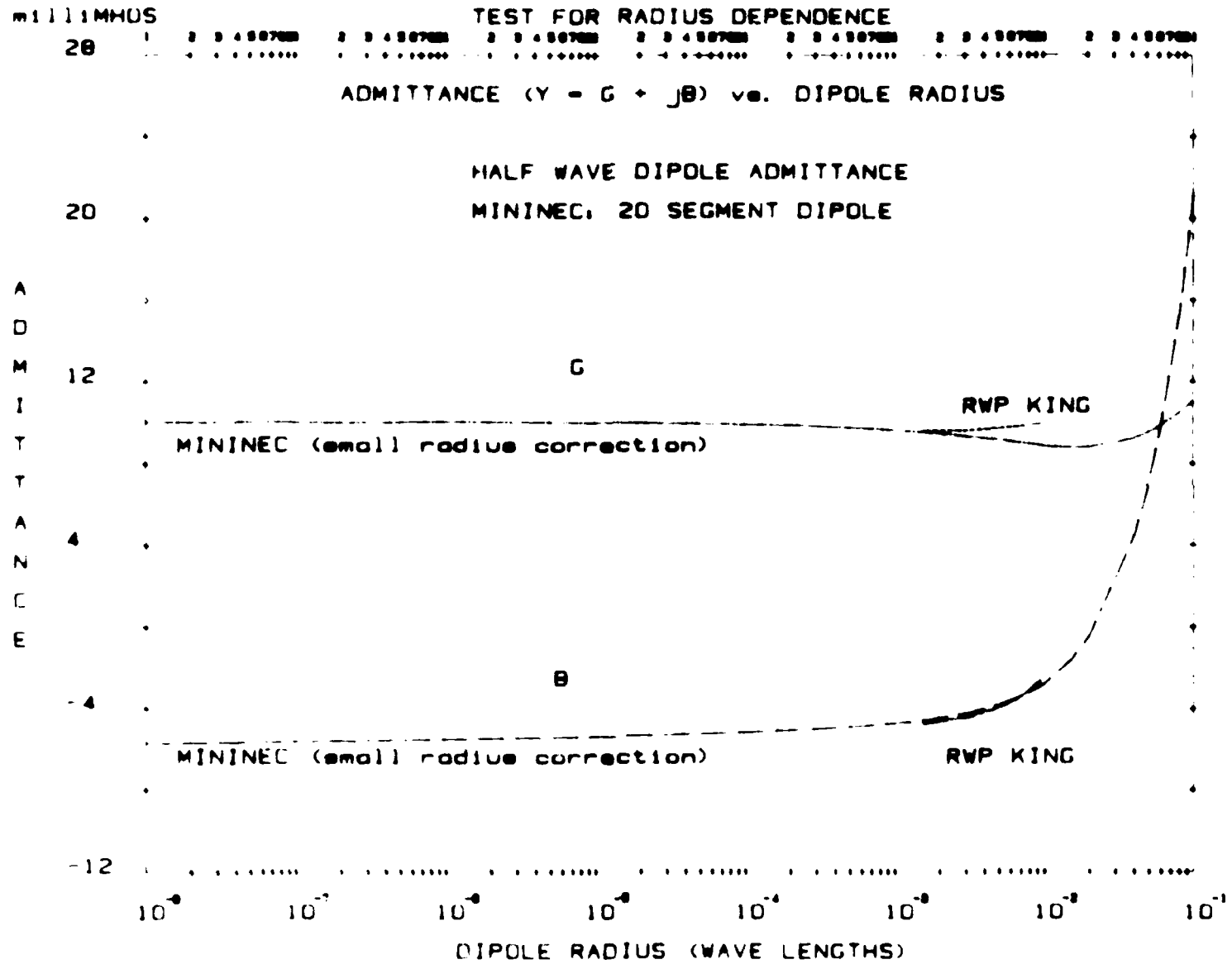

Figure 13: [Dipole admittance vs. Wire Radius] (compared to the theory of R. W. P. King [8], [9])

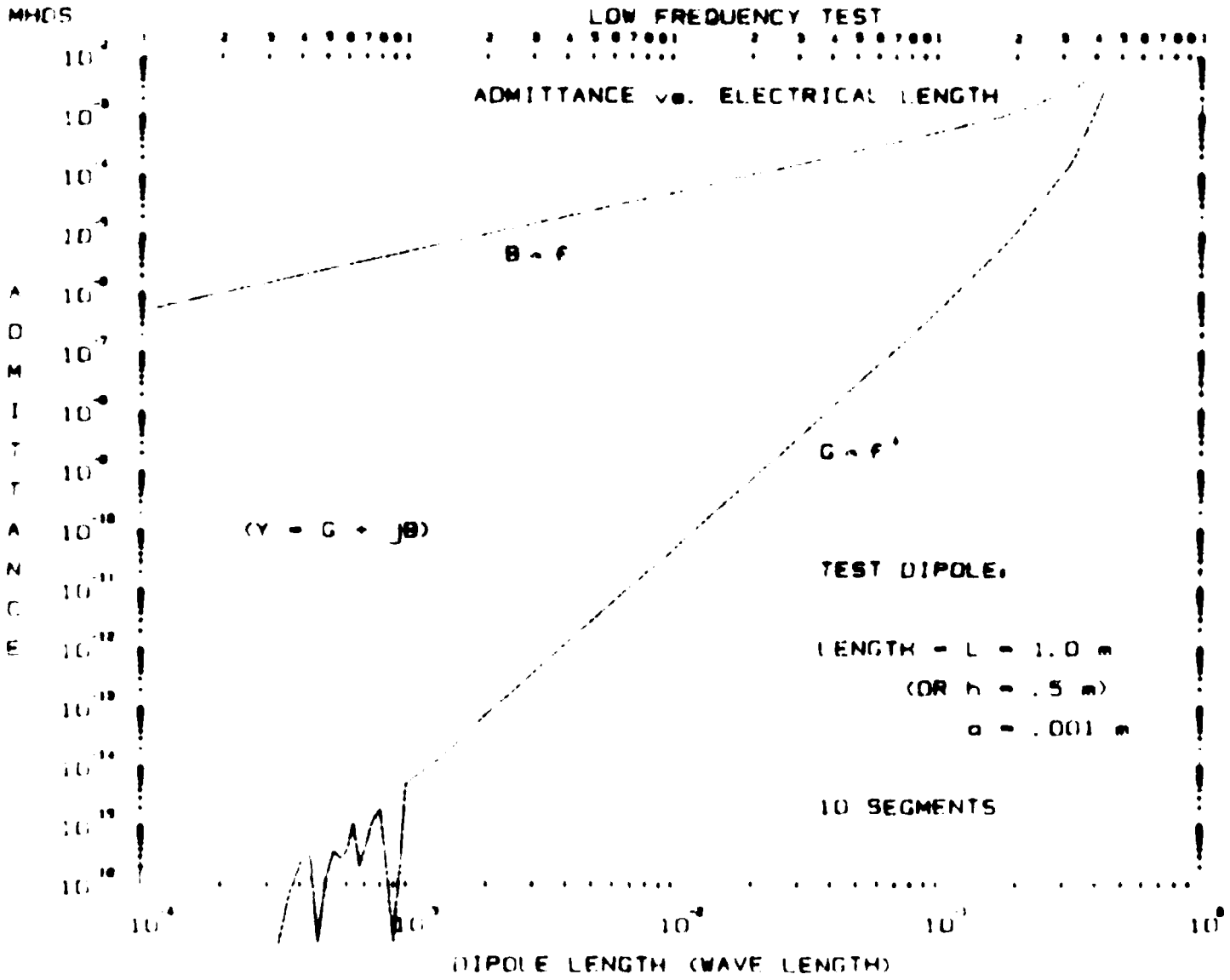

Figure 14: [Admittance vs. Dipole length] predicted by MININEC

theory. The results may be used as guidelines to model more complex antenna geometries. Natural first choices are dipoles in free space and over ground (or monopoles), followed by TEE and inverted L shaped antennas, etc. For each antenna type, a number of problems are selected involving different wire lengths and radii. MININEC is run for each antenna problem a number of times, varying segmentation (i.e., a convergence test) and other parameters to reveal the program limitations. Insight for effective application of the program is gained from comparisons with measured data or analytical solutions (when available). In this manner, modeling guidelines are derived and updated from simpler antenna problems for which there is reliable measured data or generally accepted theoretical data.

3.1 Dipole Antennas

The theoretical behavior of the dipole antenna has been studied intensely, and the literature is rich with exammples that include measured and theoretical data, [8], [9], [15], [16]. Comparison of MININEC results to this data for dipoles of various dimensions establishes validation and provides the basis for modeling guidelines. For example, convergence tests for various length dipoles reveals the accuracy that can be expected and provides a rational criterion for selection of segmentation density (the number of segments per wire) based on wire length in wave lengths.

Figure 6 through 11 show the results of convergence tests for an electrically short dipole (much shorter than the first resonance length), a dipole near resonance, and a dipole near antiresonance, respectively. Each dipole is electrically thin and center driven. Part (a) Figures (6, 8, and 10) give the variation of admittance, versus the number of segments. Part (b) Figures (7, 9, and 11) give the percent difference between MININEC and the values published by R.W.P. King, [8], [9].

The electrically short dipole, Figures 6 and 7, and the half wave dipole, Figures 8 and 9, show definitive signs of convergence and stability. No sign of convergence is seen for the antiresonant dipole, Figure 10 and 11. The authors also have seen similar convergence problems near antiresonance for other method of moment codes (notably NEC). Figures 6 through 11 can be used as guidance for selection of the segmentation density. An antenna is modeled as a collection of wires. Each wire is divided into a number of short segments selected by the user. The number of segments to achieve a desirable confidence level can be based on the results of Figures 6 through 11, depend-

ing on the wire length in wave lengths. Using this data does not guarantee convergence or the percent accuracy for a more complicated antenna, but it does provide a starting point. Convergence testing is always advisable.

Given the convergence properties of MININEC, how well does it predict dipole properties? Figure 12 is a comparison of a single, 30-segment MININEC model to the theory given by King [9]. Shown is the admittance-versus-dipole length for both MININEC and King. The difference is less that .5 millimho for most of the range, with the greatest difference of about 1.5 millimhos in the susceptance at a dipole length of .64 wave lengths. For longer or shorter antennas, the user is advised to perform suitable convergence tests.

The accuracy of the method of moments solution depends also on meeting the thin wire criterion. To illustrate, Figure 13 shows the variation of admittance versus the wire radius. The data given by King [9] are slso shown for radii betwenn 10^{-3} and 10^{-2} wave lengths. The segment to radius ratio, Δ/a, is 25 at 10^{-3} and 2.5 at 10^{-2}. For thicker wires than 10^{-2}, the thin wire criteria is not achieved and the results are expected to be not as good. The data show valid behavior for thin wires with $\Delta/a > 2.5$ or radii of 10^{-2} wave lengths and smaller.

Numerical problems may occur in the solution when quantities become too small for the inherent accuracy of the computer. An example is the erroneous results that can occur for very short segments. Figure 14 shows the results of a test designed to identify the short segment limit. Shown is the admittance-versus-dipole length in wave lengths for a 10-segment dipole in free space. The conductance and susceptance displays the proper behavior for a dipole length greater than 10^{-3} wave lengths. This corresponds to a segment length of 10^{-4} wave lengths and longer. Below 10^{-3}, the conductance oscillates about the expected values as the segment length is reduced, and at times displays negative, non-physical values. A change from single precision to double precision extends the validity range to even shorter segments, but significantly increases the solution time beyond acceptable run times for a 16-bit microcomputer. For MININEC, on a 16-bit machine in single precision, the segment length should always be greater than 10^{-4} wave lengths.

Antennas are often constructed of wires and towers or other conductors with vastly different radii. Even simple dipoles may have tapered elements. A typical MININEC model may therefore involve the connection of wires with large step changes in radii. The stepped-radius wire junction has been extensively studied by Glisson and Wilton [17]. Figure 15 is the stepped

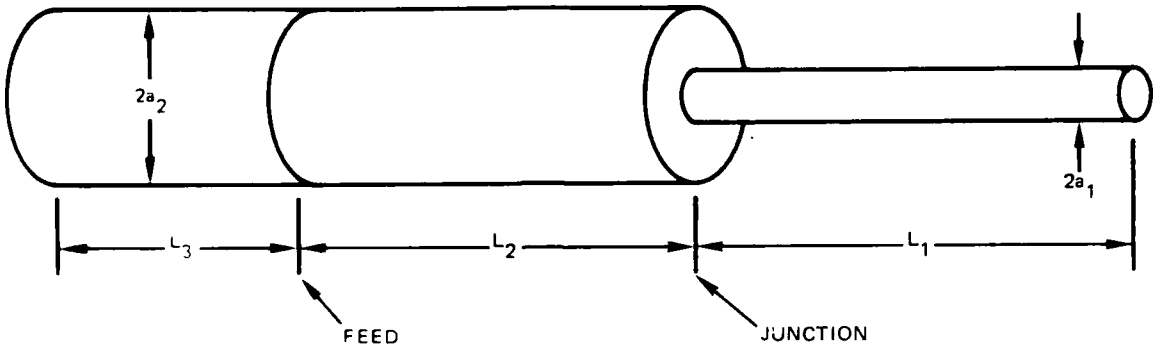

Figure 15: Geometry for the stepped radius antenna problem

wire geometry used in their study. They adapted a body of revolution computer code, PEC; to solve very accurately for currents and charges along the stepped wire antenna. The results were compared to NEC in this study.

Figures 16, 17, 18, and 19 show the current distribution predicted by PEC, NEC and MININEC for radii steps of 1:1.25, 1:5, 1:10 and 1:100, respectively. The NEC data are from their report. The MININEC results follow the PEC data surprisingly well for all step ratios. (We believe the difference between NEC and PEC may be an error in the data in the Glisson report. We have not observed this difference in NEC data.) Further investigation of MININEC for different stepped radius problems should be conducted. Suggestions include moving the feed closer to the step and switching the radii a_1 and a_2.

Multiple wire antenna structures may often require very close spacing. When the spacing is very small, the currents may not be adequately represented by a thin filament on the wire axis as it is represented in MININEC. Figures 20, 21, 22, and 23 show MININEC data for a parallel wire test used to investigate the close spacing limit. The test consists of evaluating the self and mutual admittance between two parallel half wave dipoles. One antenna is driven (i.e., the source is in the center pulse) while the second is not. The self admittance is the feed point current on the first wire if the applied voltage is 1 + j0 volts and the mutual admittance is the current for the center pulse of the second wire.

Figure 20 shows the self admittance compared to the theory by R.W.P. King [9] for dipole center to center spacings between .1 and .5 wave length. Figure 21 shows a similar comparison for the mutual admittance over the same range. The differences between MININEC and R.W.P. King are mostly

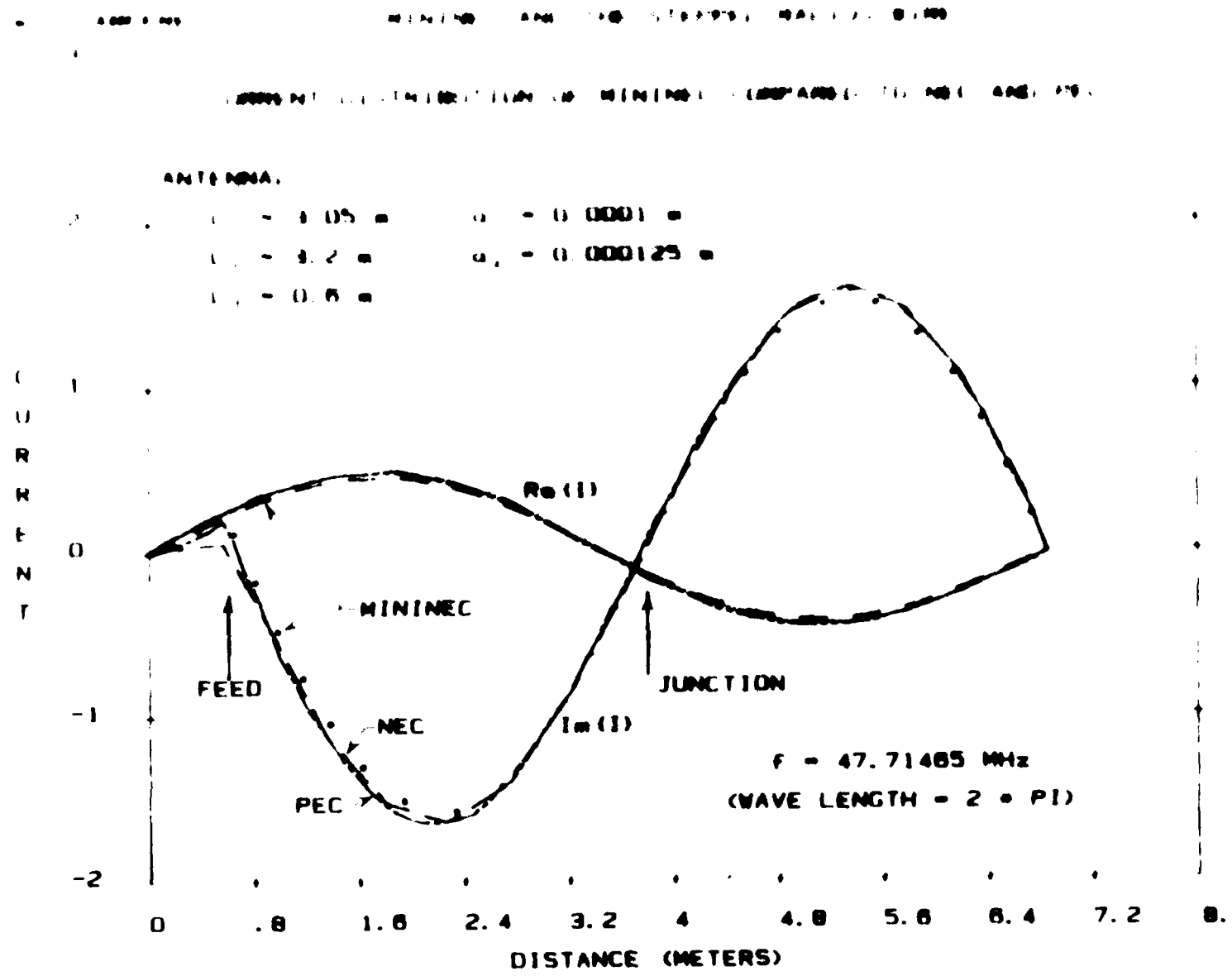

Figure 16: Currents for a stepped radius junction of $a_2/a_1 = 1.25$

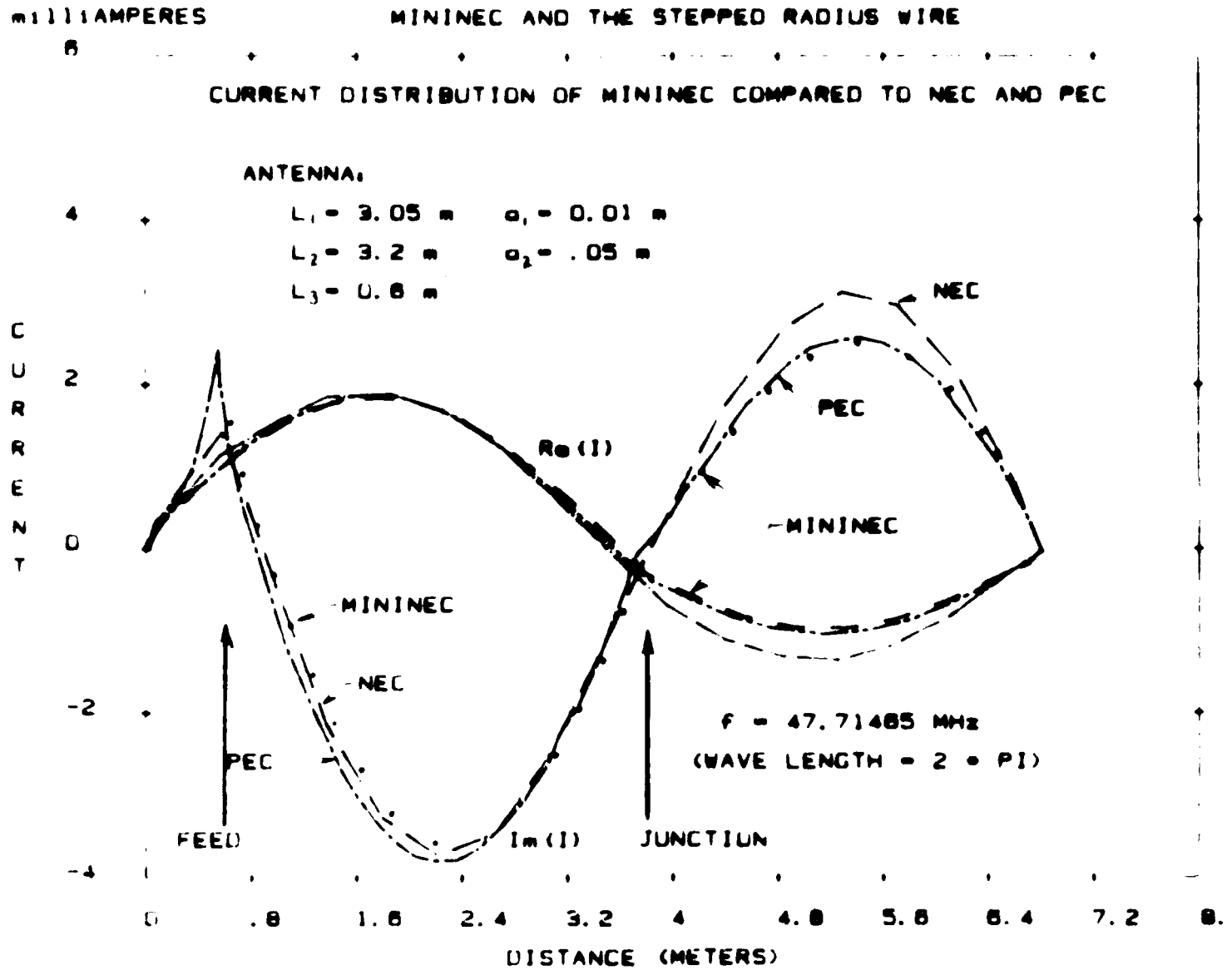

Figure 17: Currents for a stepped radius junction of $a_2/a_1 = 5$

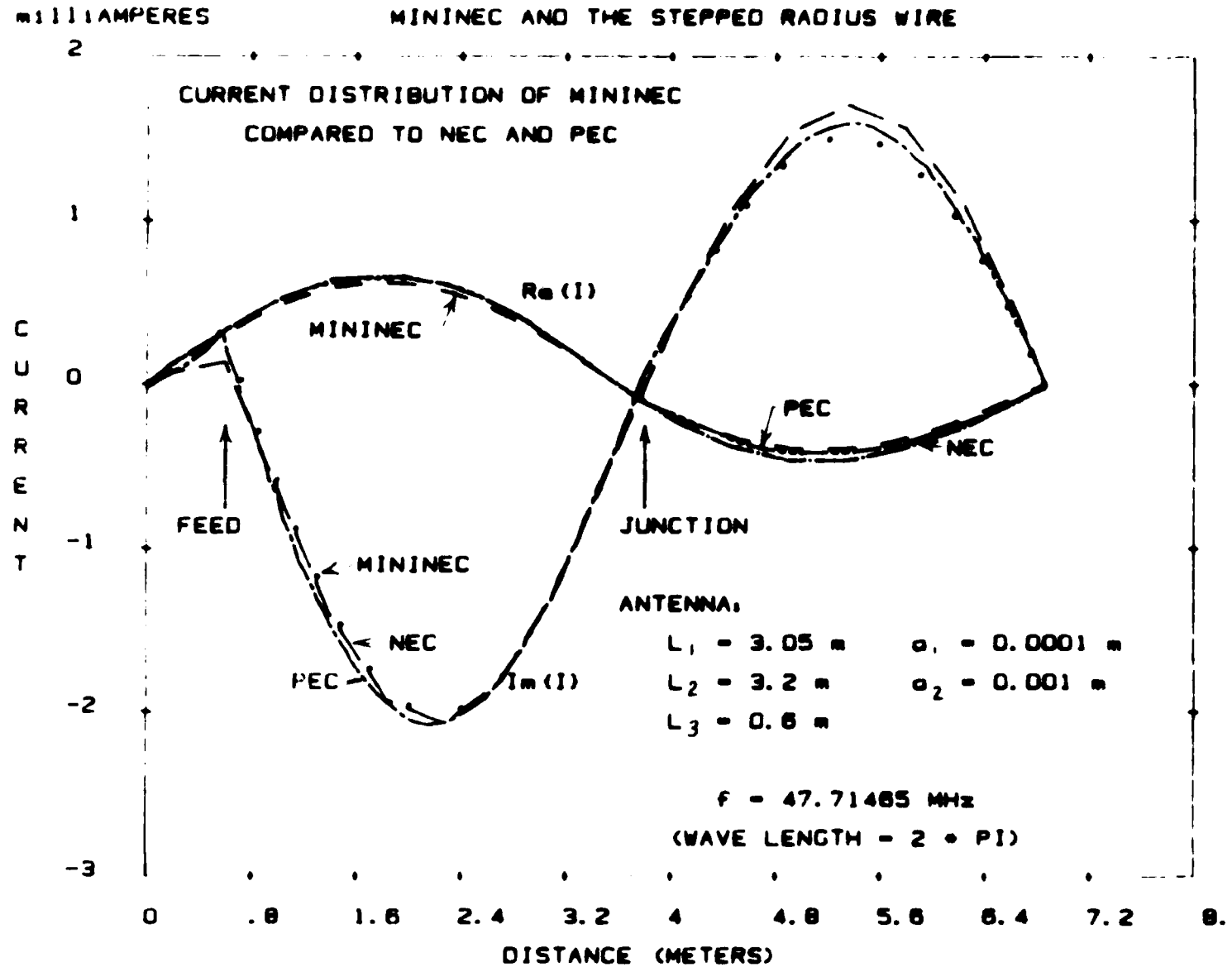

Figure 18: Currents for a stepped radius junction of $a_2/a_1 = 10$

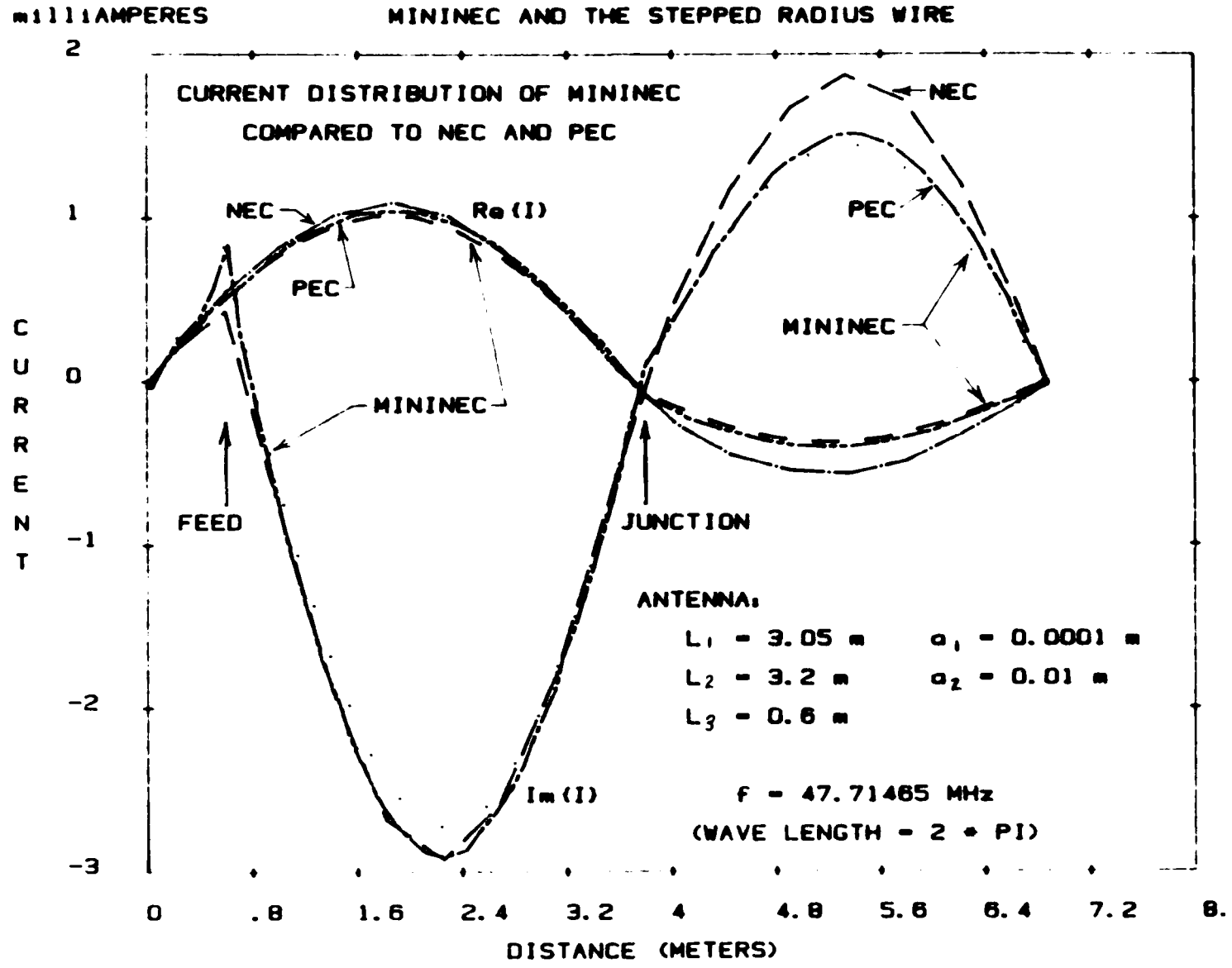

Figure 19: Currents for a stepped radius junction of $a_2/a_1 = 100$

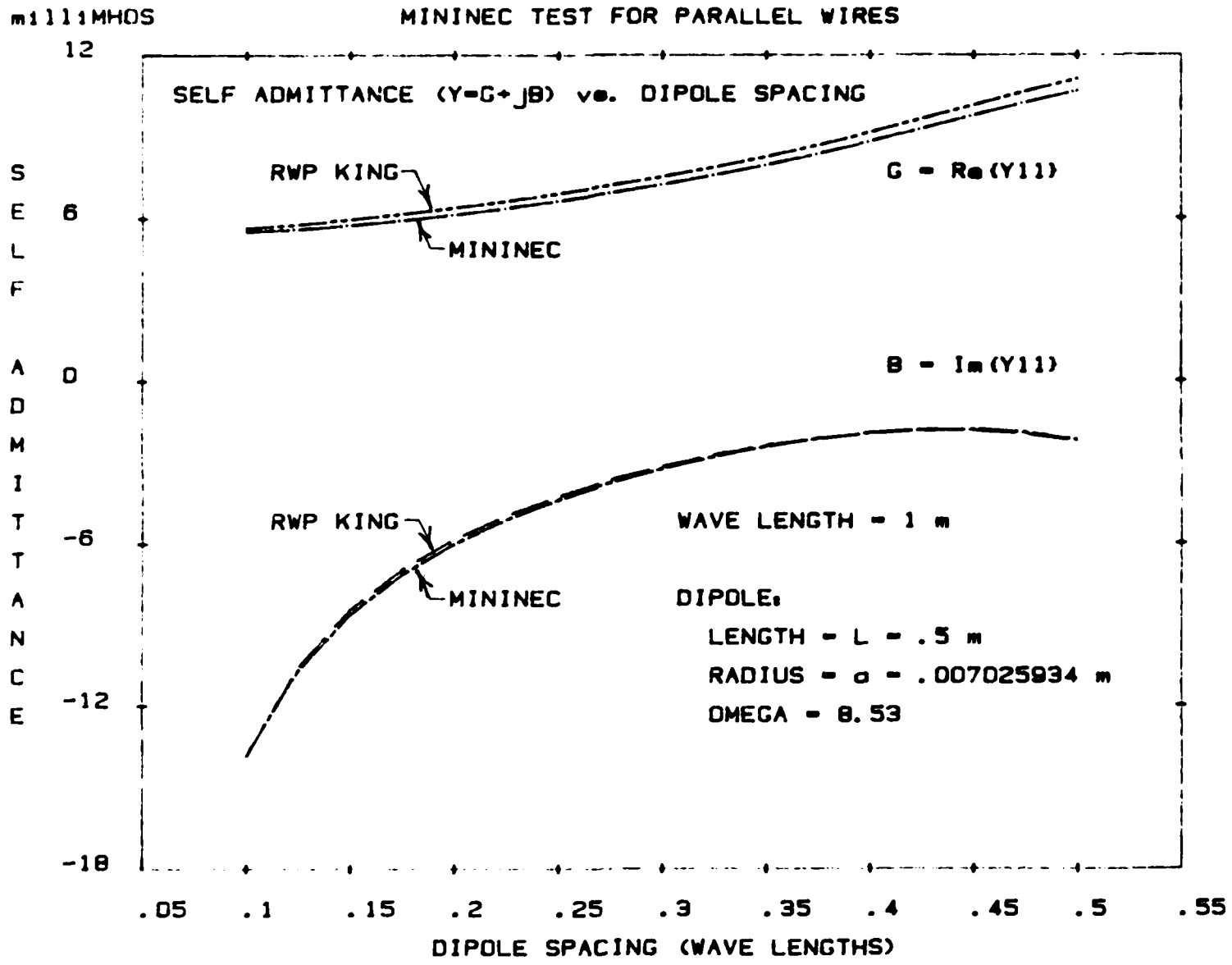

Figure 20: Self admittance computed by MININEC compared to the theory by R. W. P. King for two parallel dipoles

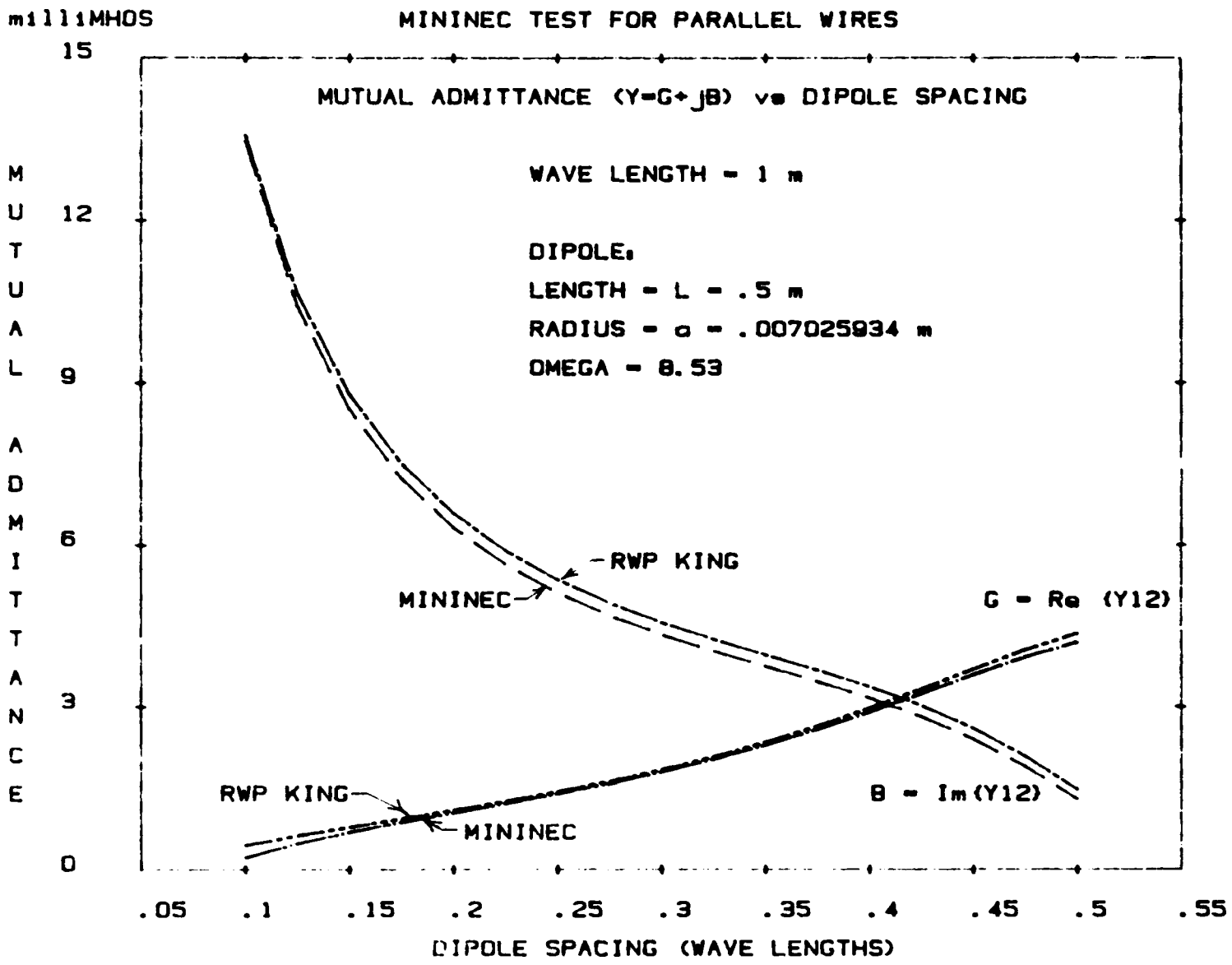

Figure 21: Mutual admittance computed by MININEC compared to the theory by R. W. P. King for two parallel dipoles

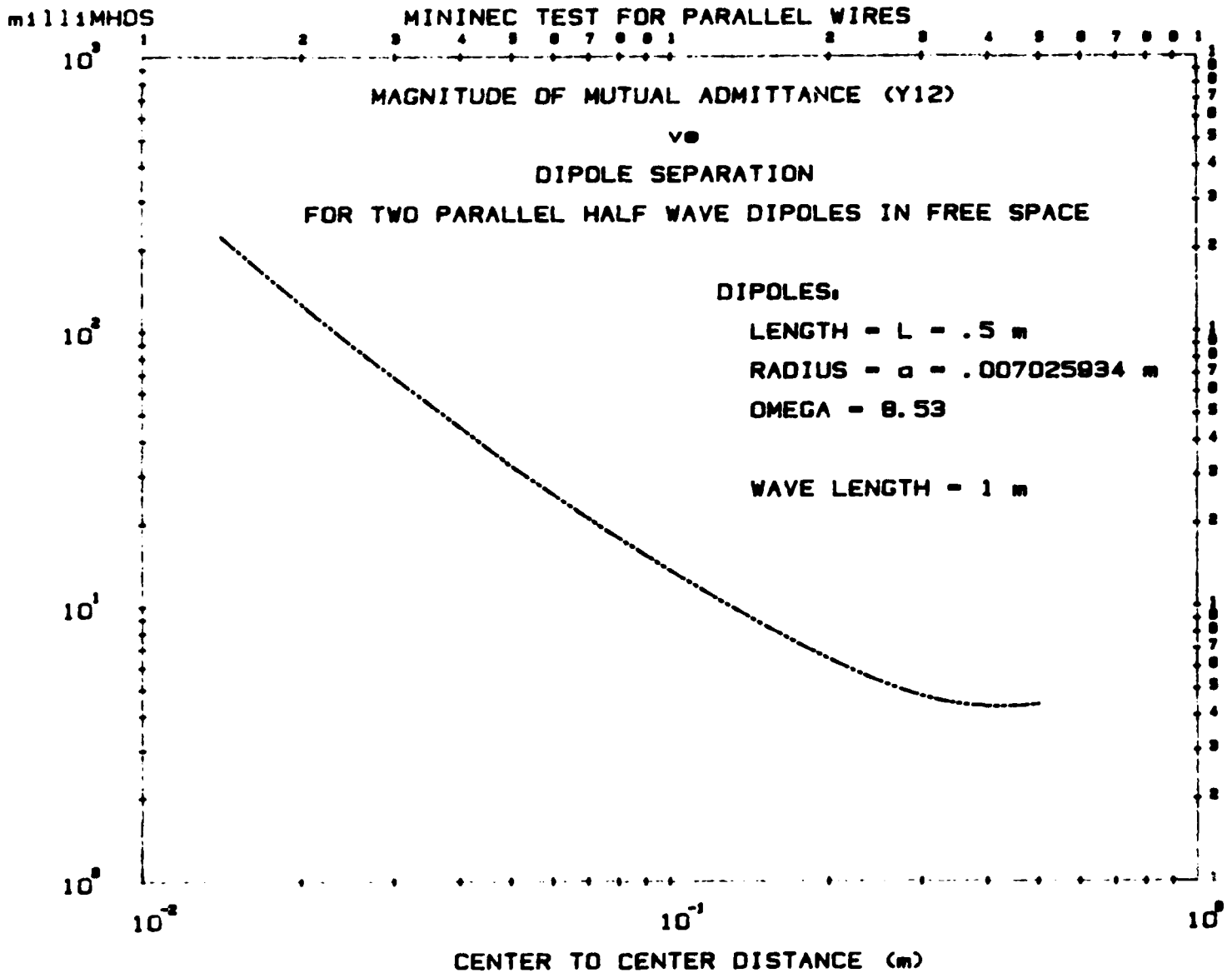

Figure 22: Magnitude of the mutual admittance between closely spaced parallel dipoles

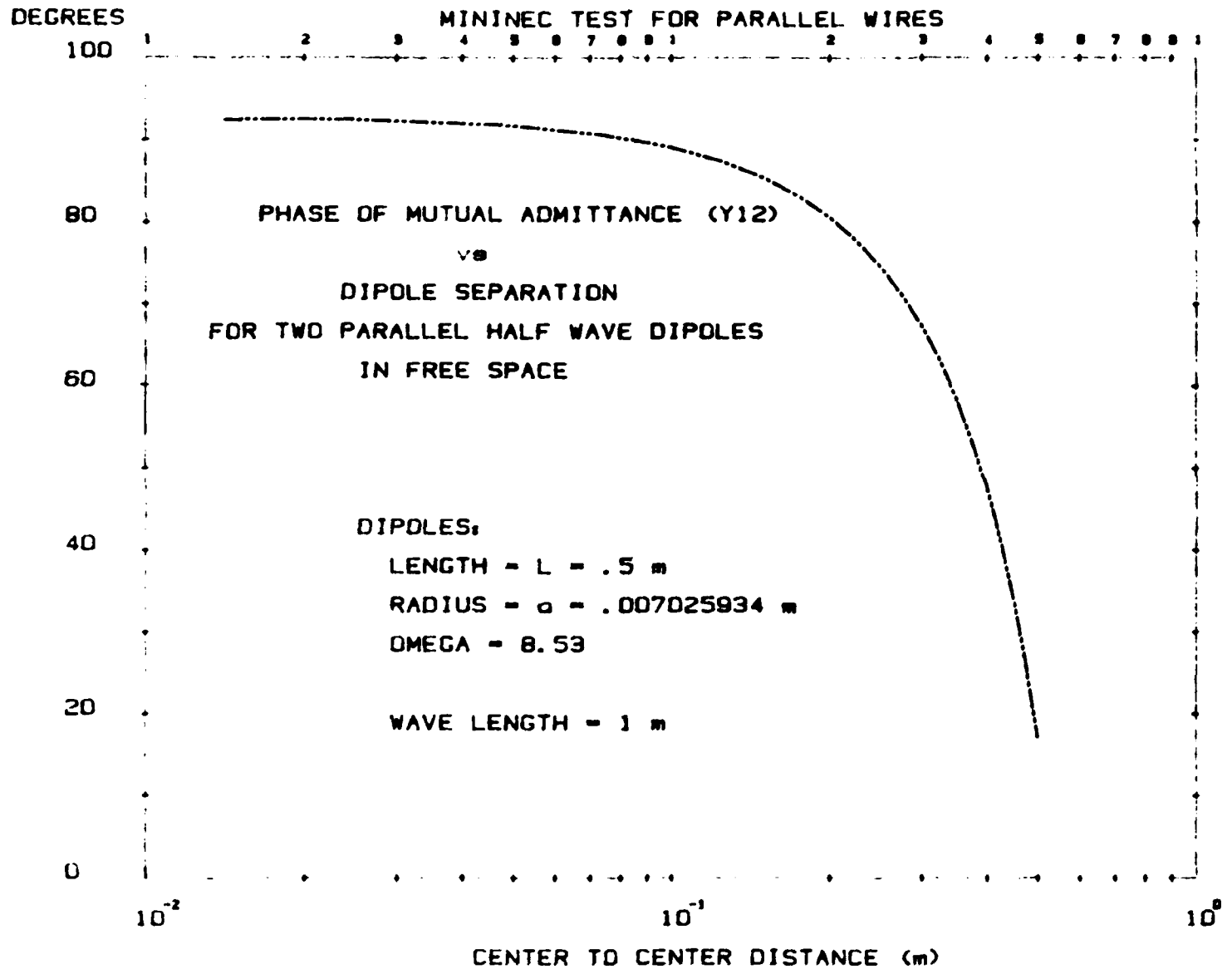

Figure 23: Phase of the mutual admittance between closely spaced parallel dipoles

less than .2 millimho and are no greater than .4 millimho in the worst case over the range shown for both self and mutual admittance.

Given the good agreement with theory down to a spacing of .1 wave length, how does MININEC fare for closer spacing? Figures 22 and 23 show the magnitude and phase of the mutual admittance for spacings down to the point of contact of the two parallel dipoles. Keep in mind the good agreement between MININEC and theory for spacings of .1 wave length and greater. (Reference [9] does not provide data for spacings less than .1, no comparison is shown.) It can be seen that the magnitude and phase continue smoothly as the spacing is reduced. Although these data are not conclusive, it can be implied that MININEC can model antenna configurations with wire spacings less than .1 wave length. Whenever a model has close spacing, however, it is advisable to examine the results very closely to ensure proper behavior.

3.2 Loop Antennas

A circular wire loop antenna may be modeled by connecting a number of wires to form a polygon approximation to the circular loop. A simple model has one segment per wire, with each wire forming one side of the polygon model, so that the number of sides and the number of segments are equal. For a given circumference, the number of wires, and hence the number of segments, can be increased until the solution stabilizes, indicating the number of sides required to model the circular loop. Figure 24 shows the results of this procedure for a loop, one wave length in circumference. The polygon model is circumscribed by a circle whose circumference is one wave length. The wire radius ($a = .00674$ meter) is chosen to correspond to the published data given by R.W.P. King [9]. At best, the real part of the MININEC admittance comes to within 3% of King's data and the imaginary part approaches to within 6%. For 22 segments (and 22 sides) the percent difference in real and imaginary is about equal, and less than 6% for each.

Figure 25 compares MININEC and R.W.P. King admittance data for a range of loop diameters from .1 to 2.0 wave lengths. The MININEC model is the 22 segment or 22 sided polygon loop. The agreement is excellent. The difference between King and MININEC is no greater than .4 millimho over the entire range. From .1 to .8 wave length, the MININEC data and King data are virtually identical.

Figures 26 and 27 show MININEC data for small loops with a circumference from 10^{-3} to just above .4 wave length. Keep in mind the excellent

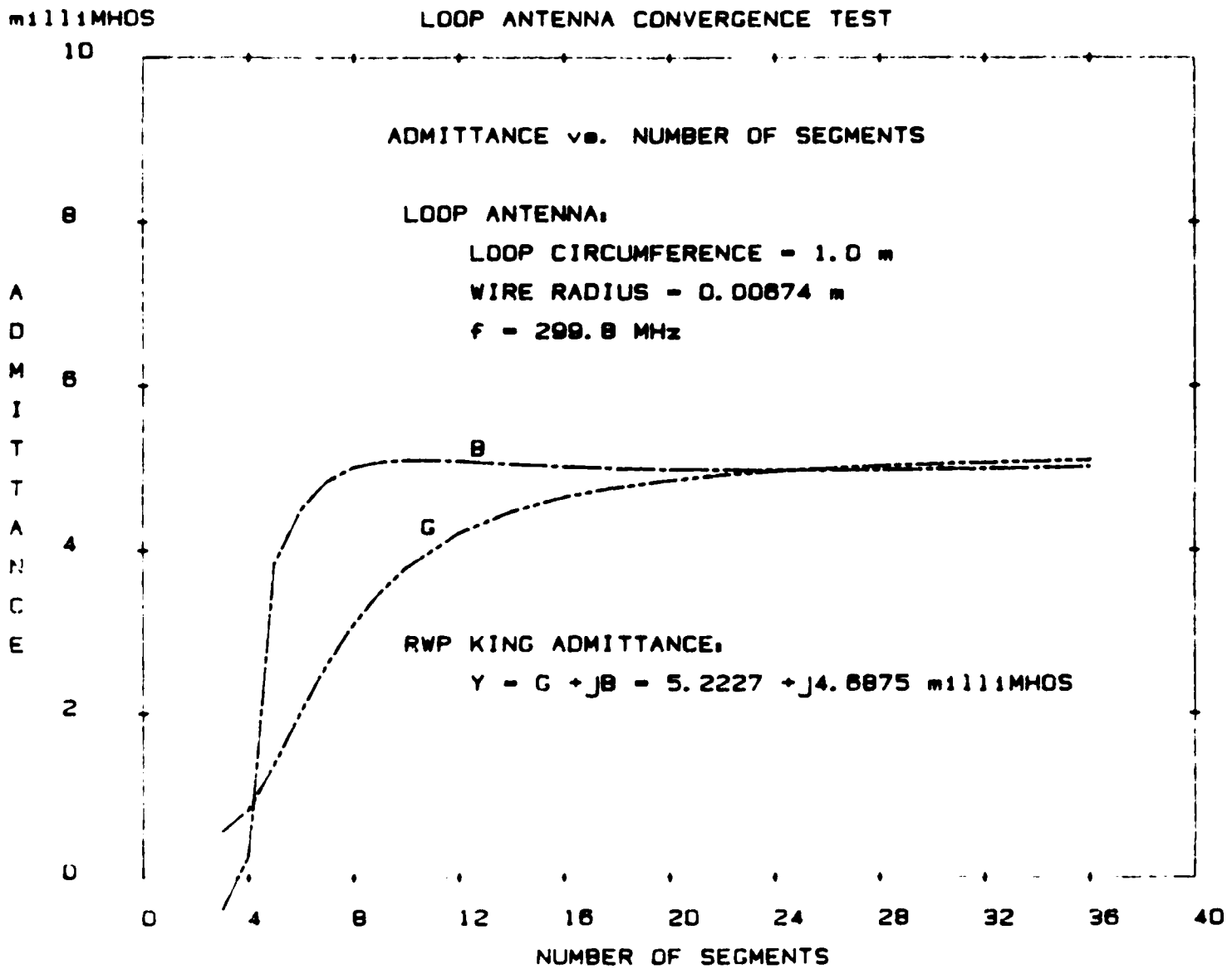

Figure 24: Admittance of a polygon model antenna. The polygon is circumscribed by a circle of one wavelength circumference.

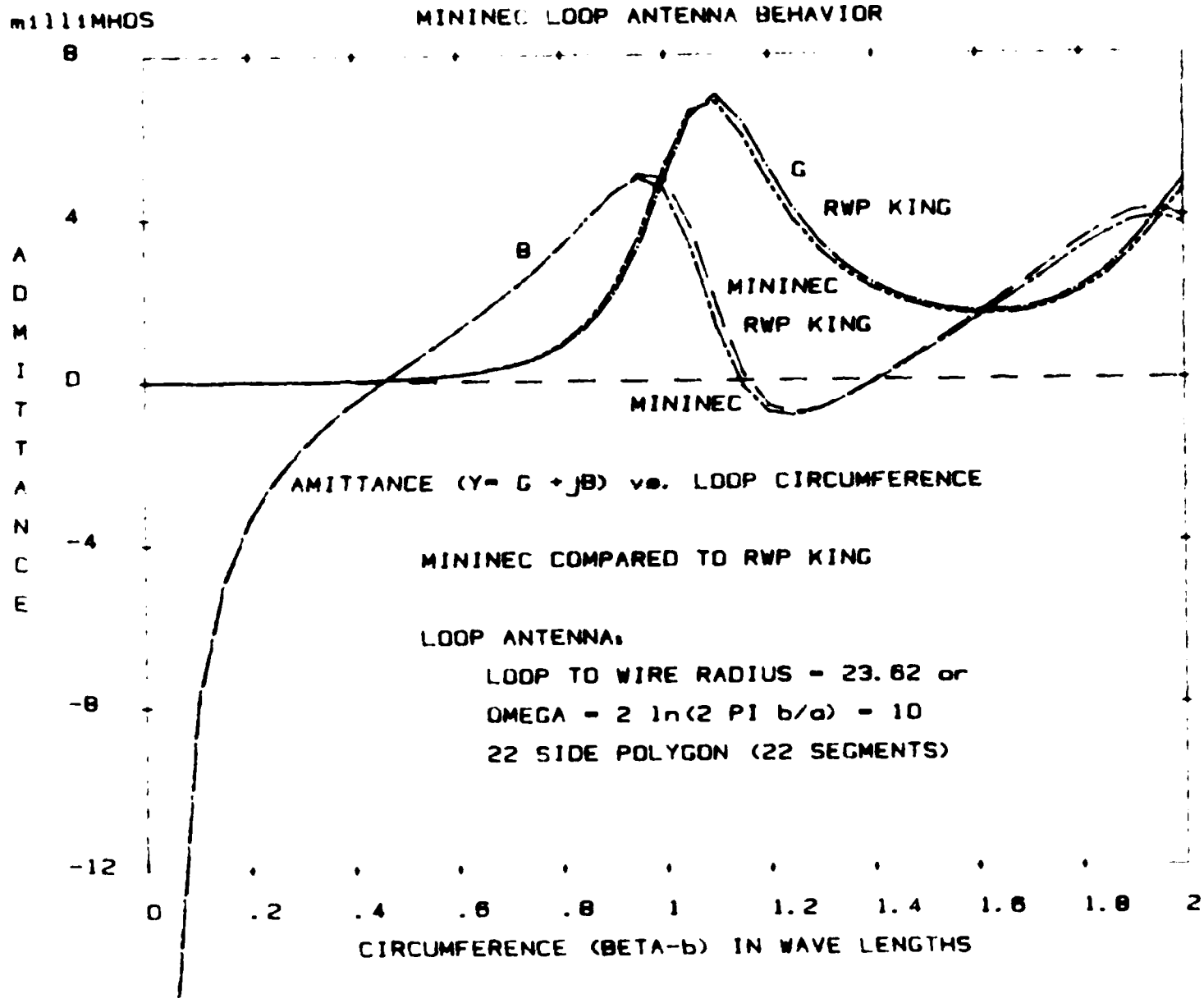

Figure 25: A comparison of MININEC data to R. W. P. King over a range of loop sizes

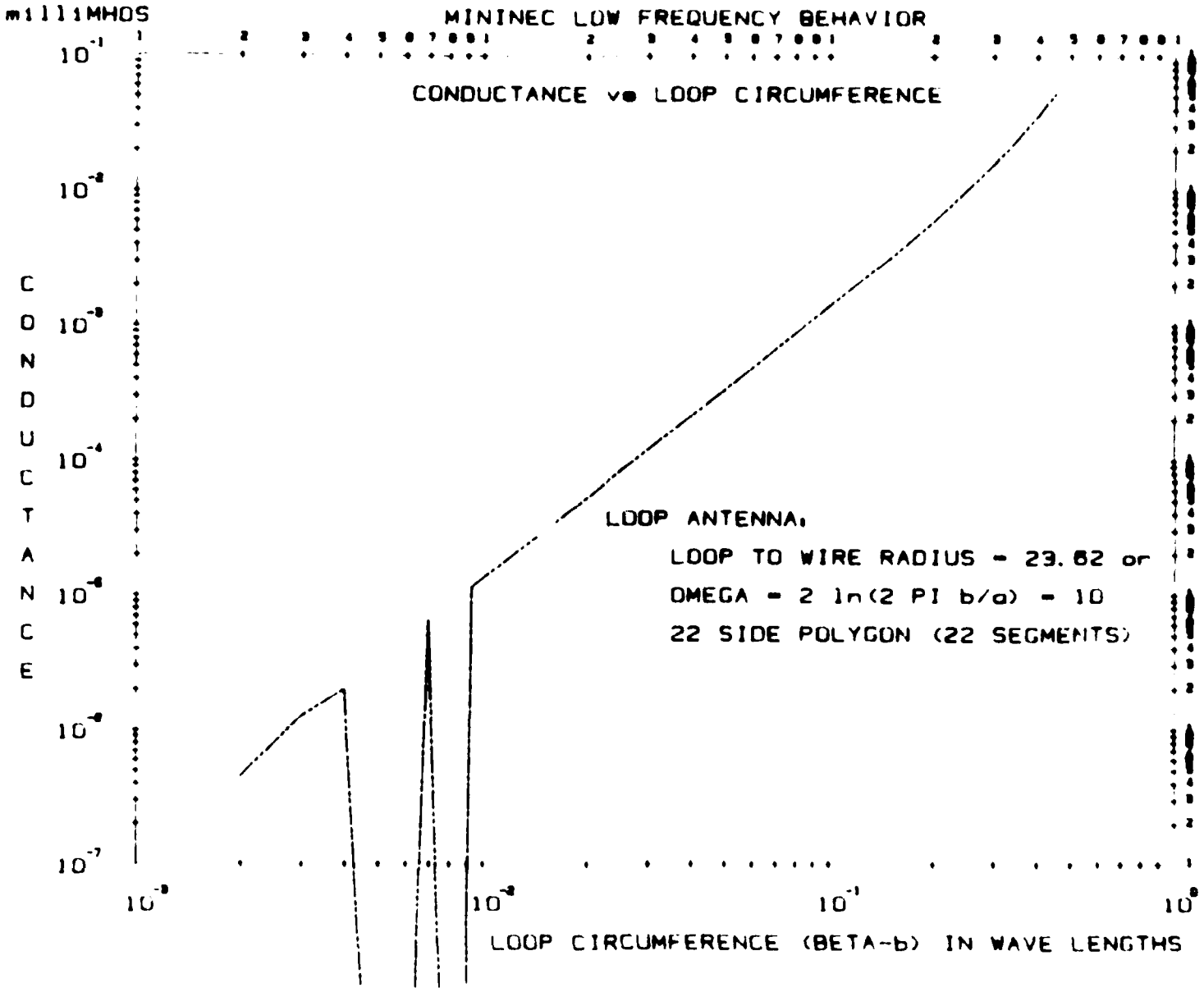

Figure 26: Admittance of small loops predicted by MININEC (Part 1)

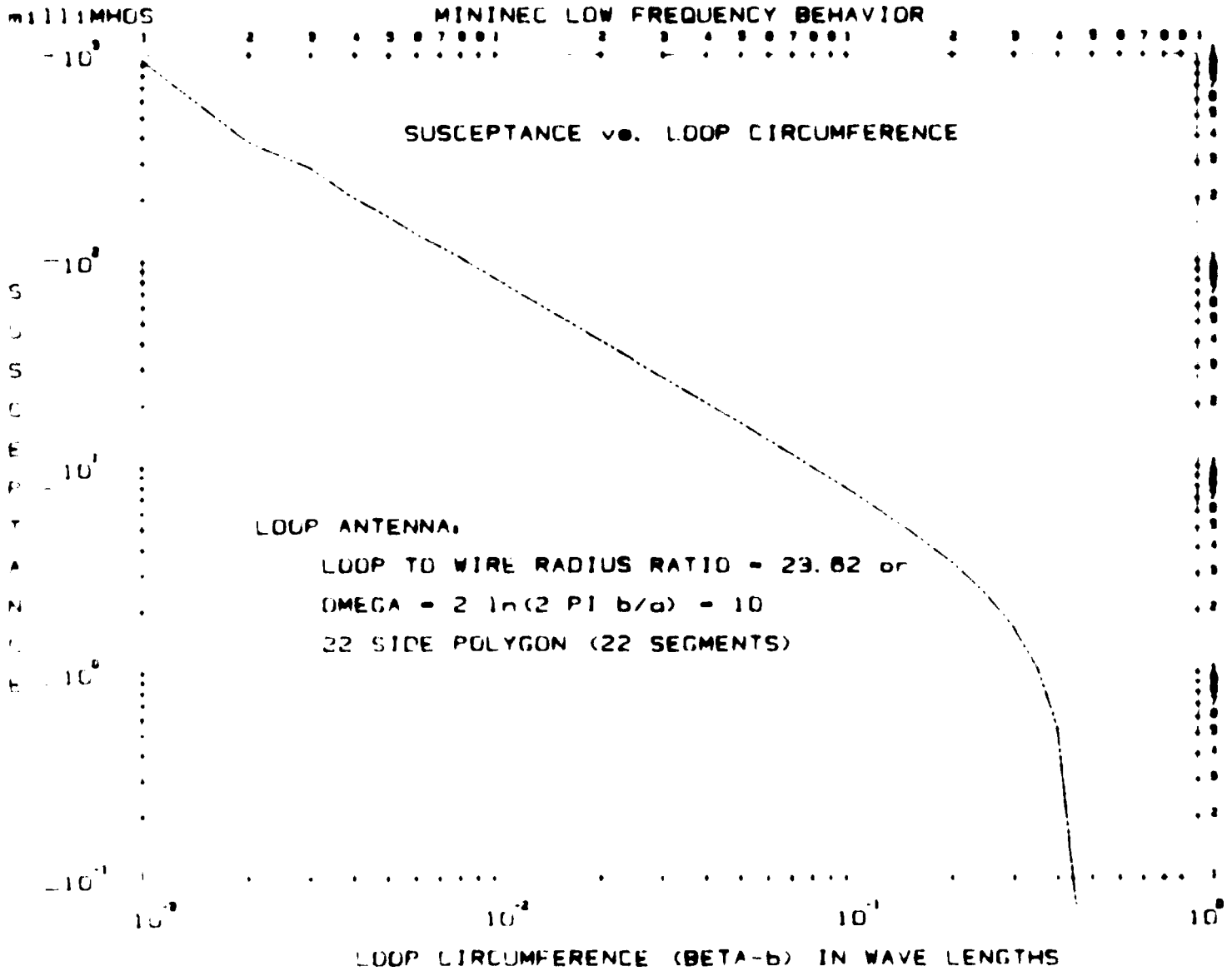

Figure 27: Admittance of small loops predicted by MININEC (Part 2)

agreement with King's data for loops of .1 and greater (Figure 25). The real and imaginary parts of the adminttance in Figures 26 and 27, respectively, are well behaved for loops greater than 10^{-2} wave lengths. Below 10^{-2}, the real part of the admittance becomes unstable due to numerical problems encountered at the limits of single precision. Note that at 22 segments, the segment size at a circumference of 10^{-3}, is very nearly the same short segment length limit displayed by the dipole test in Figure 14. The data in Figures 25, 26, and 27 suggest a small loop limit for MININEC (on a 16-bit, single precision microcomputer) of 10^{-2} wave lengths in circumference. This corresponds to a loop 18 inches in diameter at 2 MHz (about the size of a basketball goal).

3.3 Monopoles and Antennas Above Ground

Simply stated, an antenna above a perfectly conducting ground plane is equivalent to the original antenna and its mirror image in free space. Hence, all the modeling results and guidelines presented so far are directly applicable to monopoles. Specifically, the convergence properties illustrated in Figures 6 through 11 can be used for the initial selection of the segmentation required for a monopole. However, this should not preclude convergence testing whenever possible.

Figure 28 illustrates the geometry of a TEE-antenna. The antenna is driven or fed at its base from a coaxial termination at the ground plane. The dimensions for two TEE-antenna designs ($K_0h = .2$ and $K_0h = .5$) are also given. A convergence test was performed for each antenna using the segmentation scheme in the table. The results of these tests are given in Figures 29 and 30 for $K_0h = .2$ and $K_0h = .5$, respectively. A comparison of the "best" results to the measurements of Prasad and King [18] for MININEC and several other codes is given in Figure 31.

Figure 31 compares five computer programs including MININEC for the two TEE-antennas. In each case, the programs were tested for convergence and the best answer with respect to Prasad's measurements is given. NEC is the code previously described [4]. TGP (Triangular-Galerkin Procedure) is the code written by Chao and Straight [11] using triangular expansion and testing functions in a Galerkin procedure (i.e., triangles for both testing and expansion functions). PSRT (Piece-wise Sinusoidal Reaction Technique) is a sinusoidal Galerkin code written by Richmond [19]. TWTD (Thin Wire Time Domain) is a time domain method of moments code written by Van

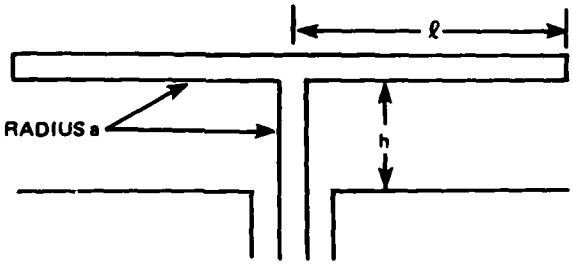

K_0h	h/λ	ℓ/λ
0.2	0.03183099	0.2181690
0.5	0.07957747	0.1704225

K_0h	Vertical Wire Segments	Horizontal Wire Segments	Total Segments
0.2	1	7	15
	2	14	30
	3	21	45
	4	28	60
0.5	1	2	5
	2	4	10
	3	6	15
	4	8	20
	5	10	25
	6	12	30
	14	14	42

Figure 28: [...] TEE antenna. Dimensions for two designs are given [...] segmentation scheme for convergence testing

Blaricum and Miller [20]. TWTD uses subsection collocation (quadratic interpolation with point matching) to solve for the time-dependent induced currents and time-dependent radiated fields. Admittance data are obtained from a discrete Fourier transform of the source current. All codes except MININEC are in FORTRAN and require mainframe (large) computers. The data show that MININEC can provide equally accurate answers.

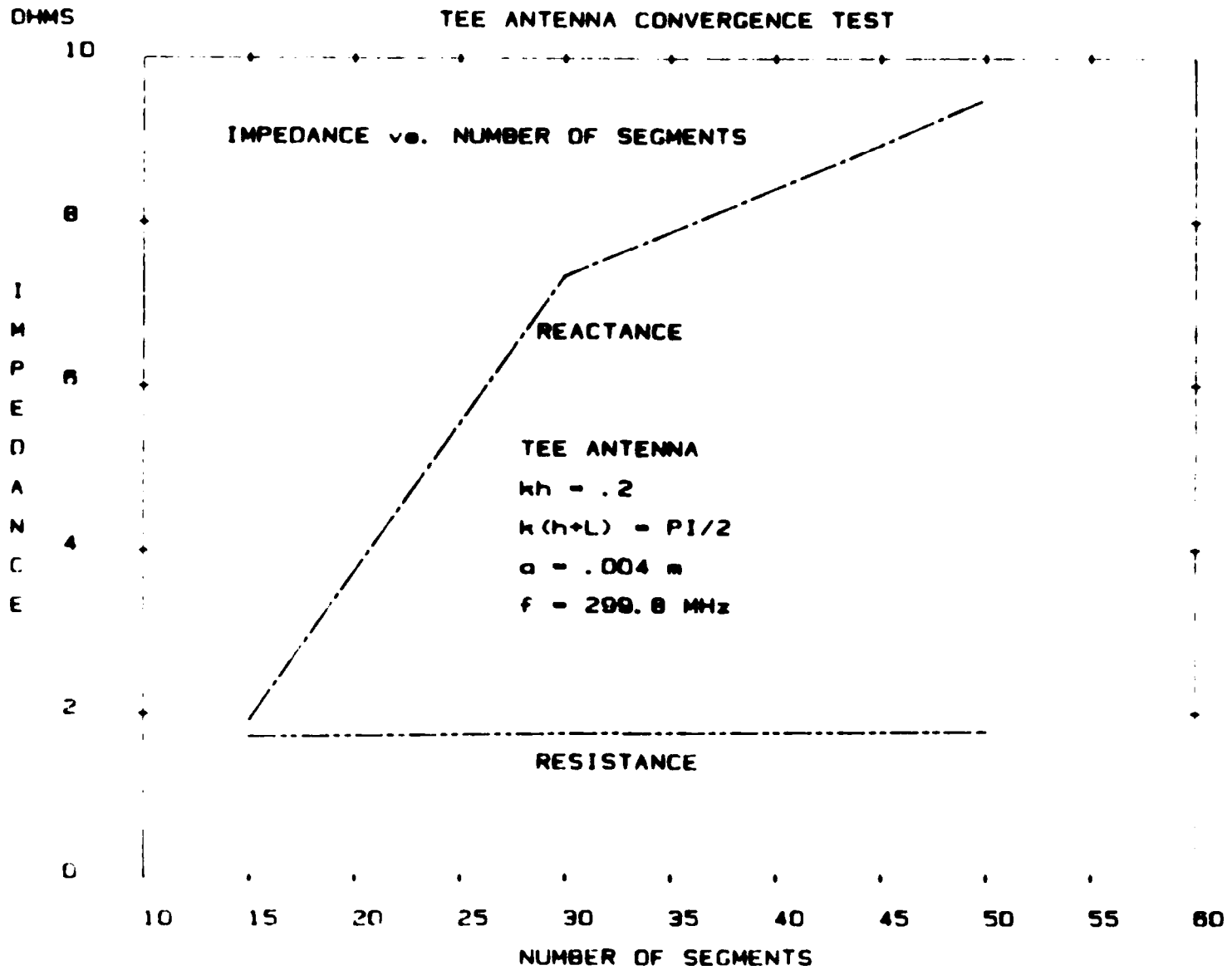

Figure 29: Convergence test for a TEE antenna with $K_0 h = .2$

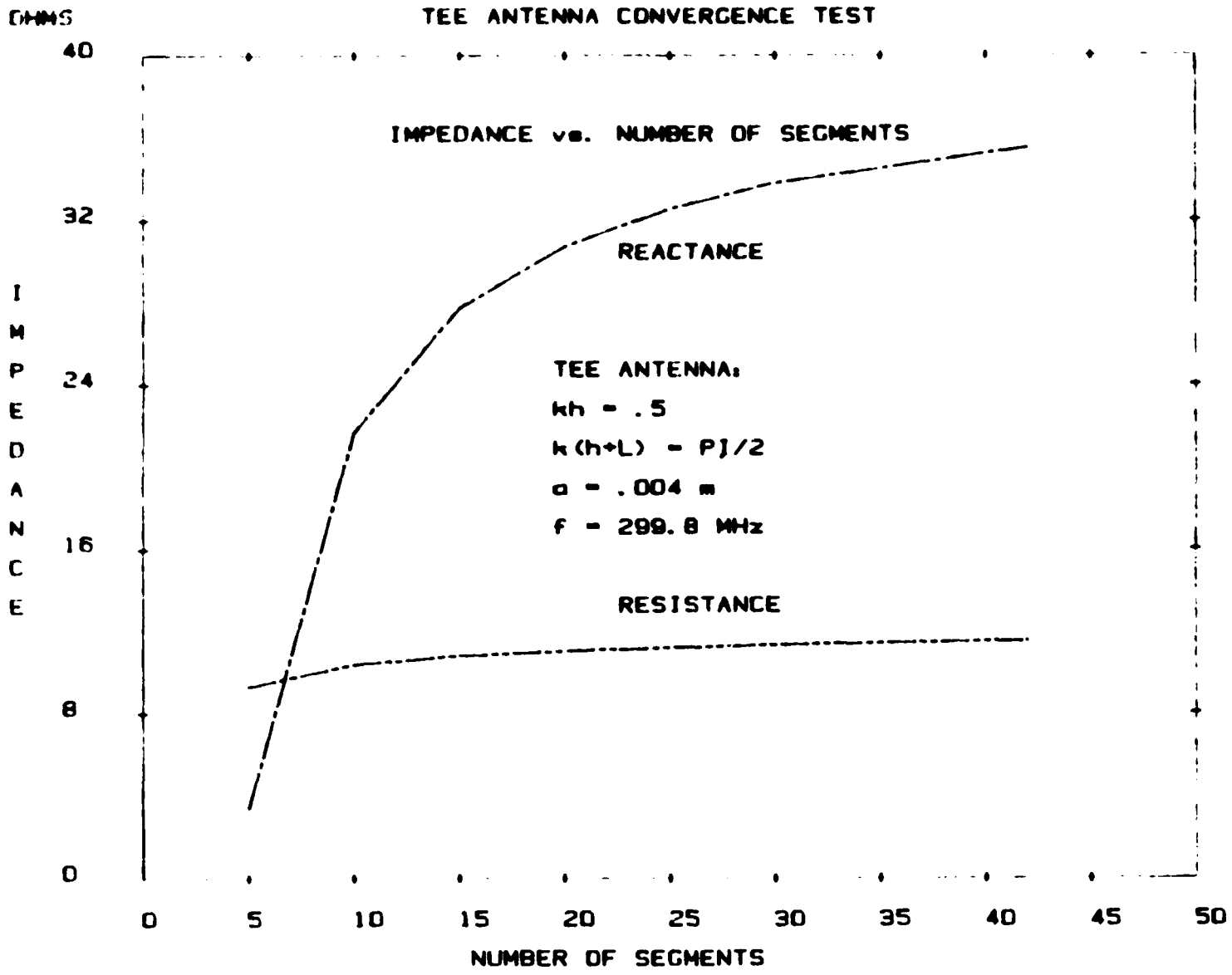

Figure 30: Convergence test for a TEE antenna with $K_0 h = .5$

Radius of Wire $= 0.004/\lambda$
$k_0 = (h + l) = \pi/2$

	$\frac{2\pi h}{\lambda} = 0.2$	$\frac{2\pi h}{\lambda} = 0.5$
MEASURED	$2.6 + \mathrm{j}\,9.0$	$11 + \mathrm{j}\,36$
MININEC	$1.8 + \mathrm{j}\,9.0$	$11.6 + \mathrm{j}\,35.5$
NEC	$1.7 + \mathrm{j}\,10.3$	$11 + \mathrm{j}\,36$
TGP	$1.78 + \mathrm{j}\,9.13$	$11.1 + \mathrm{j}\,34.3$
PSRT	$1.7 + \mathrm{j}\,3.8$	$11.4 + \mathrm{j}\,31.9$
TWTD		$11 + \mathrm{j}\,34$

Figure 31: Comparison of TEE-antenna impedance computations with the measured values of Parsad.

3.4 Near Fields

MININEC can calculate the near fields for antennas in free space and over perfectly conducting ground. Only antennas over perfectly conducting ground are considered in this section.

Figure 32 shows a comparison of MININEC and NEC and to measurements. The data are the near electric fields of a 10.67-meter monopole over a good conducting ground screen at 2 MHz. The fields are for 1 KW radiated power. The measurements were made using an E-field sensor (EFS-1) manufactured by Instruments for Industry [21]. The NEC data are from a single precision version (NEC-1) running on a VAX 11780 computer. The agreement between both codes and the measurements is acceptable over the range shown. The accuracy of the measurements is 5 to 10%, with the greatest error occurring for distances of 10 meters and greater, due to the effects of nearby structures. The differences between NEC and MININEC are due in part because the NEC data is from a single precision version.

Figures 33 and 34 are a comparison of MININEC and NEC near field data for a quarter wave monopole over perfect ground. The NEC data are from a double precision version (NEC-3) running on a VAX 11780 computer. Figure 33 gives the vertical and radial components of the electric field and Figure 34 gives the phi-component of the magnetic field. The MININEC data has been scaled to the power level of the NEC data. The NEC and MININEC

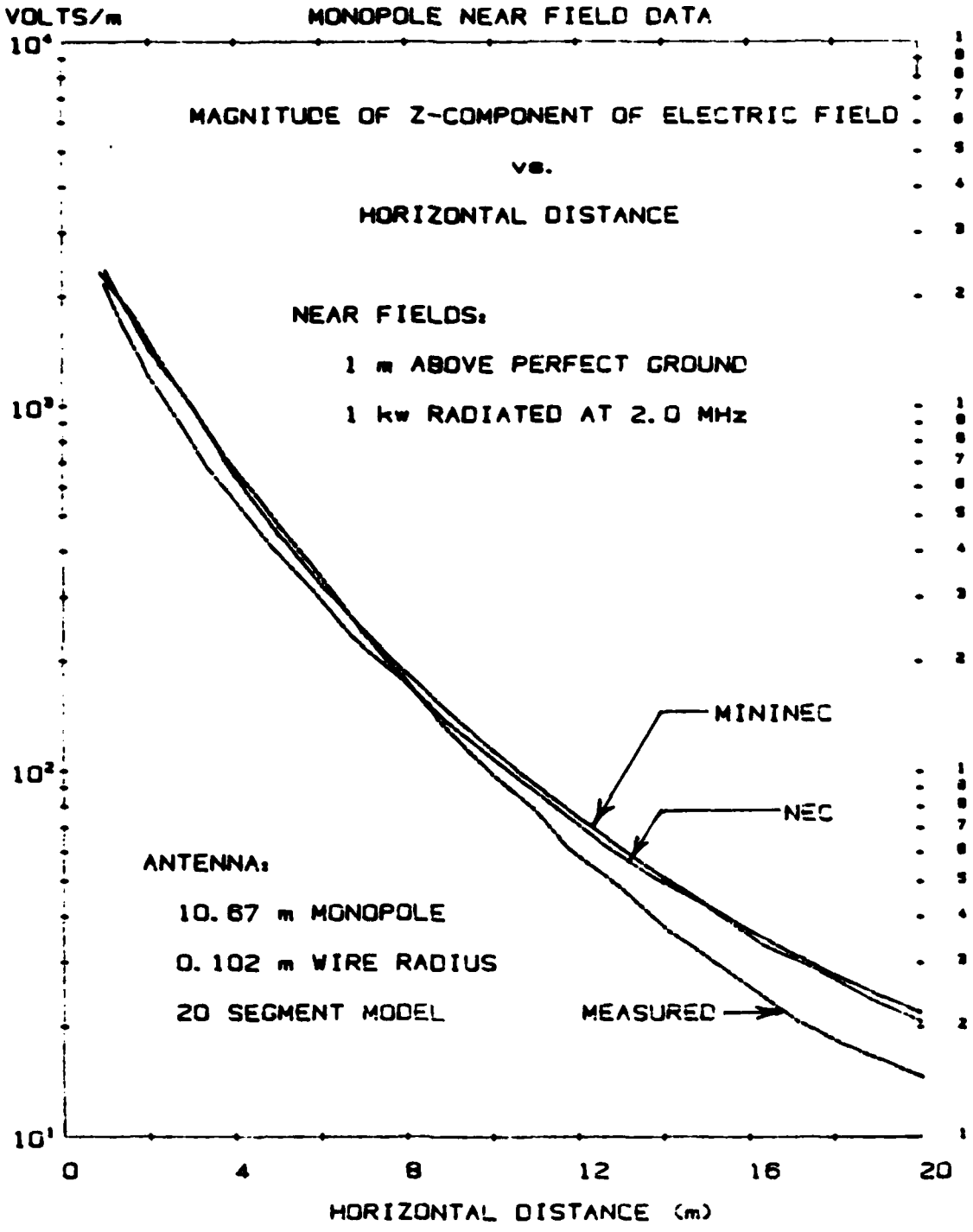

Figure 32: Comparison of near field data from MININEC and NEC to measurements

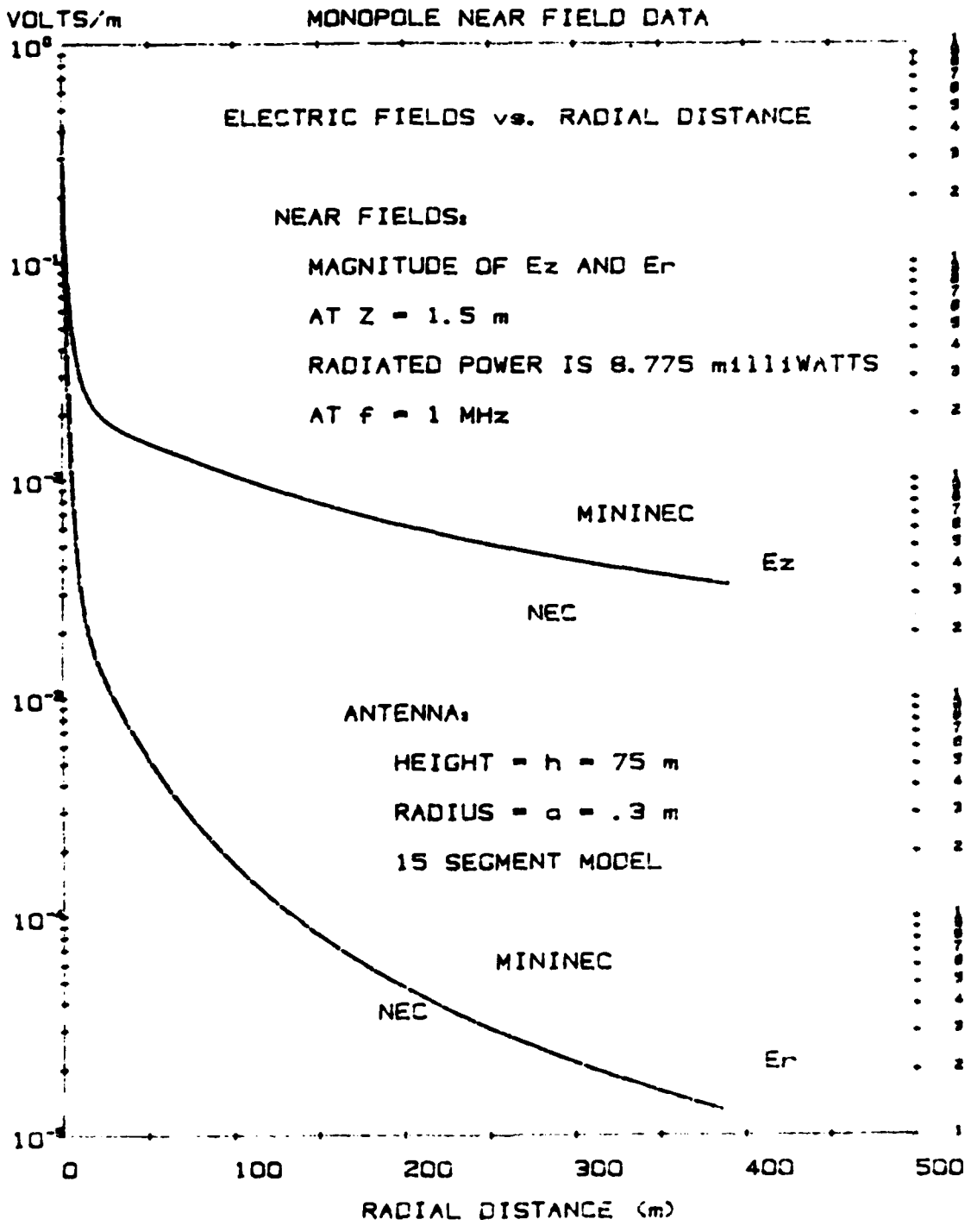

Figure 33: Near electric fields of a quarterwave monopole computed by MININEC and NEC

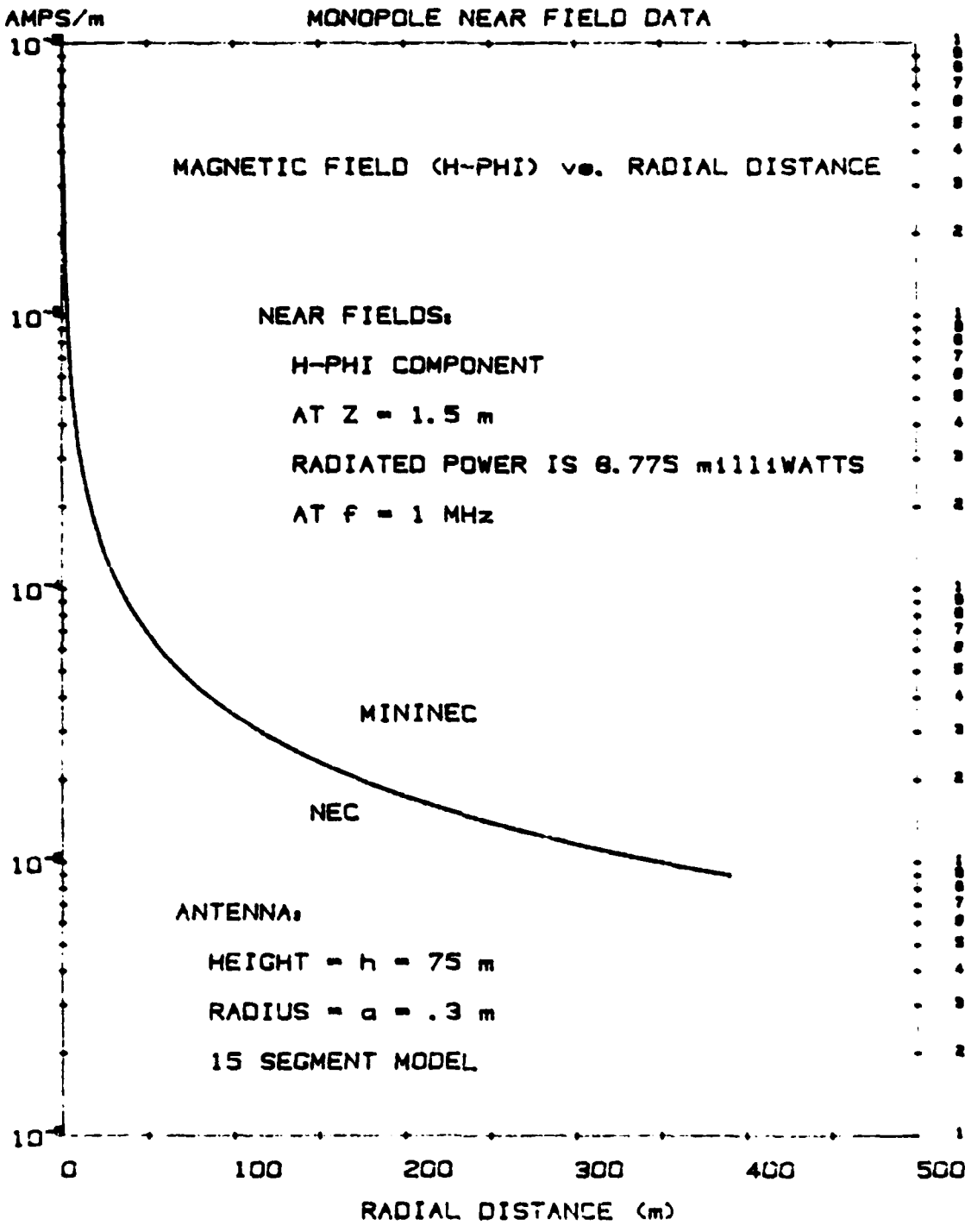

Figure 34: Near magnetic fields of a quarterwave monopole computed by MININEC and NEC

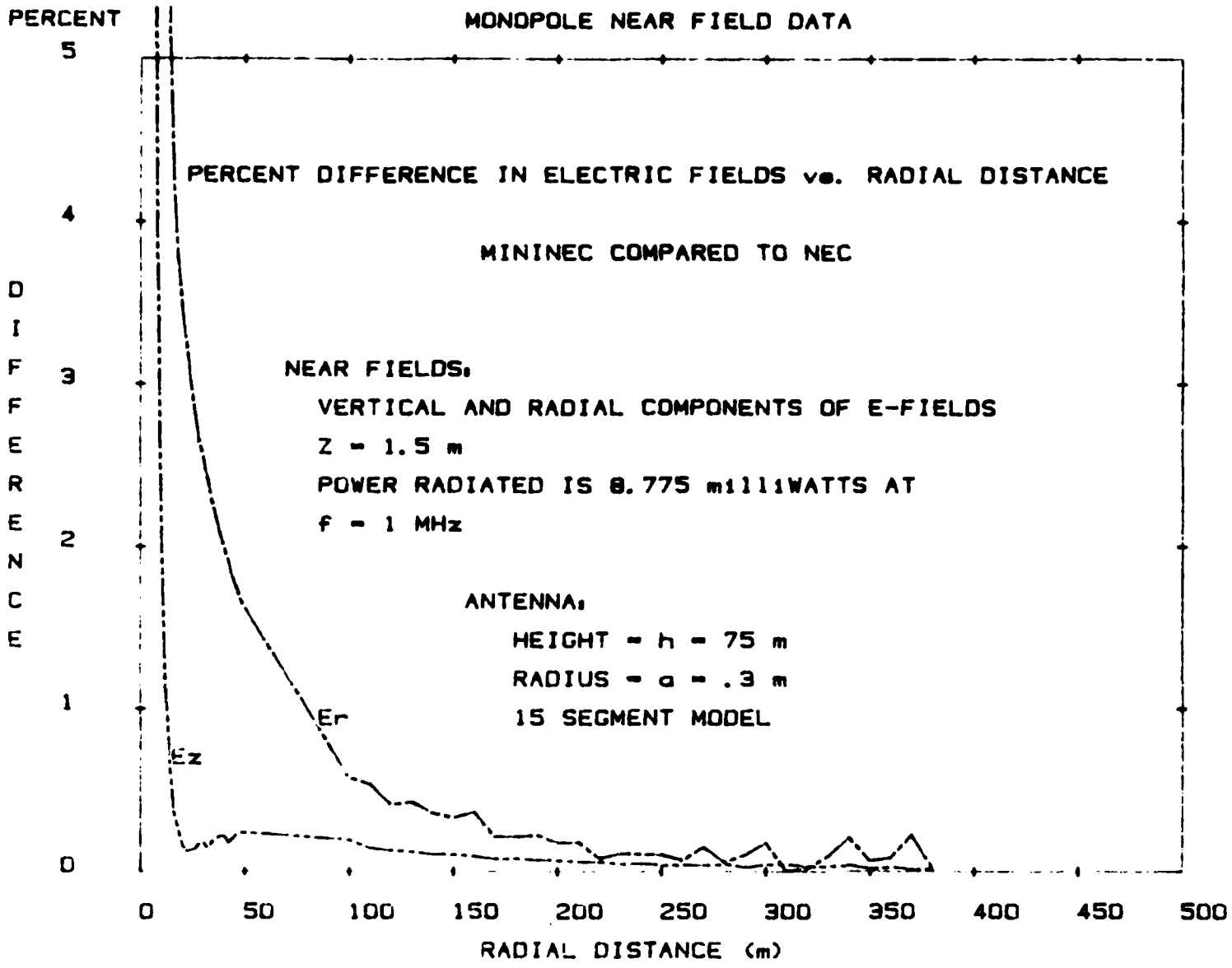

Figure 35: Percent difference between MININEC and NEC for the near field data in Figures 33 and 34 (Part 1)

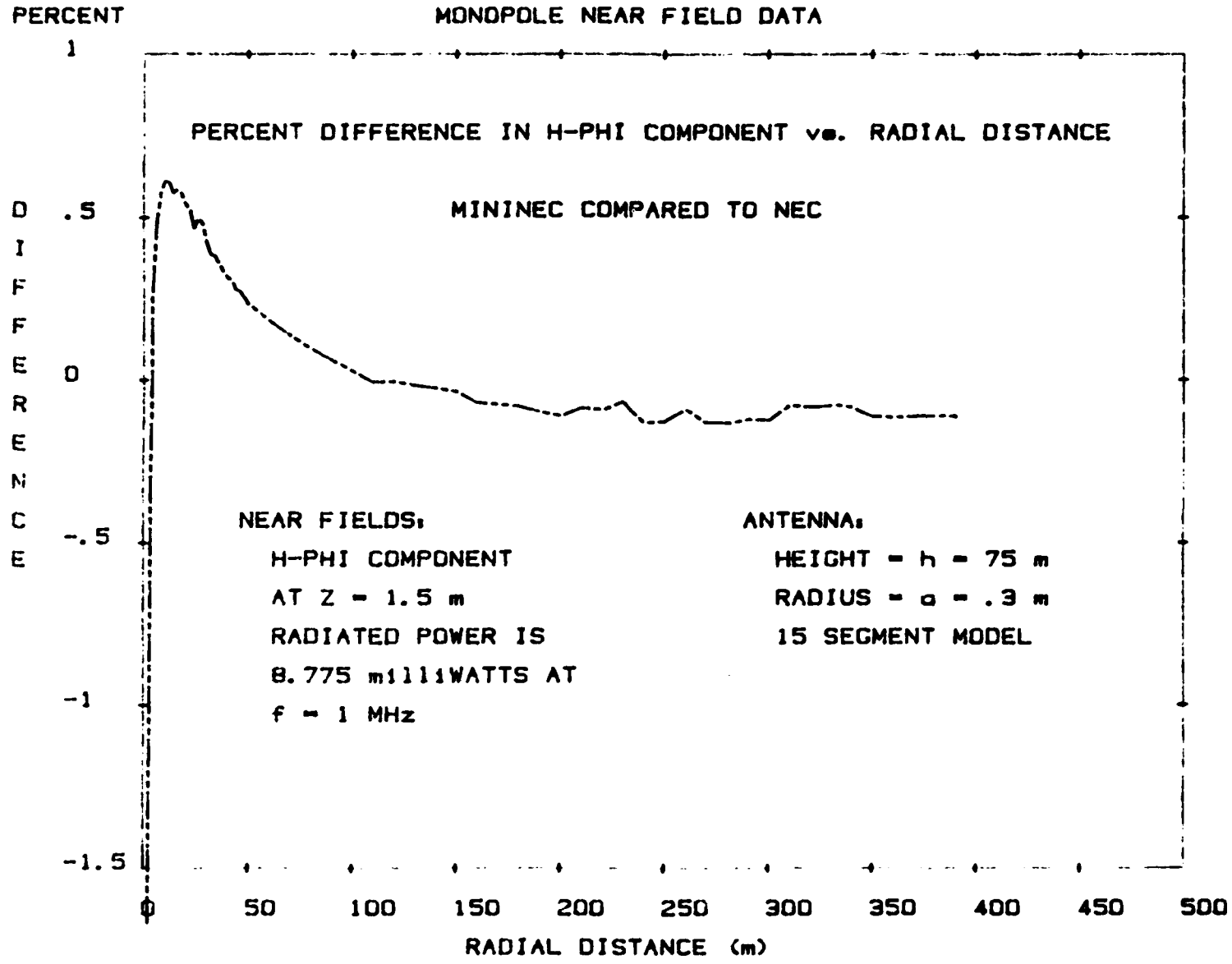

Figure 36: Percent difference between MININEC and NEC for the near field data in Figures 33 and 34 (Part 2)

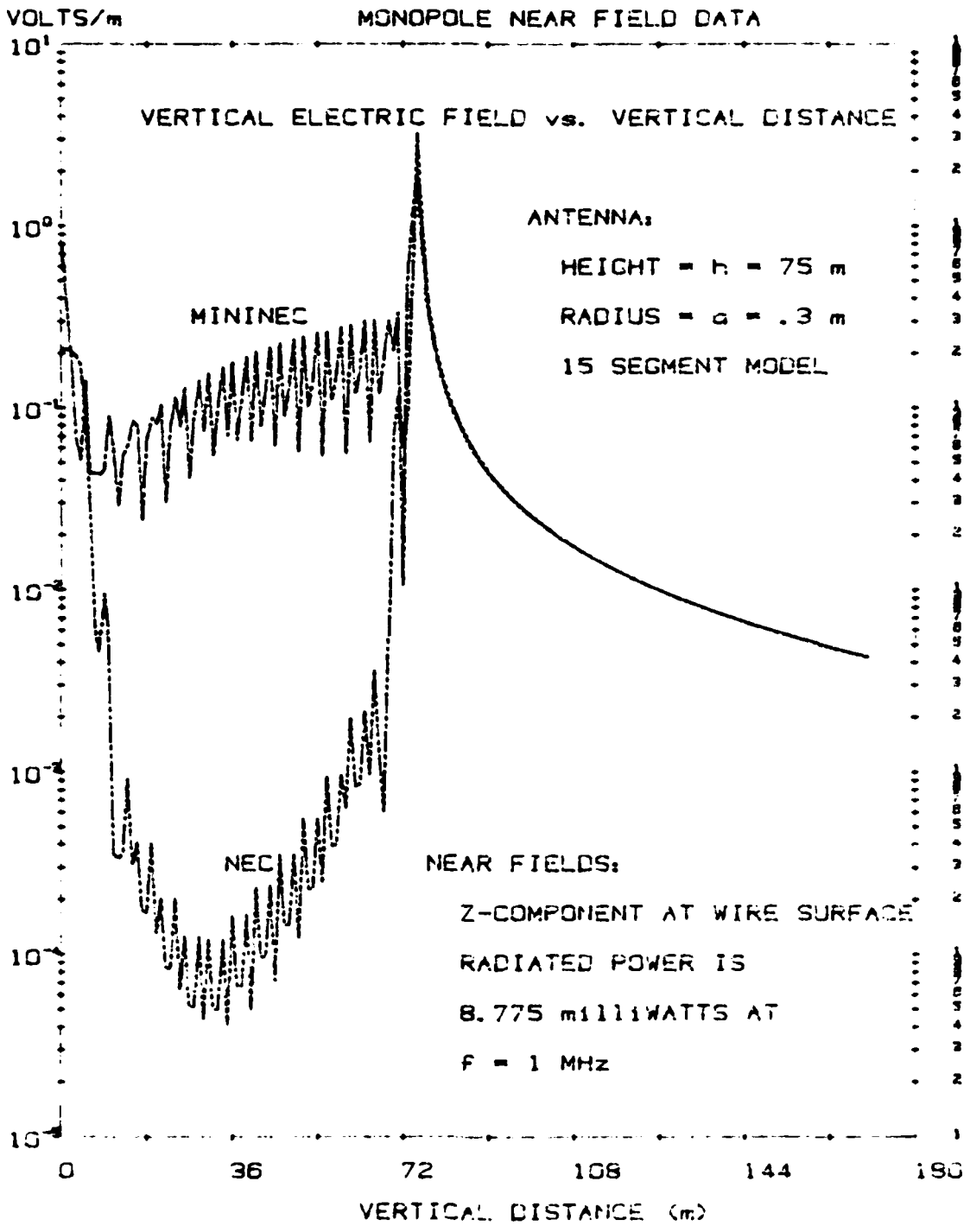

Figure 37: Vertical component of the electric field at one radius distance for a quarterwave monopole

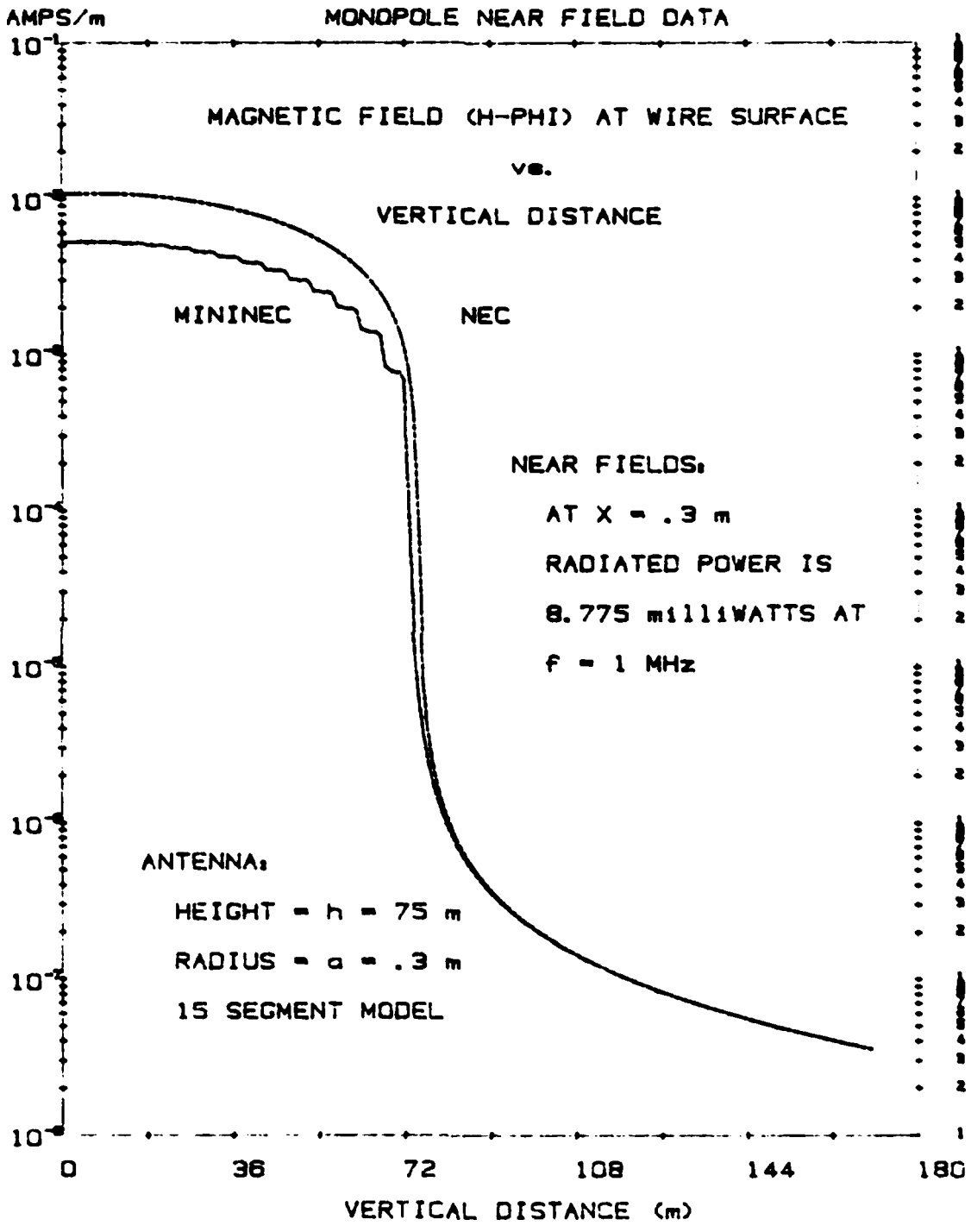

Figure 38: Horizontal component of the electric field at one radius distance for a quarterwave monopole

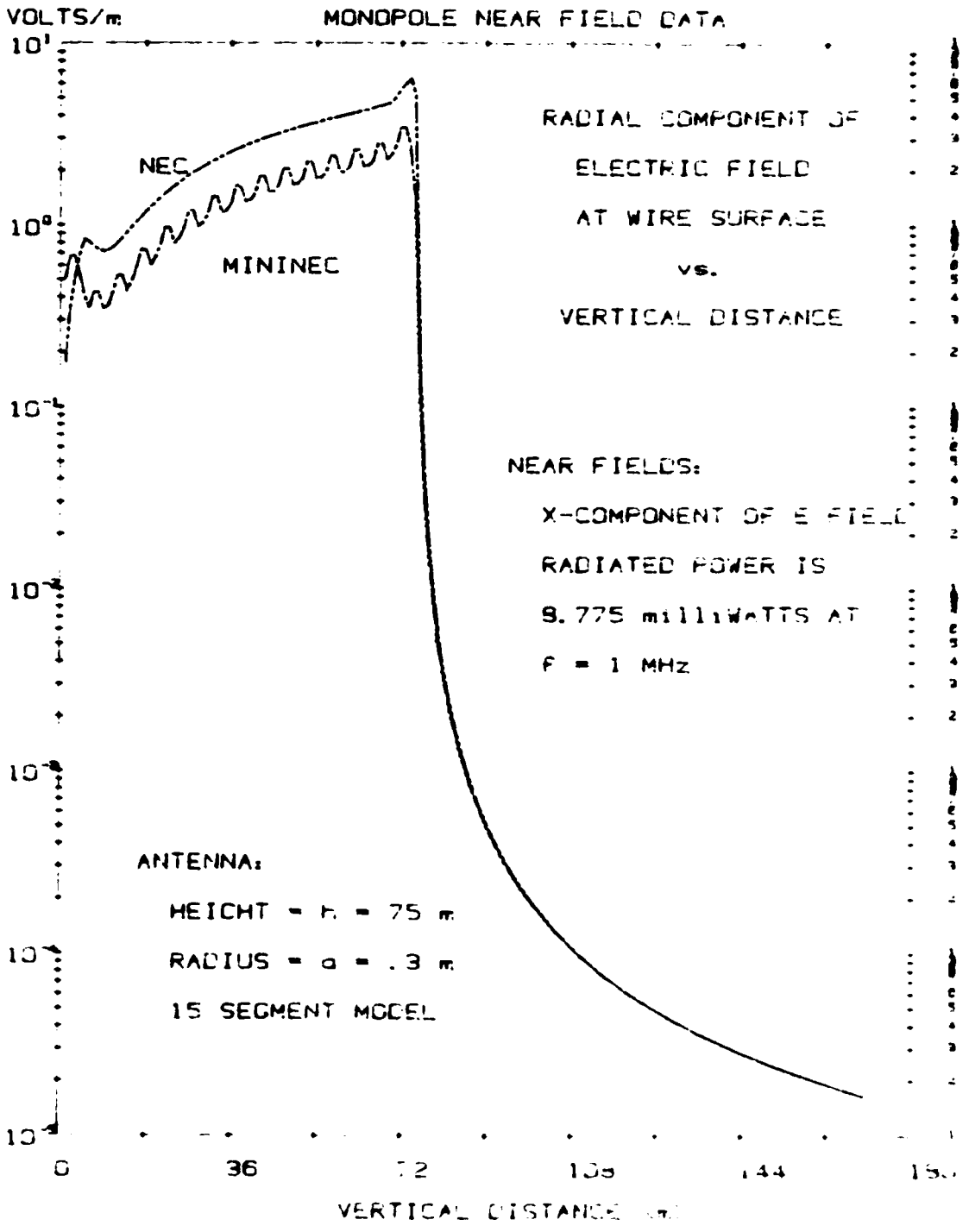

Figure 39: Phi-component of the magnetic field at one radius distance for a quarterwave monopole

Radiation Resistance and Gain for Dipole Antennas

MININEC Data	Schelkunoff Data	Jasik Data
Wire Stub:	Current Element:	Very Short Dipole:
N = 2 segments	constant current	
l = length = $.02\lambda$	l = $.02\lambda$	
a = radius = $.001\lambda$		
Z = $.0790 - \mathrm{j}\,3388$ ohms	R = $80s^2(1/\lambda)^2 = .3158$ ohms	
G = 1.754 dB	G = 1.761 dB	G = 1.76 dB
Half Wave Dipole:	Half Wave Dipole:	Half Wave Dipole:
N = 30	cosine current	
l = .5 m	l = $.5\lambda$	
a = 0.00001 m		
f = 293 MHz		
Z = 72.21+j .6485 ohms	R $\rightarrow$ 73.13 ohms as $a/\lambda \rightarrow 0$	
G = 2.13 dB	G = 2.151 dB	G = 2.15 dB (Krauss: 2.14 dB)
Full Wave Dipole:	Full Wave Dipole:	
N = 30	cosine current distribution	
l = 1 m	l = 1λ	
a = .00001 m	l = 0.00001λ	
f = 285.3 MHz	R = $(276 \log \lambda/2a) - 110l^2/199$	
Z = 6958-j26.51 ohms	= 7145 ohms	
G = 3.63 dB	G = 3.82 dB	

Monopole Radiation Resistance and Gain

MININEC	Jasik
N = 15 segments	"quarter wave dipole
h = .25 m	above perfect ground"
a = .00001 m	
f = 293 MHz	
Z = 36.10 + j .3352 ohms	
G = 5.145 dB	G = 5.15 dB

Figure 40: Comparison of MININEC impedance and gain data to classical values given by Schelkunoff and Jasik.

data are essentially identical. Figures 35 and 36 show the percent difference between the NEC and MININEC fields of Figures 33 and 34. The greatest difference occurs very close to the monopole within a segment length.

If the near fields are calculated along the surface of the monopole, the differences between MININEC and NEC are much more pronounced. Figures 37 and 38 show the electric fields along the wire surface of the monopole and Figure 39 shows the magnetic fields. The MININEC data were scaled to the same power radiated as the NEC data. The differences are due to the approximation used by MININEC to determine the fields since the current distribution (not illustrated) is nearly the same for both codes. The impedance calculated by each code is a measure of this agreement. MININEC predicts an impedance of 42.170 + j 21.478 ohms and NEC predicts 42.387 + j 24.873 ohms.

The accuracy of the MININEC near fields has been illustrated. MININEC near fields are sufficiently accurate for well converged solutions at distances greater than a segment length.

3.5 Far Fields

The correct pattern shape can often times be calculated using a coarse approximation to the antenna current distribution. However, since the antenna input impedance is used to determine gain, it is necessary to use a well-converged solution to obtain accurate gain data. Figure 40 illustrates both these points. Shown is a comparison between MININEC and the classical solutions from Schelkunoff [22] and Jasik [23]. The coarse solutions are represented by the Schelkunoff and Jasik data. Their data are obtained by assuming sinusoidal currents as noted. The MININEC data are obtained by reference to the convergence data of the previous sections and by adjusting the frequency to obtain the exact resonance condition of near zero reactance. The agreement in gain and impedance data (when available) is fairly good. Data given by Schelkunoff for antennas longer than one wave length cannot be trusted because of the assumptions he employs for the current distribution.

3.6 Memory, Disk Storage and Run Time

Computer memory, disk storage capacity, and solution time are key limiting factors in the use of all method of moments thin wire antenna codes because

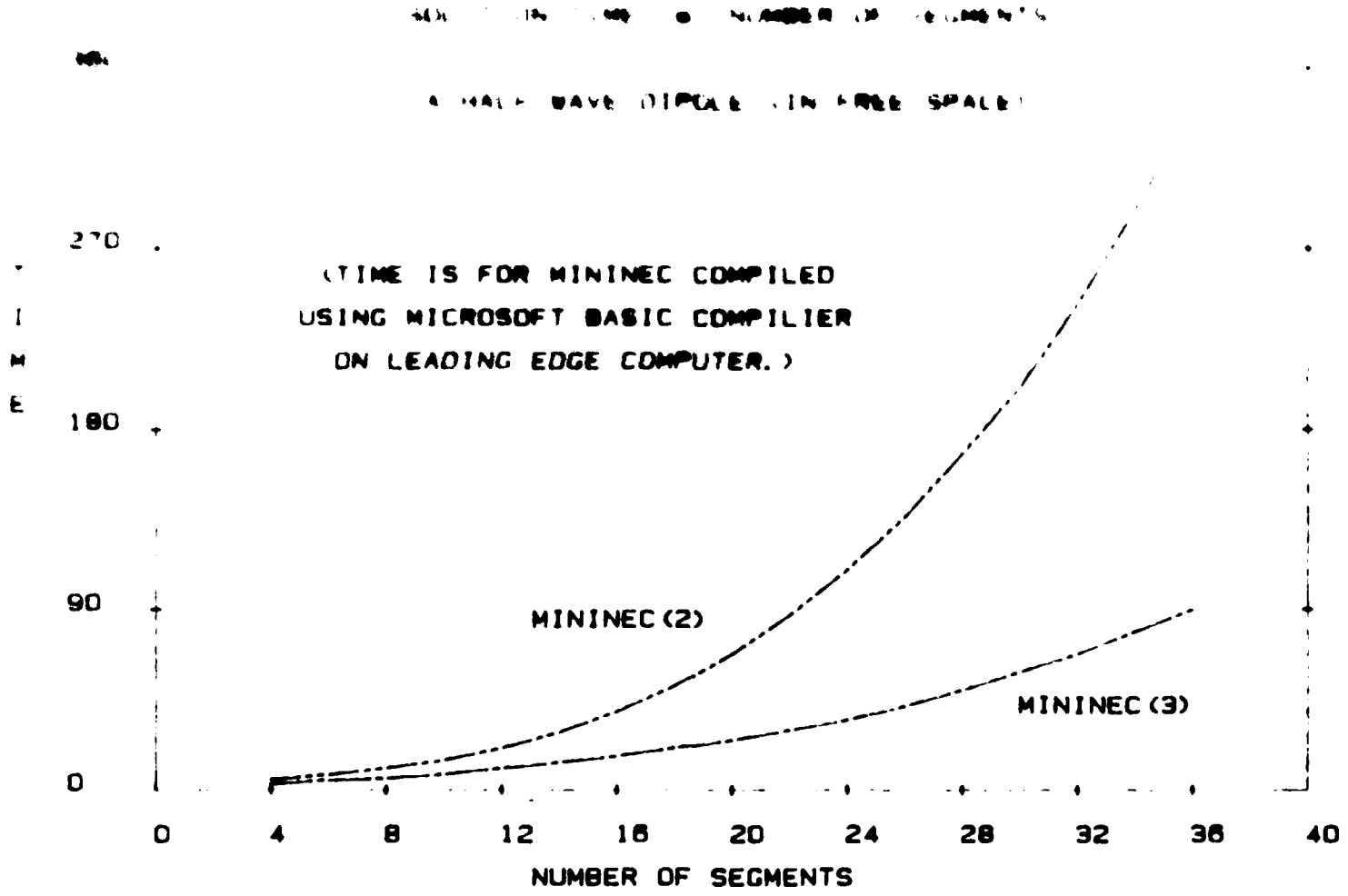

Figure 41: A comparison of the run times of MININEC version 2 and 3

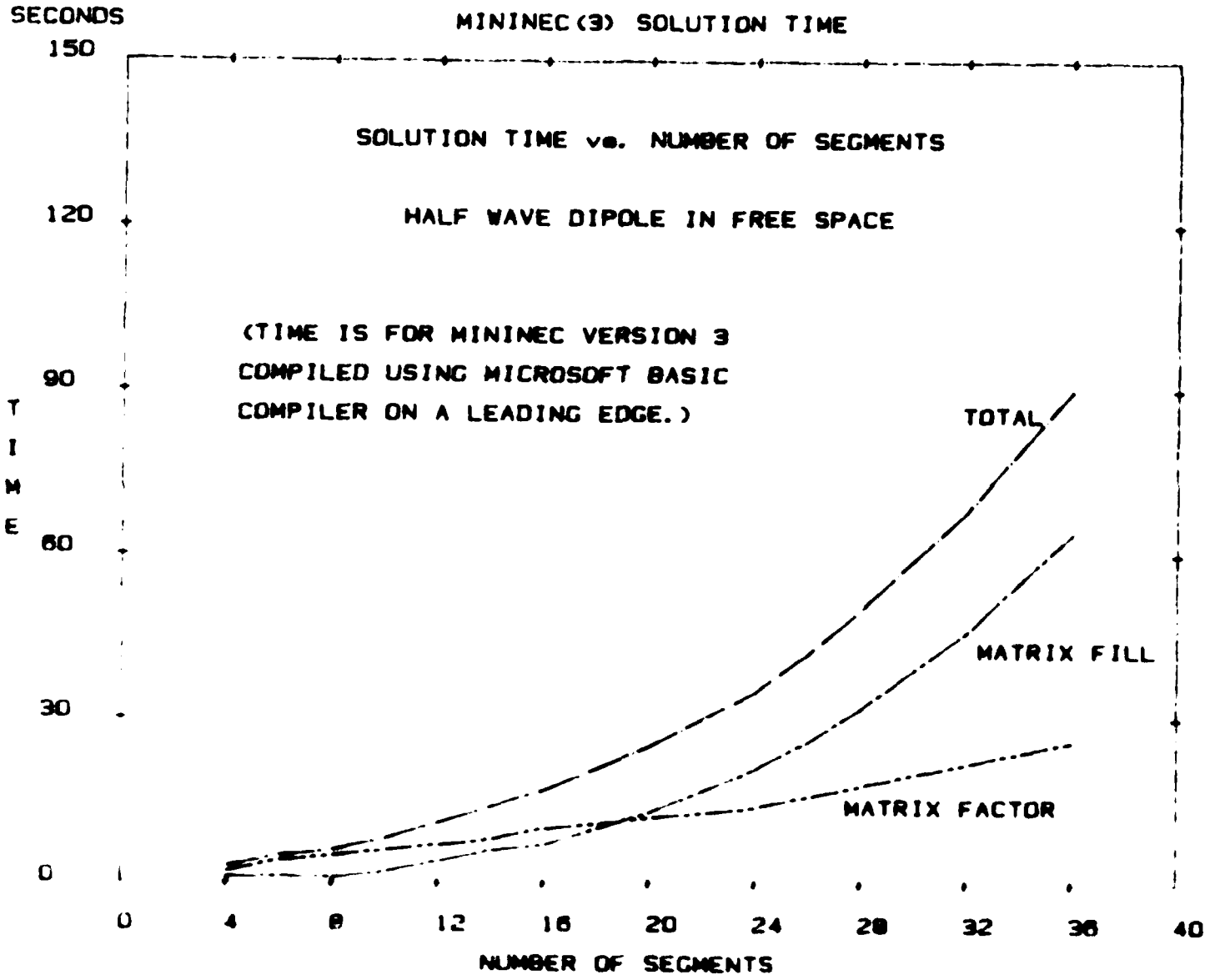

Figure 42: Solution time for MININEC(3) to solve a dipole in free space

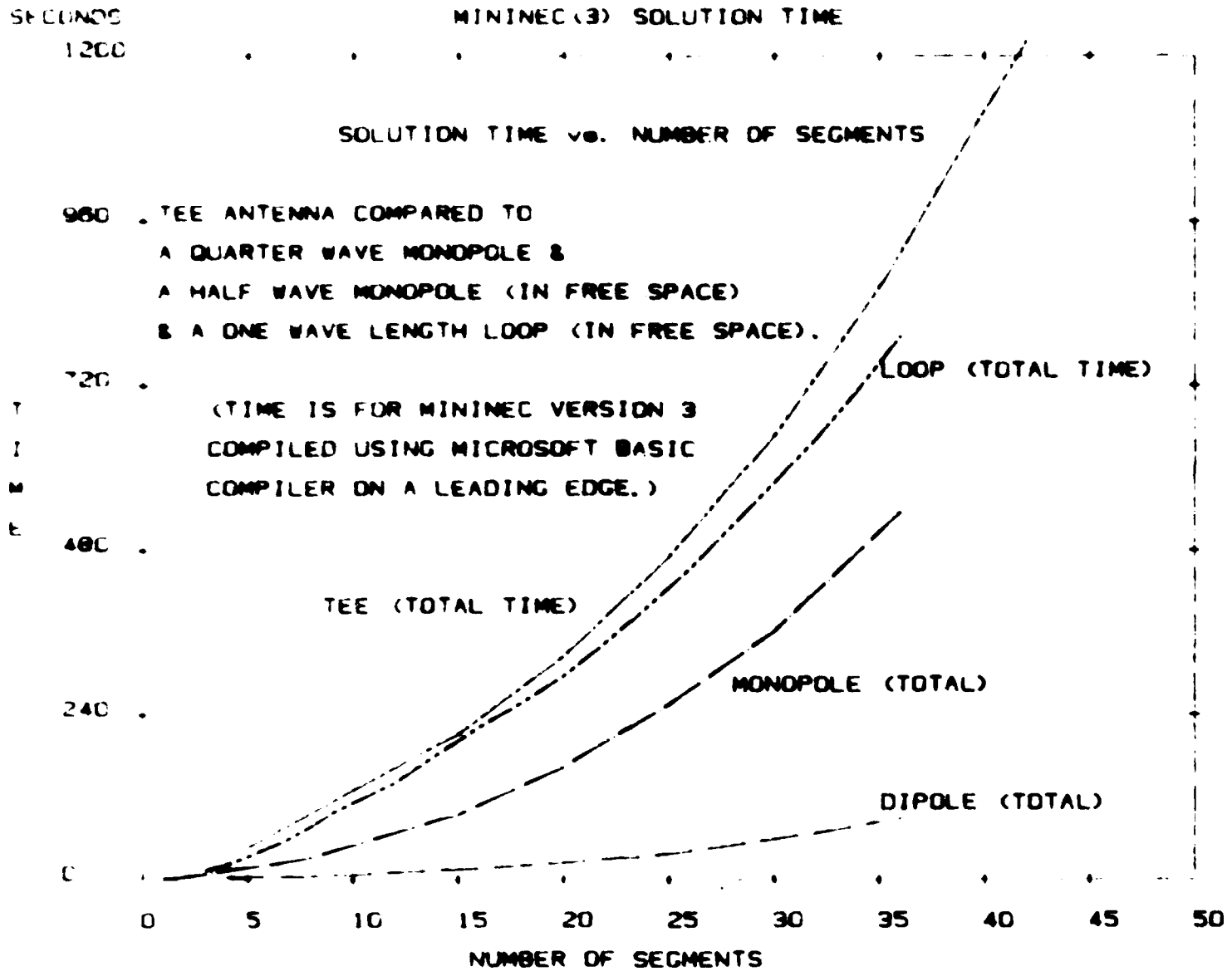

Figure 43: Solution time for MININEC(3) to solve a dipole, loop antenna, monopole and TEE antenna

of the need to store and manipulate (solve or invert) a matrix of complex numbers. These limits are particularly acute when using a microcomputer. Mega-byte hard disks and compilers can partially alleviate these limits.

MININEC has been written specifically for the use in the personal computer environment. Hence the choice of the BASIC language, and the choice of the simple pulse expansion and testing functions (to keep overhead down). Every effort has been made to produce a fast compact computer code. Earlier versions of MININEC were written to minimize program size (length). The present version, however, has sacrificed size for improved internal documentation, modularity and increased capability.

Figure 41 is a comparison of the run times between MININEC version 2 and MININEC version 3. Both codes were compiled for comparison using a Microsoft BASIC compiler. Use of a math co-processor will significantly reduce the run times. The co-processor was not used to obtain the data in Figure 41. For comparison, some other attributes of the codes are as follows:

	MININEC(2)		MININEC(3)	
	Interpreter	Compiled	Interpreter	Compiled
No. of lines	543	–	1607	–
Max. no. of wires	10	75	10	50
Max. no. of segments	50	75	30	50
Disk storage (k bytes)	13	57	44	108

The solution time and size of the executable is a function of the compiler and the compiler/linker options used.

The significant increase in speed of MININEC(3) is attributable to an improved solution routine. The matrix fill time, the time to compute all terms of the matrix, is virtually the same for both versions of MININEC. For large problems, the fill time is usually longer than the factor time, the time to solve the matrix. Figure 42 compares the matrix fill time, factor time and total solution time for MININEC(3) to solve a dipole in free space. Matrix fill time dominates for problems above 20 segments.

The solution time not only increases with the number of segments, but

also increases with the number of wire junctions. This effect can be seen in the data in Figure 43. Shown is the total solution time (fill time plus factor time) for a half wave dipole and a loop antenna in free space. The loop is an extreme case in which the number of wire junctions equals the number of segments. Also shown in Figure 43 is the total solution time for a quarter wave monopole and a TEE-antenna (previously described) over perfect ground. The wire junction in the TEE-antenna is responsible for the longer solution time compared to the monopole. The solution time is also longer for antennas over perfect ground compared to free space. For comparison, the monopole is equivalent to a dipole in free space with twice the number of segments. Even so, the dipole solution time is a little shorter than the monopole.

The brute force approach to circumvent memory and solution time limits is to seek out ever larger, faster computers. The logical extension is to rewrite MININEC in a more powerful language such as FORTRAN and use a mainframe computer. But if a mainframe is available, one really should be using the more powerful NEC program. NEC is written in FORTRAN and is designed for efficient mainframe use. The concept of MININEC is to use a personal computer (PC). In time, as PCs become more powerful, then MININEC, too, will expand in capability. In the meantime, MININEC is appropriate for application to small problems (less than 100 segments). Larger problems should be solved with NEC on an appropriate size computer.

4 Examples and User Guidance

This section is intended to be used both as a reference and as a means for first-time users to become familiar with the input and output (I/O) options of MININEC. The first-time user should spend a few minutes at the computer terminal while following along with the simple two-wire example in section 4.1. A few more minutes at the terminal (perhaps with a simpler four segment dipole) exploring all of the MININEC options should be enough to master this skill. However, the art of actually modeling a wire antenna, i.e., composing the model and properly interpreting MININEC output, is acquired through considerable study of antenna theory and properties, study of the data of section 3, and equally important, accumulating experience by using MININEC.

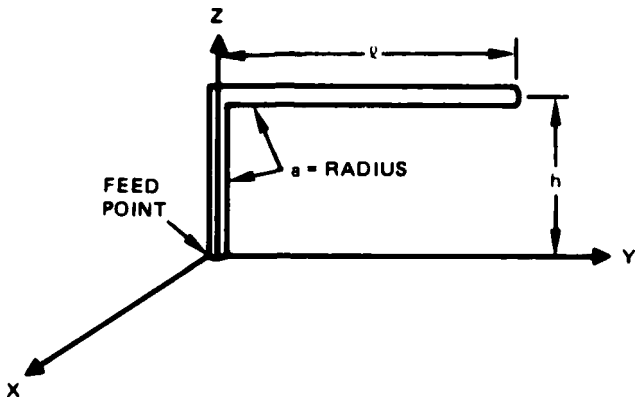

$\beta(h+\ell) = ?$
$\beta = 2\pi/\lambda$
$\beta a = .0259$
LET $\lambda = 1$, THEN
$h \simeq .191$ m
$\ell \simeq .309$ m
$a \simeq .004$ m
$Z = 263 - j457\Omega$
(Prasad [18] measured and corrected for shunt feed point loading)

	Coordinates				
Wire End	X	Y	Z	Wire No.	Wire Radius
1	0.	0.	0.	1	.004
2	0.	0.	0.191		
1	0.	0.	0.191	2	.004
2	0.	0.309	0.191		

Segmentation
Suggested Convergence Test

Wire 1	Wire 2	Total
4	6	10
6	9	15
8	12	20
10	15	25
12	18	30

Figure 44: Inverted L-antenna data for the example in Section 4.1

4.1 Getting Started

First, gather up all known information on the antenna to be modeled, including measurements or reliable analytical data, if available. It is helpful to make a sketch of the antenna using any convenient cartesian coordinate system. For this example, please consider the interted L-antenna in Figure 41. You will need to know the X, Y, Z location for each wire end of each wire relative to the origin of your choice. And you will need to know the radius of each wire. All dimensions must be in meters. This information for the example can be found in Figure 44.

You will need to decide how many segments to use on each wire. This may be done initially by calculating the length of each wire in wave lengths at the desired frequency. Then refer to Figures 6 through 11 as appropriate for the initial choice. This will not guarantee that the MININEC solution will be well converged, but it provides a good place to start. A convergence test is always a good idea. A possible segmentations scheme for the inverted L-antenna is suggested in Figure 44. Alternatively, using your prior experience on a similar antenna, you may be able to come closer to the converged solution the first time. For example, the inverted L-antenna is one wire short of being a TEE-antenna similar to the ones in section 3.3 (see Figures 28 through 31). For the purpose of this discussion, however, we will use a minimal number of segments in order to keep the solution time reasonably short.

MININEC is designed for demand mode execution. Therefore, all you need to do is answer the questions when prompted or provide the required data appropriately. In general, you must define the antenna geometry and define the environment. MININEC can then solve for the currents. Once MININEC has the solution, you may then request near and far fields (patterns).

Now run MININEC. The first question you must answer is:

```
OUTPUT TO CONSOLE, PRINTER, OR DISK (C/P/D)?
```

If you enter `C` for console, all data will be displayed on the monitor. If you answer `P` for printer, the questions or prompts will still be displayed on the monitor, but all other data will be printed. If you answer `D` for disk, you will then be prompted to supply the name of a disk file for storage of all MININEC output:

```
OUTPUT TO CONSOLE, PRINTER, OR DISK (C/P/D)?  D
FILENAMES (NAME.OUT)?
```

As with the printer, all questions and prompts appear on the monitor, but the results go to the file you specify.

Next you must supply the frequency in MHz. Enter the desired frequency or simply enter return to select the default value of 299.8 MHz (or a wave length of one meter).

```
FREQUENCY (MHz)?
    WAVE LENGTH = 1 METER
```

For the next question, you must select free space or a ground plane by entering 1 or -1, respectively.

```
ENVIRONMENT (+1 FOR FREE SPACE, -1 FOR GROUND PLANE)?
```

If you select -1 for ground, you are then prompted for the number of media, which must be an integer from zero to 5.

```
ENVIRONMENT (+1 FOR FREE SPACE, -1 FOR GROUND PLANE)?  -1
 NUMBER OF MEDIA (0 FOR PERFECTLY CONDUCTING GROUND)?
```

A zero selects a perfectly conducting ground plane. See Section 4.3 for further details. Suffice to say at this point that selection of 1 to 5 media does not effect the current distribution or the antenna impedance, but only effects far field calculations. Please select a zero to continue along with this narrative.

Next, you must specify the number of wires[1]. If you specify more than the number allowed, a warning message appears and the question is repeated.

```
NO. OF WIRES?  100
NUMBER OF WIRES EXCEEDS DIMENSION. . .
NO. OF WIRES?
```

A zero will place you at the main menu.

[1]Note to NEC users:
The MININEC post processor program is used to convert a NEC input data set into a MININEC antenna geometry description. These data are automatically stored in the `MININEC.INP` file. At this point, in the `MININEC.INP` file is not empty, MININEC will use that data for the geometry description and you will skip the normal geometry input. See Appendix A for further information.

```
NO. OF WIRES?  0

********************    MININEC MENU    ********************
   G - CHANGE GEOMETRY     C - COMPUTE/DISPLAY CURRENTS
   E - CHANGE ENVIRONMENT  P - COMPUTE FAR-FIELD PATTERNS
   X - CHANGE EXCITATION   N - COMPUTE NEAR-FIELDS
   L - CHANGE LOADS/NET    Q - QUIT
   F - CHANGE FREQUENCY
************************************************************
   COMMAND?
```

To recover from this point, select G for change geometry and answer the questions on environment again.

```
NO. OF WIRES?  0

********************    MININEC MENU    ********************
   G - CHANGE GEOMETRY     C - COMPUTE/DISPLAY CURRENTS
   E - CHANGE ENVIRONMENT  P - COMPUTE FAR-FIELD PATTERNS
   X - CHANGE EXCITATION   N - COMPUTE NEAR-FIELDS
   L - CHANGE LOADS/NET    Q - QUIT
   F - CHANGE FREQUENCY
************************************************************
   COMMAND?  G

ENVIRONMENT (+1 FOR FREE SPACE, -1 FOR GROUND PLANE)?  -1
 NUMBER OF MEDIA (0 FOR PERFECTLY CONDUCTING GROUND)?  0

NO. OF WIRES?
```

Let's assume two wires. The next prompt is for the number of segments on wire 1.

```
WIRE NO. 1
    NO. OF SEGMENTS?
```

You will be prompted for each wire in turn. If you answer zero, you will return to the question for the number of wires. This is a convenient escape mechanism, sometimes useful when you change your mind.

```
WIRE NO. 1
    NO. OF SEGMENTS?  0

NO. OF WIRES?  2
```

```
WIRE NO. 1
    NO. OF SEGMENTS?
```

If at any time you specify too many segments on any one wire, or the total number of segments on all wires specified becomes larger than the maximum allowed by the program array dimensions, an error message will be displayed, and you will return to the question for the number of wires. In this case, to keep this session short, let's choose 4 segments for wire 1.

Next, enter the X, Y, Z coordinates, in meters, for end one of the first wire. Then enter the X, Y, Z coordinates for end two; then enter the radius, as prompted.

```
NO. OF SEGMENTS?  4
END ONE COORDINATES (X,Y,Z)?  0,0,0
END TWO COORDINATES (X,Y,Z)?  0,0,.191
                     RADIUS?  .004
            COORDINATES                                  END          NO. OF
   X             Y             Z          RADIUS     CONNECTION     SEGMENTS
0             0             0                           -1
0             0            .091          .004           0              4
   CHANGE WIRE NO.  1  (Y/N)?
```

After entry of the radius, MININEC responds immediately with a table as shown above. The table gives the coordinates of the wire ends, the radius and the end connection information, so you may verify that you have entered the data correctly. If not, you have the opportunity to start again with this wire. Otherwise, you may continue to the next wire. The end connection information is useful to verify that a connection has been made. In this case, the minus one indicates that end one in connected to ground. A connection to ground is indicated by a negative integer, whose absolute value is the same as the wire number. The zero indicates that end two of this wire is not yet connected to any other wire.

Now continue on to the next wire and give the appropriate data:

```
CHANGE WIRE NO.  1  (Y/N)?  N

WIRE NO. 2
   NO. OF SEGMENTS?  6
   END ONE COORDINATES (X,Y,Z)?  0,0,.191
   END TWO COORDINATES (X,Y,Z)?  0,.309,.091
```

```
                          RADIUS?  .004
            COORDINATES                                   END          NO. OF
   X             Y             Z          RADIUS      CONNECTION      SEGMENTS
0              0              .191                        1
0              .309           .191          .004          0              6
CHANGE WIRE NO.  2  (Y/N)?
```

The connection data indicates that end one of wire two is connected to the top of wire one, i.e., end two of wire one. The absolute value of the end connection integer is the wire number to which wire two is connected. A plus sign indicates an end one connected to an end two (as in this case), or an end two connected to an end one. A negative sign indicates and end one connected to an end one, or an end two connected to an end two. And, of course, a zero means no connection.

By the way, if you happen to give either wire end a negative Z-coordinate when a ground plane is specified, you will get an error message and will have to reconsider your entry. Likewise, MININEC will not let you get away with a zero radius, or a zero wire length.

If you are now satisfied with the wire two data entry, we may proceed. MININEC will produce a table of the coordinates for the location of each current pulse on each wire. Note that the radius and connection data are also given so that you may verify your data entry.

```
CHANGE WIRE NO.  2  (Y/N)?  N

                    **** ANTENNA GEOMETRY ****

WIRE NO.  1  COORDINATES                                  CONNECTION PULSE
X              Y              Z              RADIUS       END1 END2  NO.
 0              0              0              .004         -1    1    1
 0              0              .04775         .004          1    1    2
 0              0              .0955          .004          1    1    3
 0              0              .14325         .004          1    0    4

WIRE NO.  2  COORDINATES                                  CONNECTION   PULSE
X              Y              Z              RADIUS       END 1 END 2  NO.
 0              0              .191           .004          1     2      5
 0              .0515          .191           .004          2     2      6
 0              .103           .191           .004          2     2      7
 0              .1545          .191           .004          2     2      8
 0              .206           .191           .004          2     2      9
 0              .2575          .191           .004          2     0     10
```

```
CHANGE GEOMETRY (Y/N)?
```

This table is essential to proper location of the feed point (or source excitation point) and location of loads.

You now have one last chance to change the geometry before proceeding.

```
CHANGE GEOMETRY (Y/N)?  N

NO. OF SOURCES?
```

You must now decide how many feed points to use, where they are located, and what voltages are applied. You will be prompted for this data for each source, in turn. In this case, let's keep it simple.

```
NO. OF SOURCES?  1

SOURCES NO. 1:
PULSE NO., VOLTAGE MAGNITUDE, PHASE (DEGREES)?  1,1,0
```

Sources are always co-located with current pulse functions. Hence, you may have to refer to the above table of antenna geometry to select an appropriate pulse to apply the source. In this example, the source is at the ground plane, i.e., pulse number one, located on wire one. I have chosen one volt at zero degree phase angle for this example.

The next set of questions provide the opportunity to add impedance loading to the antenna. To keep things simple, let's avoid loading and continue on. Please refer to section 4.5 for more detailed information on loading options.

```
NUMBER OF LOADS?  0

********************    MININEC MENU    ********************
   G - CHANGE GEOMETRY     C - COMPUTE/DISPLAY CURRENTS
   E - CHANGE ENVIRONMENT  P - COMPUTE FAR-FIELD PATTERNS
   X - CHANGE EXCITATION   N - COMPUTE NEAR-FIELDS
   L - CHANGE LOADS/NET    Q - QUIT
   F - CHANGE FREQUENCY
*********************************************************
   COMMAND?
```

You are now faced with the main menu again. By selection of an appropriate command letter, you may change the geometry (G), change the environment (E), change the source or excitation (X), change the loads and networks (L), and change the frequency. When satisfied with the antenna geometry and environment, you are ready to determine the antenna properties. The preferred choice at this point is C, compute and display the currents. If you select P for patterns or N for near fields, MININEC will check to see if the currents have been calculated; if not, MININEC will compute the currents before you can proceed. So let's select C.

```
COMMAND?  C

BEGIN MATRIX FILL
MATRIX FILL 10% COMPLETE - APPROX TIME REMAINING 1:48
```

MININEC responds almost immediately with an estimate of the time in minutes and seconds required to complete filling the impedance matrix. At intervals, the estimate will be updated and the total time will be given when this step is completed. Similarly, MININEC will estimate the time to solve the matrix for the currents and in turn display the total times.

```
BEGIN MATRIX FILL
MATRIX FILL 100% COMPLETE - APPROX TIME REMAINING 0:00
FILL MATRIX:  1:27

FACTOR MATRIX 100% COMPLETE - APPROX TIME REMAINING 0:00
FACTOR MATRIX:  0:04
```

When the solution is complete, MININEC computes and displays the impedance and power input for each source in turn. If there is more than one source, the sum total power input will also be displayed. The solution is also displayed in terms of the current distribution, wire by wire.

```
********************    SOURCE DATA     ********************
PULSE  1      VOLTAGE = ( 1 , 0 J)
              CURRENT = ( 9.852278E-04 , 1.479977E-03 J)
              IMPEDANCE = ( 311.6818 , -468.1982 J)
              POWER =  4.926139E-04  WATTS

********************    CURRENT DATA    ********************
```

```
WIRE NO.  1:
PULSE        REAL          IMAGINARY     MAGNITUDE     PHASE
NO.          (AMPS)        (AMPS)        (AMPS)        (DEGREES)
 1           9.852278E-04   1.479977E-03  1.777922E-03  56.3481
 2           .000962       -7.880544E-04  1.243573E-03 -39.32376
 3           8.940962E-04  -2.186383E-03  2.362143E-03 -67.75855
 4           7.867739E-04  -3.248648E-03  3.342563E-03 -76.38595
J            6.45715E-04   -3.943692E-03  3.996205E-03 -80.70126

WIRE NO.  2:
PULSE        REAL          IMAGINARY     MAGNITUDE     PHASE
NO.          (AMPS)        (AMPS)        (AMPS)        (DEGREES)
J            6.45715E-04   -3.943692E-03  3.996205E-03 -80.70126
 6           5.160325E-04  -4.466384E-03  4.496095E-03 -83.40944
 7           3.756805E-04  -4.519859E-03  4.535446E-03 -85.24862
 8           2.408057E-04  -4.093055E-03  4.100132E-03 -86.633
 9           1.252218E-04  -3.201494E-03  3.203942E-03 -87.76009
 10          4.12146E-05   -1.891714E-03  1.892163E-03 -88.75189
E            0              0             0             0

SAVE CURRENTS TO A FILE (Y/N)?
```

Notice that the current is zero at the free end of wire two. And since there is no pulse number, an `E` is displayed to help identify a free end. Kirchoff's current law has been used to solve for the currents on each respective wire at the junction. And a `J` is substituted for the pulse number, indicating a wire junction or connection point.

Notice that the real part of the impedance, the resistance, is within 19% of the measured value given by Prasad [18], (see the data in Figure 44) and the reactance is within 2.4%. When I tried the convergence test suggested by the scheme in Figure 44, MININEC was pretty well converged at 30 segments to an impedance of 167 + j395 ohms. Prasad used an approximate method to correct her measured data for the loading effects of the coaxial termination at the feed point. I suspect the method may not be sufficiently accurate in this case.

You must now decide whether to save the currents to a disk file. If you answer `Y`, you will be prompted for a disk file name and the currents will be saved. If not, you will return to the main menu.

```
SAVE CURRENTS TO A FILE (Y/N) ? N

********************    MININEC MENU    ********************
   G - CHANGE GEOMETRY     C - COMPUTE/DISPLAY CURRENTS
   E - CHANGE ENVIRONMENT  P - COMPUTE FAR-FIELD PATTERNS
   X - CHANGE EXCITATION   N - COMPUTE NEAR-FIELDS
   L - CHANGE LOADS/NET    Q - QUIT
   F - CHANGE FREQUENCY
************************************************************
   COMMAND?
```

If you decide that you want to look at the impedance or currents again, you simply chose `C`. There is no wait this time because MININEC does not re-compute and solve the matrix. You will get an immediate display of the impedance and currents.

You may now elect to calculate patterns or near fields. Please refer to the appropriate sections for details on these operations.

Good luck!

4.2 Change Geometry

The `G` option on the MININEC menu provides the means to change the antenna configuration without changing the frequency. The entry point is the question to choose the environment, free space or ground. Please see section 4.3 for details. After choosing the environment, you will begin defining the wire configuration, i.e., specify the number of wires and the location, radius and segmentation for each wire. Please see section 4.1 for an example.

4.3 Change Environment

The `E` option on the MININEC menu provides the means to change the antenna environment, without changing the frequency, feed point, loading or geometry. Note that changing from free space to a ground plane does not change the connection data or location of wires already specified. Hence, erroneous and strange results may occur if the geometry is not also changed appropriately.

Selecting free space will return you to the main menu.

If you choose a ground plane, you may specify 0 for perfectly conducting ground or you may select up to 5 changes in surface impedance (up to 5

media). Changing the surface impedance does not alter the current distribution on antennas over ground. MININEC uses the surface impedance to correct far field pattern only. If you select 1 surface impedance, you will be prompted for the relative dielectric constant and the conductivity, in mhos per meter. The far field subroutine will use this information in a Fresnel reflection coefficient correction to the radiation fields.

For two or more impedance surfaces, you must choose between a linear or circular boundary between surfaces. The linear boundary is parallel to the Y-axis. The circular boundary is centered at the origin. The first surface (and the perfectly conducting ground plane) is always at the level of the X-Y plane (Z=0). For each surface in turn, you must specify the height of the surface (or media) relative to the first surface. A negative value is a step down; a positive value is a step up. A zero value means a flat ground. Note that there is no diffraction coefficient correction in MININEC for a cliff edge. There is also no correction for blockage due to a large step up, i.e., the antenna cannot be in a well. For each media in turn, you must supply the distance in meters from the origin to the media boundary.

When you choose a circular boundary with two or more media, you will be prompted for the number of radial wires in the ground screen. This approximation is really accurate for dense ground screens only. One hundred or more should be used for best results. Zero, of course, is also a valid choice. You must also supply the wire radius of the wires in the ground screen. The length of the wires in the ground screen is the same as the distance to the interface between media one and two.

4.4 Change Excitation

The `X` option in the MININEC menu provides the means to change the antenna feed excitation (i.e., number of feeds, feed location and magnitude and phase) without changing the geometry, environment, frequency or loading. Changing only the excitation does not require re-filling or re-factoring of the matrix. Hence, after solving for the currents for the initial excitation, you can rapidly try out all possible source locations or try multiple source excitation. Source locations must coincide with the locations of the current pulse functions. You cannot put source excitations on non-existent pulses. At least one source must be given. MININEC will not allow more sources than the maximum set by the dimension statement (see the first 30 lines of MININEC to determine this limit).

There is but one source model in MININEC. The model imposes a constant field over a pulse width, with amplitude and location, coincident with a current pulse, chosen by the user. In spite of the simplicity, this source model is a good approximation for most transmit cases. What do you do then to evaluate the performance of a receive only antenna? One way to evaluate the receive properties of an antenna is to place a transmitting dipole at a great distance (i.e., in the far field of the receive antenna). The field incident on the receive antenna is a good approximation to a plane wave.

4.5 Change Loads

The `L` option on the MININEC menu provides the means to alter or add lumped parameter loads to an antenna. Changing the load requires re-filling and re-factoring of the matrix. Each load location must coincide with a current pulse function. MININEC will not allow more loads than the maximum for which it is dimensioned (see the first 30 lines of MININEC to determine this limit). There are two kinds of loads; impedance loading and S-parameter loading. You may select the loading type when prompted after specifying the number of loads.

The simplest load type is impedance loading. You must supply the pulse location, resistance and reactance for each load, in turn. The reactance value you specify will not change when you change the frequency. If you desire the load impedance to change appropriately with frequency, you must change the impedance load every time you change frequency. Alternatively, you may specify your load in terms of an equivalent S-parameter function.

One convenient method of circuit analysis makes use of the concept of a complex frequency, or S-paramter. Generally, S is defined as $S = G + \mathrm{j}\,\omega$ where G is the neper frequency and ω is the angular frequency [24]. For steady state, sinusoidal time varying signals, $G = 0$.

The impedance of an RLC circuit can always be expressed as a function of S. With a little bit of algebra, the impedance can be represented as a ratio of polynomials in S. The S-parameter impedance function is a polynomial in S with the form:

$$Z(S) = \frac{A_0 S^0 + A_1 S^1 + A_2 S^2 + \ldots A_n S^n}{B_0 S^0 + B_1 S^1 + B_2 S^2 + \ldots B_m S^m}$$

where the coefficients A_i and B_i are functions of R, L and C. For example a series RC circuit has an impedance of

$$Z = R + \frac{1}{j\omega C} = R + \frac{1}{SC} = \frac{RC+1}{CS}$$

hence

$$A_0 = RC + 1$$

$$A_1 = 0 \text{ for } i > 0$$

and

$$B_0 = 0$$

$$B_1 = C$$

$$B_i = 0 \text{ for } i > 1$$

When you select the S-parameter load option, you will be prompted for the pulse number (at which to locate each load) and the order of the S-parameter impedance function. The order is the highest exponent of S occurring in either the numerator or denominator. For the example cited above, the order is one. After supplying these two numbers, you will be prompted for the magnitude of the coefficients of S in order, starting with the order zero and up to the order you have specified. The coefficients are given in pairs, i.e., numerator and denominator for each order.

The advantage of the S-parameter load is that the impedance changes appropriately with frequency. Each time you change frequency, you need not re-specify the load. Almost any series-parallel combination of RLC elements can be expressed in terms of a polynomial in S, with a little bit of algebraic effort.

4.6 Change Frequency

The `F` option on the MININEC menu provides a way to alter the frequency. You will be prompted for the frequency in MHz. MININEC will compute and display the wave length and return to the menu. Changing the frequency will require re-filling and re-factoring of the impedance matrix. The current geometry will be used.

4.7 Compute/Display Currents

The `C` option on the MININEC menu triggers filling and factoring of the matrix for the antenna configuration most recently specified. If a solution has already been computed, and no changes have been made to the environment, excitation, loads and frequency, then the `C` option will simply display the impedance and current distribution.

4.8 Compute Far Field Patterns

The `P` option on the MININEC menu is used to specify the far field pattern calculation. If the currents have not already been computed, they will be computed before you can proceed. You may choose to compute the patterns in dBi, i.e., in dB above an isotropic radiator, or in volts per meter, i.e., the electric field.

When you choose dBi, you are prompted for the zenith angle and the azimuth angle. In each case you must supply three numbers, the initial angle, the angle increment and the number of angles. If you specify zero for the number of angles, one is assumed. The zenith and azimuth angles are the theta and phi angles, respectively, as shown in Figure 45. When the patterns are calculated in dBi, the e^{-jkR}/R dependence of the far field is suppressed, i.e., the pattern is at infinite range.

When you choose to compute the patterns in volts per meter (i.e., the electric field strength), the power (radiated) level is displayed and you are prompted to change this level. The fields will be scaled to the level you specify. Next, you must specify the range in meters. If you specify zero, the e^{-jkr}/R dependence is suppressed. For accuracy, be sure the range you specify is sufficient for the far field.

For both dBi and volts per meter, you will be prompted to save the pattern data. When you answer yes, you are prompted for a file name. The pattern data will be saved as ASCII images in this file. You may use an editor or the MININEC post processor to prepare this data for plotting (see Appendix B).

4.9 Compute Near Fields

The `N` option on the MININEC menu is used to specify the location of points for calculation of the near electric and magnetic fields. If the currents have

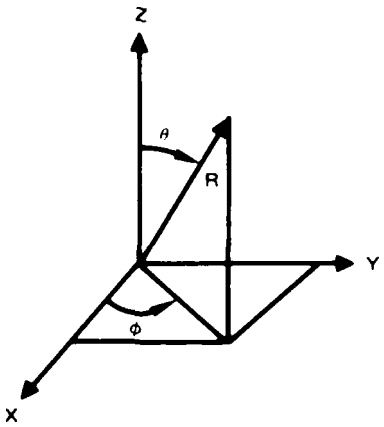

Figure 45: Coordinate system for far field pattern

not already been computed, they will be computed before you can proceed. You must choose electric or magnectic fields. Then you will be prompted for the field location in cartesian coordiantes. You are prompted for the initial coordinate, the increment and the number of steps for each of the principle directions. All dimensions must be in meters. Next, the radiated power level is displayed and you are given a chance to change this level. The near fields will be scaled to the power level you specify. If you specify zero, the original power level will be used. You will also be prompted to save the near field data. The field data will be stored in the disk file you specify. Use `MMPOST` (see Appendix B) or an editor of your choice to process this data for plotting.

4.10 Quit

The `Q` option on the MININEC menu provides a clean and efficient termination of the MININEC session.

References

[1] A. J. Julian, J. C. Logan, and J. W. Rockway. MININEC: A Mini-numerical Electromagnetics Code. Technical Report NOSC TD 516, September 1982.

[2] D. R. Wilton. Wire Problems. Lecture Notes for Short Course on Computational Methods in Electromagnetics, 1981.

[3] S. T. Li, J. C. Logan, J. W. Rockway, and D. W. Tam. *Microcomputer Tools for Communications Engineering*. Artech House, Inc., Dedham, MA, 1984.

[4] G. J. Burke and A. J. Poggio. Numerical Electromagnetics Code (NEC)—Method of Moments. Technical Report NOSC TD 116, January 1981.

[5] R. F. Harrington. *Field Computation by Moment Methods*. Macmillan Company, New York, 1968.

[6] M. Abramowitz and I. Stegun, editors. *Handbook of Mathematical Functions*, pages 590–592. Number 35 in NBS Applied Mathematics Series. Government Printing Office, New York, November 1980.

[7] A. Ralston. *A First Course in Numerical Analysis*. McGraw-Hill, New York, 1965.

[8] R. W. P. King. *The Theory of Linear Antennas*. Harvard University Press, Cambridge, MA, 1956.

[9] R. W. P. King. *Tables of Antenna Characteristics*. IFI/Plenum Data Corporation, New York, 1971.

[10] J. C. Logan. A Comparison of Techniques for Treating Radiation and Scattering by Bent Wire Configurations with Junctions. Technical Report TR-73-10, Syracuse University, August 1973. National Science Foundation Grant GK-4227.

[11] H. H. Chao and B. J. Strait. Computer Programs for Radiation and Scattering by Arbitrary Configurations of Bent Wires. Scientific Report 7, September 1970. Contract F19628-68-0180, AFCRL-700374.

[12] A. T. Adams, B. J. Strait, D. E. Warren, D. Kuo, and T. E. Baldwin, Jr. Near Fields of Wire Antenna by Matrix Methods. *IEEE Transactions on Antennas and Propagation*, AP-21(5):602–610, 1973.

[13] A. T. Adams and E. Mendelovicz. The Near Field Polarization Ellipse. *IEEE Transactions on Antennas and Propagation*, AP-21(1), January 1973.

[14] J. R. Wait. Characteristics of Antennas Over Lossy Earth. In Collin and Zuker [15], Part II, pages 386–437.

[15] R. E. Collin and F. J. Zuker, editors. *Antenna Theory*. McGraw-Hill, New York, 1969.

[16] W. L. Stutzman and G. A. Thiele. *Antenna Theory and Design*. John Wiley and Sons, New York, 1981.

[17] A. W. Glisson and D. R. Wilton. Numerical Procedures for Handling Stepped-Radius Wire Functions. Final report for contract N66001-E-0156, University of Mississippi, March 1974.

[18] S. Prasad and R. W. P. King. Experimental Study of Inverted L-, T-, and Related Transmission Line Antennas. *Journal of Research of the National Bureau of Standards—D Radio Propagation*, V. 65D(5), September-October 1961.

[19] J. H. Richmond. Computer Program for Thin-Wire Structures in a Homogeneous Conducting Medium. NASA Technical Report 2902-12, Grant No. NGL 36-008-138, August 1973.

[20] M. Van Blaricum and E. K. Miller. TWTD: A Computer Program for Time Domain Analysis of Thin Wire Structures. Lawrence Livermore Laboratory Report UCRL-51277, October 1972.

[21] J. W. Rockway and J. C. Logan. Thin-Wire Modeling Techniques Applied to Antenna Analysis. NELC TD 359, October 1974.

[22] S. A. Schelkunoff and H. T. Fries. *Antennas: Theory and Practice*. John Wiley and Sons, New York, 1952.

[23] H. Jasik. *Antenna Engineering Handbook*. McGraw-Hill, New York, 1961.

[24] N. Balabarrian. *Fundamentals of Circuit Theory.* Allyn and Bacon, Boston, 1961.

A A Pre-Processor for MININEC

MNPRE.BAS converts NEC input data sets to MININEC geometry specifications. First prepare an input data file suitable for NEC (see reference [5] for instructions). Then run MNPRE.BAS. MNPRE.BAS will prompt you for a disk file name containing the NEC data set. It will convert the geometry portion of the NEC data set into the geometry specifications required by MININEC and write the results into a binary file named MININEC.INP. When you run MININEC, it will check MININEC.INP for data. If empty, data entry is normal keyboard entry. If not empty, MININEC will read the data and display the segmentation data. The MININEC session will then proceed as normal starting with the question:

```
CHANGE GEOMETRY (Y/N)?
```

A source listing of MNPRE.BAS follows:

B A Post-Processor MININEC

MNPOST.BAS processes MININEC output data for plotting using the GRAPS program (See NOSC TD 820, "GRAPS: Graphical Plotting System" by R. T. Laird, July 1985). You may store MININEC currents, near fields and pattern data in a file of your choice. Election to store output data in disk files is accomplished during a MININEC session. MNPOST.BAS will read these files and prompt you for the data to be plotted. MNPOST.BAS will recognize the type of data and display it for your convenience. After you have chosen the data for plotting, the minimum and maximum values are computed and displayed. You will be prompted to adjust the scale limits or use these values. Then the data will be written to a file you designate in the format required by GRAPS. A program listing of MNPOST.BAS follows:

C MININEC Program Listing

MININEC Compilation

Fastest run times for MININEC3 have been achieved using 87BASIC/ INLINE(TM), MicroWay's BASIC compiler post processor which generates in-line 8087 code for all floating point expressions. The following table gives

some ideas of the difference in run times for the matrix fill in the sample problem in NOSC TD 516, Appendix B.

BASICA Interpreter	4 1/2 hours
IBM BASIC Compiler	22 minutes
87BASIC Compiler	8 minutes
87BASIC/INLINE	4 minutes

87BASIC/INLINE is available from MicroWay, P.O. Box 79, Kingston, Mass. 02364 Phone (617) 746-7341. The current price of the package is two hundred dollars.

MININEC3.BAS may be run with the BASICA Interpreter, but the maximum number of pulses must be reduced to 42 with 10 wires. A maximum of 50 wires and 50 pulses may be used with the IBM BASIC Compiler. The other compilers allow 70 pulses.

A program listing dimensioned for the IBM BASIC Compiler follows: